Updating Standard Shape Material Properties Database for Design and Reliability (k-Area 4)

Report on a Research Project funded by

American Institute of Steel Construction
One East Wacker Drive, Suite 3100
Chicago, IL 60601-2001

by

F. M. Bartlett,
J. J. Jelinek,
and B. J. Schmidt

Dept. of Civil and Environmental Engineering
University of Western Ontario
London Canada N6A 5B9

(519) 661-3659
fax: (519) 661-3779
email: f.m.bartlett@uwo.ca

R. J. Dexter,
M. D. Graeser,
and T. V. Galambos

Dept. of Civil Engineering
University of Minnesota
500 Pillsbury Drive S.E.
Minneapolis, MN 55455-0220

(612) 624-0063
fax: (612) 626-7750
email: dexter@tc.umn.edu

Final 04 December 2001

ABSTRACT

This report summarizes the mechanical properties of ASTM A992 steel as determined by tests of 207 flat-strap tensile test specimens at the University of Minnesota and the University of Western Ontario carried out in accordance with ASTM A370. Samples were obtained from 38 heats of steel from eight different shapes provided by three producers. The objectives of the study were to quantify statistical parameters for the mechanical properties of A992 steel and to investigate the necessity of updating the resistance factor for steel in the AISC LRFD Specification (AISC, 1999). The lower tail of the yield strength data is accurately represented by the lognormal distribution reported by Dexter et al. (2000). The ratio of the observed yield stress to the corresponding value reported on the Mill Test Report averaged 1.002, with a coefficient of variation of 0.044. The ratio of the flange yield strength to web yield strength averaged 0.95, suggesting that producing steel from near-net-shape blooms instead of ingots may not significantly affect this ratio. The difference between the static yield strength and the yield strength recorded at ASTM A370 strain rates averaged 4.4 ksi. It is concluded that A992 steel has smaller bias coefficients and smaller coefficients of variation compared to the parameters for A36 steel used in the original calibration that have increased the reliability index slightly. At the AISC LRFD calibration point of a live-to-dead ratio of three, the reliability index for a braced compact beam with a resistance factor of 0.9 increases from 2.5 to 2.6 if the discretization factor is ignored or to 2.8 if the discretization factor is included. However, an increase of resistance factor from 0.90 to 0.95 is not recommended without further study.

ACKNOWLEDGEMENTS

Funding for this research was provided by the American Institute of Steel Construction in the form of separate contracts with the University of Minnesota (R. J. Dexter, Principal Investigator) and the University of Western Ontario (F. M. Bartlett, Principal Investigator). Jacques Cattan, Sergio Zoruba and Tom Schlafly served as the coordinating managers for this project. The authors would like to thank Trade ARBED Inc., Nucor-Yamato Steel Sales Corp., and Corus CIC Inc. for their generous donation of steel specimens. The assistance of Bob Stuart of the University of Western Ontario Machine Shop is also gratefully acknowledged.

TABLE OF CONTENTS

LIST OF TABLES

LIST OF FIGURES

1. INTRODUCTION

Resistance factors, ϕ, presently used in the AISC Load and Resistance Factor Design (LRFD) Specification (AISC, 1999) are largely based on tensile test data for A36 steel collected in the 1960s and 1970s (Galambos & Ravindra, 1978). Since then, the processes used to make steel have changed, the producers of structural shapes are different, and the ASTM specifications for structural steel have evolved considerably.

Past steel production involved ingots produced from raw iron ore in basic oxygen furnaces. Most shapes currently produced for use in the United States are rolled from beam blanks, blooms, or near-net-shapes cast continuously. The steel is melted in electric-arc furnaces using recycled material. The continuous casting reduces the amount of rolling necessary to form the final shape, and so reduces the energy requirements and overall cost.

Most steel shapes are now produced to a single material grade specification, ASTM A992, which meets or exceeds the A36 and A572 Grade 50 (and CSA G40.21 Grades 300 and 350) specifications. The A992 specification tightens previous chemistry limits, sets new limits on residual elements, and includes the following minimum mechanical property requirements:

- yield strength, F_y : 50-65 ksi (345-448 MPa)
- minimum ultimate tensile strength, F_u : 65 ksi (448 MPa)
- maximum yield strength to ultimate tensile strength ratio, *Y/T*: 0.85
- minimum elongation at failure in 2 in. (50.8 mm): 21%

The change from A36 to A992 steel potentially affects the shape and character of the steel stress-strain curve because the minimum specified yield stress has increased by over 38% whereas the minimum ultimate tensile strength has increased by only 12%.

The location of the test specimen used to verify the mechanical properties of wide flange shapes, specified in ASTM A6, has also changed. At the time of the original resistance factor calibration, the test coupon was obtained from the quarter-depth of the web. Since 1996, it has been obtained from the flange for W-shapes with flange widths of six inches (150 mm) or greater. This potentially impacts the resistance factor because the yield strength of the flange is typically less than that of the web, and so the strength of steel produced may be increased to meet minimum specified values.

To quantify the mechanical and chemical properties of current structural shape production, the Structural Shape Producers Council (SSPC) compiled an extensive data base from approximately 25 000 mill test reports of A36, A572 Grade 50, and A992 material (Dexter et al., 2000). However, to fully incorporate these data into the resistance factor calibration process, it is necessary to determine the relationships between information reported on the mill test certificate and various properties of the steel.

1.1 Objectives of Research

The objectives of the research are as follows:

1. Determine various mechanical properties by tests of flat-strap tensile test specimens representing current A992 steel production. Specific objectives are:
    a. to determine the statistical parameters for the yield strength F_y, the ultimate tensile strength F_u, the Y/T ratio, the elastic modulus E, the strain at commencement of strain hardening ε_{st}, and the ultimate strain, ε_u;
    b. to quantify the correlation between the strength of steel in the flange of the shape and the strength in the web;

c. to verify the accuracy of mechanical properties reported on mill test certificates, and so determine whether information in the SSPC database of mechanical properties must be rectified before being adopted for resistance factor calibration;

d. to quantify the relationship between the yield strength observed at strain rates specified in ASTM A370 and the static yield strength, that defines the strength of steel in a structural member loaded at a slower rate; and,

e. to compute typical inter-laboratory precision statistics.

2. Using these findings, compute statistical parameters for the resistance of typical steel members.

3. Carry out reliability-based analyses to investigate the necessity of updating the ϕ factors, and recommend revised ϕ factors if necessary.

The current study has been ongoing with a parallel investigation entitled "Review of the Resistance Factor for Steel" (Schmidt, 2000; Schmidt & Bartlett, 2001a, 2001b), funded by the Steel Structures Education Foundation of the Canadian Institute of Steel Construction. Data have been shared between the two studies, and the findings of both studies have been progressively reviewed for consistency. Carrying out the work in parallel between Canada and the United States recognizes that today this is really one marketplace for structural steel shapes. Further, this collaboration will facilitate the ongoing harmonization of all North American steel design codes.

2. TESTING PROGRAM

Samples of A992 steel investigated in this study were provided by Trade ARBED Inc., Nucor-Yamato Steel Sales Corp., and Corus CIC Inc. As shown in Table 1, the samples represented a total of 38 heats of steel from eight different shapes. A total of 207 flange and web coupons were obtained from these shapes, and were tested at the University of Western Ontario (UWO) and the University of Minnesota (UM).

Two producers, identified simply as Producers A and B for the remainder of this report, sent two-foot lengths of complete shapes to the University Machine Shop at UWO. Coupons were obtained from each shape from the six locations shown in Fig. 1, and were machined to the dimensions shown in Fig. 2, which conform to the ASTM A370 standard (ASTM, 1997). Mill test certificates were provided by each producer that represented flange material from the same heat as each length of shape provided.

The third producer, Producer C, sent web and flange coupons obtained from the locations shown in Fig. 1 instead of the complete shapes. The coupons were shorter and thinner than the standard ASTM A370 sizes as shown in Fig. 2. Mill test results were provided for one flange coupon from each shape, corresponding to location 6 on Fig. 1.

At UM, the specimens were tested using an MTS machine with a capacity of 600 kips (2670 kN), and elongation of the reduced section was recorded using an extensometer with an 8-inch gauge length. At UWO, the specimens were tested using the Tinius Olsen Deluxe Super "L" Model 120 Universal Testing Machine, with a capacity of 120 kips (530 kN), and elongation of the reduced section were recorded using an MTS extensometer with a 2-inch gauge length. At both laboratories, load, crosshead movement, and elongation data were logged electronically.

Both laboratories controlled the speed of testing as determined by the rate of crosshead separation in accordance with ASTM A370. At UM, the crosshead separation in the elastic region was 0.0175 inches per inch of reduced section per minute, and increased to 0.275 inches per inch of reduced section per minute in the strain-hardening region. At UWO, the loading rates were approximately half these values. Static yield stress readings were obtained for all coupons tested at UM in accordance with the procedure specified in SSRC Technical Memorandum #8.

The capacity of the UWO testing machine limited the maximum test specimen thickness to 1 inch (25 mm) for coupons from the material provided by Producers A and B. Some coupons from the 14-inch column shapes exceeded this limit. It was postulated that, if material strength variation is symmetric about the mid-thickness of the flange or web, milling a specimen on one side to exactly half the original thickness should not impact its average strength properties. Therefore half thickness coupons were fabricated for testing at UWO, and the results were compared with full thickness coupons from the same shape tested at UM. Subsequent analysis indicated no significant difference between the mechanical properties measured on full thickness specimens and those measured on half thickness specimens.

A complete summary of test results for all specimens tested at both UWO and UM is presented in Appendix A.

3. DATA ANALYSIS

In this section, the statistical parameters for the elastic modulus, E, yield strength, F_y, ultimate tensile strength, F_u, strain at commencement of strain hardening, ε_{sh}, and strain at failure, ε_u for the tests conducted in the present investigation are presented and compared with results reported in previous investigations. These various material properties are shown in Fig. 3, which is typical of stress-strain responses recorded. The main statistical quantities investigated are the bias, the ratio of the mean value to the nominal value, and the coefficient of variation, CoV, the ratio of the standard deviation to the mean. The mechanical properties of flange and web material are presented and compared. Inter-laboratory precision statistics are also presented and compared to values published in the literature.

3.1 Elastic Modulus

The statistical parameters for elastic modulus from the 119 specimens tested at UWO are shown in Table 2. The elastic modulus for each coupon was determined by: graphing the recorded load-elongation data; identifying data in the elastic region that were not affected by any initial slip of the specimen in the testing machine grips; and, fitting a straight line to these data by least-squares regression. Scatter plots indicated no discernible trend between the elastic modulus, E, and either the specimen thickness, t, or yield strength, F_y. The final statistical parameters for E, shown in Table 2, based on a nominal value of 29 000 ksi (200 000 MPa), are a bias of 0.993 and a CoV of 0.034. As shown in the table, these parameters are similar to those obtained in previous investigations.

3.2 Yield Strength

The current edition of ASTM A370 (ASTM, 1997) permits the yield strength of steel to be determined by several different methods. It is permissible to report the upper yield point, F_{yu}, which corresponds to the drop of the beam of older testing machines, or the yield plateau stress, which can be determined using the 0.2% offset or 0.5% absolute elongation methods. In this report, the yield plateau stress, F_y, will be adopted as the basis for the definition of the yield strength because not all steels exhibit an upper yield point. At both laboratories, F_{yu} and F_y values were recorded for all specimens tested to quantify the difference between the yield strengths as obtained by these definitions.

Yield strengths reported on mill test certificates correspond to specimens loaded at relatively high strain rates specified in ASTM A370. These must be converted to static yield strengths observed for zero strain rates, F_{ys}, that are more appropriate for design because the majority of loads on structures are essentially static. Conventionally, the static yield strength has been assumed to be four ksi less than the strength observed at normal testing rates (Galambos & Ravindra, 1978; Kennedy & Gad Aly, 1980). Static yield stress readings were obtained for all coupons tested at the UM in accordance with the procedure specified in SSRC Technical Memorandum #8 (Galambos, 1998).

An initial review of the yield strength data indicated that the average strengths reported by UWO were approximately 0.4 ksi less than those reported by UM. As noted previously, the rate of loading at UM was approximately twice that at UWO, which accounts for approximately half of the difference. Before the overall yield strength parameters were computed, the inter-laboratory precision was computed using criteria presented in ASTM E691 (ASTM, 1992) for the 27 shapes that had two flange specimens tested by each lab. The repeatability standard deviation, a measure of the within-laboratory variability, ranged from 0.16 to 2.33 ksi (1.1 to 16.1 MPa) and averaged 0.75 ksi (5.2 MPa). The reproducibility standard deviation, a measure of the between-laboratory variability, ranged from 0.21 to 2.33 ksi (1.5 to 16.1 MPa), and averaged 1.19 ksi (8.2 MPa). The within-laboratory consistency statistic, k, a measure of the relative within-laboratory variability, ranged between 0.163 and 1.413 with an average value of 0.780 for the specimens tested at UWO and between 0.064 and 1.405 with an average of 1.025 for the specimens tested at UM. These values are just less than the average values reported in ASTM E8 (ASTM, 1996) for metal specimens and so were combined to give one large data set. No adjustment was made to account for the rate of loading because the rates adopted at each laboratory conform to ASTM A370.

The statistics for the combined set of flange yield strengths are shown in Table 3. Generally there is remarkable consistency between the parameters obtained in the current investigation and those reported for A992 by Dexter et al. (2000), and for A572 Grade 50 steel by Jaquess and Frank (1999) and Frank and Read (1993). Regression analysis of flange data indicated that the differences of mean strengths for material from Producers A, B and C are statistically significant. However, as shown in the table, the between-producer variation noted in the current study is similar to that observed in past studies.

Table 4 shows the yield strength statistical parameters for the various ASTM Shape Groups investigated. The mean strengths for specimens from Group 2 and three shapes tend to be slightly larger than those from Group 1 and four shapes. However, it is difficult to make strong inferences here because the numbers of specimens from each producer in each group category are not constant, and so any difference between producers may influence any difference between ASTM group categories. Also, Schmidt (2000) documented the use of different chemical compositions for different thickness ranges of steel plate produced to a single specification: it is probable that a similar variation of chemical composition of steel produced for different shape groups may occur in practice. No trend between yield strength and coupon thickness was observed.

Figures 4 and 5 show the frequency histogram and cumulative distribution values of yield strengths, respectively, for the 131 flange coupons tested in the current investigation. Figure 5 also shows the 20 259 data points from the SSPC survey and the lognormal fit corresponding to a mean strength of 55.8 ksi and a CoV of 0.058 as reported by Dexter et al. (2000). The horizontal axis of Fig. 5 is the natural logarithm of the yield strength, and the vertical axis is the Z value from the standard normal distribution, so a population with a lognormal distribution plots as a straight line on the figure. Although the yield strength values do not plot as a straight line, the values in the lower tail with $-2 \leq Z \leq -1$ are linear and close to the distribution reported by Dexter et al. (2000). The data also imply that the distribution may be truncated at $F_y = 50$ ksi, or $ln(F_y) = 3.91$, because the sample CDF is nearly vertical at that point. Thus the distribution reported by Dexter et al. (2000) is very suitable for reliability analysis because it provides an excellent fit to much of the lower tail and, conservatively, neglects any truncation at the specified yield stress value.

The observed yield strengths of the flange coupons were on average very consistent with the values reported on the mill test certificates. For the 131 flange specimens tested, the ratio of observed yield strength to that reported on the mill certificate ranged from 0.91 to 1.18, with a mean value of 1.002 and a coefficient of variation of 0.044.

To investigate the correlation between the flange yield strength and the web yield strength, data were analyzed from 64 specimens where two or three flange coupons and one or two web coupons from the same shape were tested. The ratio of average flange yield strength to web yield strength ranged from 0.85 to 1.21, with a mean of 0.953 and a CoV of 0.064. These findings are consistent with the five per cent allowance considered in past investigations (Galambos & Ravindra, 1978; Kennedy & Gad Aly, 1980) and suggest that producing steel from near-net-shape blooms instead of ingots may not significantly affect this ratio. Jaquess and Frank (1999) reported 95% for most producers, but data from one producer with widely varying flange-to-web yield strength ratios increased the overall average to 98%.

To investigate the relationship between the upper yield point and the yield (plateau) strength, data from all 207 web and flange specimens tested at both laboratories were analyzed. The upper yield point, where it existed, was consistently greater than the yield plateau strength, ranging from 0 to 5.2 ksi (0 to 36 MPa) with a mean difference of 1.8 ksi (12.4 MPa) and a standard deviation of 1.2 ksi (8.0 MPa).

To investigate the difference between the yield strength observed at a typical testing strain rate and the static yield strength, data from 86 web and flange specimens tested at UM were analyzed. On average the static yield strength was 4.41 ksi (30.4 MPa) less than the yield strength observed at typical testing rates, with a standard deviation of 0.59 ksi (4.1 MPa). This average value is very consistent with that assumed in past calibration studies (Galambos & Ravindra 1978; Kennedy & Gad Aly, 1980). It is slightly greater than that for A572 Grade 50 steel where a difference of approximately 2.44 ksi (16.8 MPa) was reported for 101 flange and web specimens (Jaquess & Frank, 1999).

3.3 Ultimate Tensile Strength

An initial review of the ultimate tensile strength data indicated that the strengths reported by UM averaged 2.6 ksi (18 MPa) greater than those reported by UWO. Inter-laboratory precision was again computed for the 27 shapes that had two flange specimens tested by each lab. The repeatability standard deviation ranged from 0.04 to 1.30 ksi (0.3 to 10.7 MPa) and averaged 0.51 ksi (3.5 MPa). The reproducibility standard deviation ranged from 1.30 to 2.68 ksi (8.9 to 18.5 MPa) and averaged 1.19 ksi (8.2 MPa). The within-laboratory consistency statistic, *k*, ranged between 0.065 and 1.315with an average value of 0.693 for the specimens tested at UWO and between 0.520 and 1.413 with an average of 1.143 for the specimens tested at UM. The repeatability is less than the average value for metal specimens reported in ASTM E8 (ASTM, 1996) but the average reproducibility exceeds the average value in ASTM E8 by a factor of approximately two. We are unable to find any rational explanation for this difference.

The data from the tests at UM and UWO are therefore presented separately and together in Table 5. Despite any difference between the UM and UWO results, there is again general consistency between the parameters obtained for the combined data sets from the current investigation and those reported for A992 by Dexter et al. (2000), and for A572 Grade 50 steel by Jaquess and Frank (1999) and Frank and Read (1993). Regression analysis indicated that the differences of the mean ultimate tensile strengths for material from Producers A, B and C are statistically significant. However, as shown in the table, the between-producer variation noted in the current study is similar to that observed in past studies.

Figures 6 and 7 show the frequency histogram and sample cumulative distribution, respectively, of ultimate tensile strengths for the specimens tested at UM and UWO. It also shows the ultimate tensile strengths of the 20 259 coupons from the SSPC survey and the lognormal fit corresponding to a mean strength of 73.3 ksi and a CoV of 0.043 as reported by Dexter et al. (2000). The data from the current study are not lognormal, although a lognormal distribution can be readily fitted to the lower four-fifths of the data, say for $Z \leq 1$. The upper fifth of the distribution deviates from lognormal, perhaps due to the effect of combining material from different producers. The distribution reported by Dexter et al. (2000) has a slope (and therefore a CoV) that is consistent with the data from the present investigation, and has ordinates that are in the order of two per cent larger than suggested by the data.

The observed ultimate tensile strengths of the flange coupons were on average very consistent with the values reported on the mill test certificates. For the 131 flange specimens tested, the ratio of observed ultimate tensile strength to that reported on the mill certificate ranged from 0.91 to 1.08, with a mean value of 0.996 and a coefficient of variation of 0.030.

To investigate the correlation between the ultimate tensile strengths of the flange and the web, data were analyzed from 64 specimens where two or three flange coupons and one or two web coupons from the same shape were tested. The ratio of average flange ultimate tensile strength to web ultimate tensile strength ranged from 0.93 to 1.17, with a mean of 0.986 and a CoV of 0.037.

The ratio of the yield to ultimate tensile strength, *Y/T*, was also investigated. For the 131 flange coupons tested, the *Y/T* ratio had a mean value of 0.768, a standard deviation of 0.026, and a maximum value of 0.830. For the 76 web coupons tested, the mean *Y/T* ratio was 0.789, with a maximum of 0.862 and a standard deviation of 0.039. Six web coupons exceeded the limit of 0.85 specified for flanges in ASTM A992, but not by much.

3.4 Strains

Table 6 summarizes the strain at the commencement of strain hardening for the flange and web specimens tested at UWO and UM. The coefficients of variation are reasonably stable at about 0.3 as shown. A statistically significant relationship was noted between the strain at the onset of strain hardening and the thickness of the coupon, as shown in Fig. 8. The figure also illustrates the scatter of the data, which made analysis of other trends in the data difficult.

Table 7 summarizes the ultimate strain values for all 207 specimens tested. The average ultimate strains for steel supplied by Producer B were significantly less than those for steel supplied by Producers A and C, and there was a slight negative correlation between the coupon thickness and the ultimate strain, as shown in Fig. 9.

Table 8 summarizes the percent elongation at failure, which on average was significantly greater for steel supplied by Producer C than those for steel supplied by Producers A and B. This difference may be due in part to the different specimen geometries shown in Fig. 2. Also elongations were measured using a two-inch gauge length for specimens provided by Producer C, and were measured using an eight-inch gauge length for coupons from the steel provided by Producers A and B. There was no significant correlation between the percent elongation at failure and the coupon thickness, as shown in Fig. 10.

4. PRELIMINARY RELIABILITY ANALYSIS

Commentary Section A5 of the AISC LRFD specification (AISC, 1999) states that the point at which the LRFD criteria are calibrated to the previous Allowable Stress Design (ASD) criteria is $L/D = 3$ for braced compact beams in flexure and tension members at yield. For the resistance factor, ϕ, equal to 0.9, the implied reliability index β at this calibration point is approximately 2.6 for members. The following equation, numbered A-C5-3 in the commentary, is used to define β:

$$\beta = \frac{ln(R_m / Q_m)}{\sqrt{V_R^{\,2} + V_Q^{\,2}}} \tag{1}$$

where R_m and V_R are the mean value and coefficient of variation of the resistance, respectively, and Q_m and V_Q are the mean value and coefficient of variation of the total load effect. In this section, new resistance distributions based on the material properties of steel presented in Section 3 will be derived and reliability indices corresponding to $\phi =$ 0.90 and 0.95 will be computed.

ASCE 7-98 (ASCE 2000) specifies a dead load factor of 1.2 and a live load factor of 1.6 for the basic combination of dead plus live load. To assess the impact of changing the resistance factor, Eq. (1) was rearranged to give the reliability index, β, for a given live-to-dead load ratio, L/D and ϕ as follows:

$$\beta = \frac{1}{\sqrt{V_R^2 + V_Q^2}} \ln\left[\frac{R_m}{\phi R_n}\left(\frac{1.2 + 1.6(L/D)}{(D_m/D) + (L_m/L)(L/D)}\right)\right] \tag{2}$$

where D_m and L_m are the mean dead and live load effects, respectively, and R_n is the nominal resistance.

Statistical parameters for the effects of dead load and live load due to use and occupancy were obtained from the literature. The dead load effect was assigned bias $D_m/D = 1.05$ and $V_D = 0.10$ in accordance with Ellingwood et al. (1980). An equivalent lognormal distribution was fit to the upper tail of the Gumbel distribution for maximum office live load in a 50-year reference period reported by Ellingwood and Culver (1977), with resulting parameters $L_m/L = 0.93$ and $V_L = 0.288$. (As a check, analyses were repeated with $L_m/L = 1.0$ and $V_L = 0.25$ as reported by Ellingwood et al. (1980) and similar β values were obtained).

Three sets of reliability analyses were carried out, using the resistance parameters shown in Table 9. The resistance factors used in the original calibration did not include any factor for discretization. This is conservative (e.g. Technical Memorandum #10 in Galambos, 1998), so the current calibration check has been carried out for two cases: one neglecting discretization and the other considering it.

The effect of discretization is a factor in steel design that generally improves the resistance statistics. When a designer chooses a section with factored resistance greater than or equal to the sum of the factored load effects, extra capacity is usually provided because only discrete shapes are available to resist the continuum of applied load effects.

For example, the light dotted line with markers in Fig. 11 shows the ratio of the factored braced compact beam bending resistance to the factored demand versus the factored demand for 174 W shapes listed in the beam selection tables of the AISC *LRFD Manual of Steel Construction* (AISC, 1993). The vertical line that defines the left side of each peak represents a transition point where the capacity of a shape becomes insufficient and the next larger shape, with excess capacity, must be selected. For the range of capacities shown, the average discretization factor is 1.027 with a coefficient of variation of 0.022. If the set of possible shapes is reduced to the 47 most efficient shapes that provide the necessary capacity and have the least weight, represented by the heavy line in Fig. 11, the average discretization factor is 1.051 with a coefficient of variation of 0.043. These values represent an upper bound on the discretization effect, and so have been adopted for one of the current calibration checks, as shown in Table 9.

The resistance parameters shown in Table 9 under the heading "Original Calibration" are as presented in Appendix C of Ellingwood et al. (1980). The material factor represents the static yield strength of the flanges of rolled W-shapes (Galambos & Ravindra, 1978). The mean value of the professional factor, 1.02, seems low if significant strain hardening can occur in the flanges of a braced compact beam, and values as high as 1.10 have been adopted for calibration of other steel resistance factors (Kennedy & Gad Aly, 1980; Schmidt & Bartlett, 2001b).

The resistance parameters shown in Table 9 for the current calibration were selected recognizing that the main focus of the current study is the impact of new material properties on the resistance factor. The statistical parameters for geometric properties, in this case the plastic section modulus, Z, are as reported in recent studies

(Schmidt & Bartlett, 2001a; Jaquess & Frank, 1999) of geometric tolerances in rolled W-shape production. The material property statistics based on the SSPC study data (Dexter et al., 2000): the mean yield strength reported for 20 295 ASTM A992 steel coupons of 55.8 ksi (Table 3) has been reduced by 4.4 ksi (Section 3.2) to give an equivalent mean static yield strength of 51.4 ksi and an associated bias coefficient of 1.028. The uncertainty of the conversion to static yield strength has been assumed negligible, so the coefficient of variation of the static yield strength equals the value reported in the SSPC study, 0.058.

The variation of the reliability index, β, with the live-to-dead load ratio, L/D, is shown in Fig. 12. The lower boundary of the shaded areas on the figure represent the β values for the case where discretization is neglected and the upper boundary represents the case where discretization is included. The range of β values computed for $\phi = 0.95$ straddle the set of values computed using the resistance parameters adopted for the original calibration. If ϕ is maintained at 0.90, the range of β values fall above that obtained using the resistance parameters from the original calibration.

At the calibration point of $L/D = 3$, the β value computed using the resistance parameters from the original calibration is 2.52. For the new resistance parameters, the corresponding β values range between 2.61 and 2.77 for $\phi = 0.9$ and between 2.37 and 2.54 for $\phi = 0.95$.

Thus the new statistical parameters for A992 steel give slightly higher reliability indices than those adopted for the original calibration, but they are insufficient by themselves to permit increasing the resistance factor from 0.90 to 0.95 unless the full beneficial effect of the discretization factor is assumed. Further studies might be carried out to review the professional factors for steel shapes and to broaden the investigation to consider other load combinations and resistance categories. At this stage it can simply be stated that A992 steel has smaller bias coefficients and smaller coefficients of variation compared to the parameters for A36 steel used in the original calibration, and the new parameters have increased the reliability index slightly.

5. SUMMARY AND CONCLUSIONS

This report summarizes the mechanical properties of ASTM A992 steel as determined by tests of 207 flat-strap tensile test specimens at the University of Minnesota and the University of Western Ontario carried out in accordance with ASTM A370. Samples were obtained from 38 heats of steel from eight different shapes provided by three producers. The objectives of the study were to quantify statistical parameters for the mechanical properties of A992 steel, investigate the correlation of the strengths of web and flange material, verify the accuracy of information reported on mill test certificates, quantify the rate-of-loading effect on yield strength, compute inter-laboratory precision statistics, and carry out reliability-based analyses to investigate the necessity of updating the resistance factor for steel in the AISC LRFD Specification (AISC, 1999).

The conclusions of the study are as follows:

1. The elastic modulus of A992 steel with a nominal value of 29 000 ksi has a bias of 0.993 and a coefficient of variation of 0.024. These parameters are similar to those observed in previous investigations involving A36 and A572 Grade 50 material.

2. The yield strength of 131 flange coupons, corresponding to rates of loading specified in ASTM A370, averaged 55.0 ksi (379 MPa) with a standard deviation of 3.1 ksi (21.4 MPa). The differences between the mean strengths of steel provided by the three producers are statistically significant. These findings are consistent with recent studies by others of A992 (Dexter et al. 2000) and A572 Grade 50 (Jacques & Frank, 1999) steels. The lower tail of the data is particularly well represented by the lognormal distribution with a bias of 1.116 and a coefficient of variation of 0.058 reported by Dexter et al. (2000).
3. The ratio of average flange yield strength to average web yield strength had a mean of 0.953 and a coefficient of variation of 0.064. These findings are consistent with the 5% allowance considered in past investigations (Galambos & Ravindra, 1978; Kennedy & Gad Aly, 1980) and suggest that producing steel from beam blanks, blooms, or near-net-shapes instead of ingots may not significantly affect this ratio.
4. The difference between the static yield strength and the yield strength recorded at testing rates specified in ASTM A370 averaged 4.41 ksi (30.4 MPa), with a standard deviation of 0.59 ksi (4.1 MPa). This average value is very consistent with that assumed in past calibration studies (Galambos & Ravindra 1978; Kennedy & Gad Aly, 1980).
5. The ultimate tensile strength of 131 flange coupons averaged 71.6 ksi (494 MPa) with a standard deviation of 3.7 ksi (25.5 MPa). The differences between the mean ultimate tensile strengths of steel provided by the three producers are statistically significant. These findings are reasonably consistent with recent

studies by others of A992 (Dexter et al., 2000) and A572 Grade 50 (Jacquess & Frank, 1999) steels.

6. The ratio of the yield to ultimate tensile strength averaged 0.768, with a standard deviation of 0.026 for the flange coupons and averaged 0.789, with a standard deviation of 0.039. Six web coupons and no flange coupons exceeded the limit of 0.85 specified for flange coupons in ASTM A992.
7. On average, values reported on mill certificates corresponded closely to the material properties determined in the investigation. The ratio of the observed yield strength to that reported on the mill certificate ranged from 0.91 to 1.18, with a mean value of 1.002 and a coefficient of variation of 0.044. The ratio of observed ultimate tensile strength to that reported on the mill certificate ranged from 0.91 to 1.08, with a mean value of 0.996 and a coefficient of variation of 0.030.
8. The resistance parameters for a braced compact A992 steel beam are a bias of 1.049 and a coefficient of variation of 0.090 if the discretization factor is neglected, or a bias of 1.101 and a coefficient of variation of 0.100 if the discretization factor is considered.
9. At the calibration point of $L/D = 3$ used to calibrate the AISC LRFD specification, the β values for a braced compact A992 beam range between 2.61 and 2.77 for $\phi = 0.9$ and between 2.37 and 2.54 for $\phi = 0.95$. The target β value computed at this calibration point using the resistance parameters from the original calibration is 2.52. Thus the new statistical parameters for A992 steel give slightly higher reliability indices than those adopted for the original calibration, but they are

insufficient by themselves to permit increasing the resistance factor from 0.90 to 0.95 unless the full beneficial effect of the discretization factor is assumed.

10. A992 steel has smaller bias coefficients and smaller coefficients of variation compared to the parameters for A36 steel used in the original calibration that have increased the reliability indices slightly. However, an increase of resistance factor from 0.90 to 0.95 is not recommended without further study.

6. REFERENCES

American Institute of Steel Construction (1999), "Load and resistance factor design specification for steel buildings," American Institute of Steel Construction, Chicago.

American Institute of Steel Construction (1993), "LRFD manual of steel construction, 2nd edition," American Institute of Steel Construction, Chicago.

American Society of Civil Engineers (2000), "Minimum design loads for buildings and other structures (ASCE 7-98)," ASCE, Reston, Virginia.

American Society for Testing and Materials (1997), "Standard test methods and definitions for mechanical testing of steel products," ASTM Standard A370-97a, American Society for Testing and Materials, West Conshohocken, PA.

American Society for Testing and Materials (1996), "Standard testing methods for tension testing of mechanical materials," ASTM Standard E8-96a, American Society for Testing and Materials, West Conshohocken, PA.

American Society for Testing and Materials (1992), "Standard practice for conducting an interlaboratory study to determine the precision of a test method,". ASTM Standard E691-92, American Society for Testing and Materials, West Conshohocken, PA.

Chernenko, D. E., and Kennedy, D. J. L. (1991), "An analysis of the performance of welded wide flange columns," Canadian Journal of Civil Engineering, Vol. 18, pp. 537-555.

Dexter, R. J., Graeser, M., Saari, W. K., Pascoe, C., Gardner, C. A., and Galambos, T. V. (2000), "Structural shape material property survey," Technical report for Structural Shape Producers Council, University of Minnesota, Minneapolis, MN.

Ellingwood, B. R., and Culver, C. (1977), "Analysis of live loads in office buildings," Journal of the Structural Division, American Society of Civil Engineers, Vol. 103, No. ST8, pp. 1551-1560.

Ellingwood, B. R., Galambos, T.V., MacGregor, J. G., and Cornell, C. A. (1980), "Development of a probability-based load criterion for American National Standard A58," NBS Special Publication 577, National Bureau of Standards, United States Department of Commerce, Washington, D.C.

Galambos, T.V. (editor) (1998), "Guide to stability design criteria for metal structures (5th edition)," John Wiley & Sons, Inc., New York, NY.

Galambos, T. V. and Ravindra, M. K. (1978), "Properties of steel for use in LRFD," Journal of the Structural Division, American Society of Civil Engineers, Vol. 104, No. ST9, pp. 1459-1468.

Jaquess, T. K., and Frank, K. H. (1999), "Characterization of the material properties of rolled sections," Technical Report for SAC Joint Venture, University of Texas at Austin, Austin, Texas.

Kennedy, D. J. L. and Gad Aly, M. (1980), "Limit states design of steel structures—performance factors," Canadian Journal of Civil Engineering, Vol. 7, pp. 45-77.

Schmidt, B. J. (2000), "Review of the resistance factor for steel," MESc thesis, University of Western Ontario, London.

Schmidt, B. J., and Bartlett, F. M. (2001a - in press), "Review of resistance factor for steel: data collection," Accepted for publication in Canadian Journal of Civil Engineering, 13 November 2001.

Schmidt, B. J., and Bartlett, F. M. (2001b - in press), "Review of resistance factor for steel: resistance distributions and resistance factor calibration," Accepted for publication in Canadian Journal of Civil Engineering, 13 November 2001.

Table 1: Scope of Testing Program

Shape Designation		Size		No. of Coupons Tested at			
				UWO		UM	
US	Metric	Group	No.	FL	Web	FL	Web.
6x25	150x37	1	3	5	3	6	3
8x31	200x46	1	6	12	6	12	6
12x65	310x97	2	4	9	5	6	3
14x176	360x262	3	5	11(8)[a]	6	8	4
14x257	360x382	4	7	8(8)	10(4)	6(6)	4
24x76	610x113	2	3	5	3	6	3
30x99	760x147	2	5	12	7	6	3
36x150	920x223	2	5	11	6	8	4
Total			38	73	46	58	30

[a] – number of half-thickness specimens shown in parentheses

Table 2: Elastic Modulus Parameters for Nominal Value of 29 000 ksi

Source	n	Bias	CoV
Current Investigation	119	0.993	0.034
Galambos & Ravindra (1978)[a]	197	1.01 to 1.02	0.010 to 0.014
Galambos (1998)[b]	341	1.036	0.045
Chernenko & Kennedy (1990)	7	1.038	0.026

[a] – tension and compression coupon specimens

[b] – combined results for all data presented by Galambos and Ravindra (1978)

Table 3: Flange Yield Strength Parameters for Nominal Value of 50 ksi

Source	Producer	Grade	n	$\bar{x}$ (ksi)	s (ksi)	Bias	CoV
Current Investigation	A	A992	106	54.1	2.3	1.082	0.043
	B	A992	10	61.5	2.1	1.231	0.034
	C	A992	15	56.9	1.9	1.138	0.033
	overall	A992	131	55.0	3.1	1.100	0.056
Dexter et al. (2000)	D	A992	4 942	52.0	2.2	1.04[a]	0.042
	E	A992	10 794	56.0	2.9	1.12	0.052
	F	A992	2 873	58.0	2.7	1.16	0.046
	G	A992	987	58.5	3.3	1.17[a]	0.056
	H	A992	407	52.5	1.9	1.05[a]	0.037
	overall	A992	20 295	55.8	3.2	1.116	0.058
Jaquess & Frank (1999)	I	A572	4	49.0	0.6	0.980	0.013
	J	A572	19	52.5	1.7	1.050	0.033
	K	A572	14	54.8	2.2	1.097	0.040
	L	A572	22	56.8	4.6	1.136	0.081
	overall	A572	59	54.4	3.9	1.088	0.071
Frank & Read (1993)	overall	A572	13 536	54.9[b]	4.9[b]	1.097	0.0089

[a] – value shown is 0.97 x reported upper yield point value

[b] – value shown is 0.95 x reported web yield strength value

Table 4: Flange Yield Strength for Various Shape Groups

ASTM Group	n	$\bar{x}$ (ksi)	s (ksi)	Bias	CoV
1	35	54.0	1.3	1.08	0.025
2	63	55.4	3.2	1.11	0.058
3	19	56.4	3.9	1.13	0.069
4	14	53.7	3.4	1.07	0.064

Table 5: Flange Ultimate Tensile Strength Parameters for Nominal Value of 65 ksi

Source	Producer	Grade	n	$\bar{x}$ (ksi)	s (ksi)	Bias	CoV
Current Investigation: UM	A, B	A992	58	72.4	3.3	1.113	0.045
Current Investigation: UWO	A, B, C	A992	73	71.0	3.8	1.092	0.054
Current Investigation (combined)	A	A992	106	70.4	2.5	1.084	0.036
	B	A992	10	80.4	2.0	1.238	0.025
	C	A992	15	73.8	1.7	1.135	0.023
	overall	A992	131	71.6	3.7	1.101	0.051
Dexter et al. (2000)	D	A992	4 942	72.8	2.5	1.12	0.035
	E	A992	10 794	72.2	2.9	1.11	0.040
	F	A992	2 873	76.7	2.3	1.18	0.030
	G	A992	987	76.7	3.6	1.18	0.047
	H	A992	407	73.5	2.4	1.13	0.032
	overall	A992	20 295	73.5	3.2	1.13	0.044
Jaquess & Frank (1999)	I		4	70.1	0.6	1.079	0.008
	J		19	71.0	2.4	1.092	0.034
	K		16	73.0	1.9	1.123	0.027
	L		22	73.3	3.5	1.128	0.047
	overall	A572	61	72.3	2.9	1.113	0.040
Frank & Read (1993)	overall	A572	13 536	75.6	6.2	1.163	0.082

Table 6: Strain at Commencement of Strain Hardening

	n	$\overline{x}$ ($\mu\varepsilon$)	s ($\mu\varepsilon$)	CoV
Flange	131	22290	6324	0.284
Web	76	24875	7352	0.296
Overall	207	23239	6817	0.293

Table 7: Ultimate Strain

	n	$\overline{x}$ ($\mu\varepsilon$)	s ($\mu\varepsilon$)	CoV
Flange	131	158745	15668	0.099
Web	76	151452	17196	0.114
Overall	207	156067	16583	0.106

Table 8: Elongation at Failure

		n	$\bar{x}$ ($\mu\varepsilon$)	s ($\mu\varepsilon$)	CoV
Flange	Producers A + B	57	0.289	0.027	0.092
	Producer C	15	0.443	0.030	0.067
	Combined	72	0.321	0.069	0.215
Web	Producers A + B	30	0.262	0.035	0.134
	ProducerC	16	0.403	0.071	0.176
	Combined	46	0.311	0.084	0.270
Overall	Combined	118	0.317	0.075	0.236

Table 9: Resistance Parameters for Reliability Analysis

Factor	Original Calibration		Current Calibration			
			No Discretization		With Discretization	
	bias	CoV	Bias	CoV	Bias	CoV
Geometric	1.00	0.05	1.00	0.034	1.00	0.034
Material	1.05	0.05	1.028	0.058	1.028	0.058
Professional	1.02	0.06	1.02	0.06	1.02	0.06
Discretization	1.00	0.00	1.00	0.00	1.05	0.043
Total	1.07	0.127	1.049	0.090	1.101	0.100

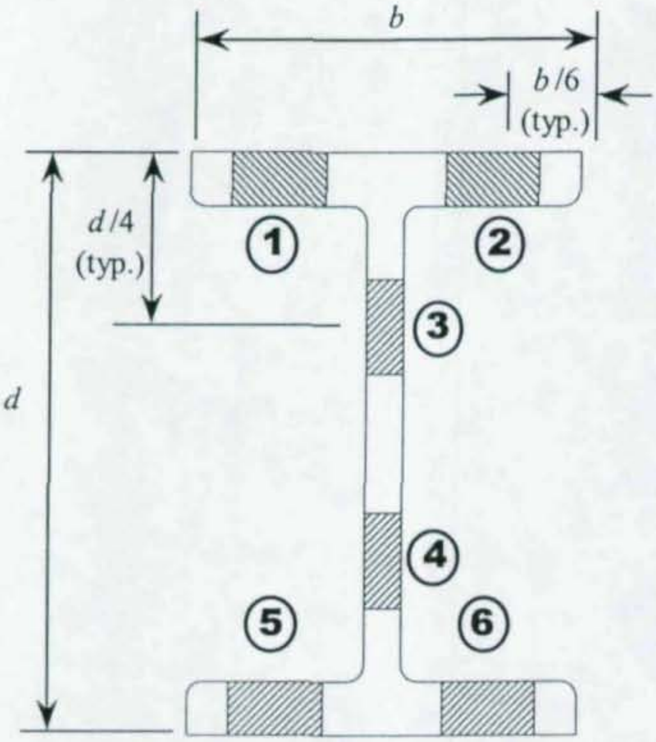

Figure 1: Coupon Locations.

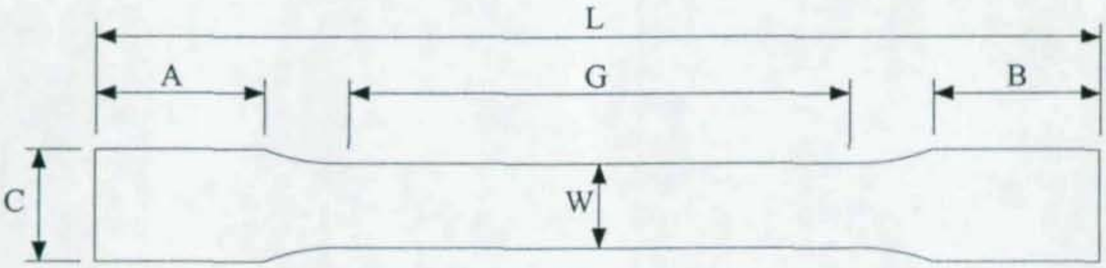

Dimension	Producer A	Producer B	Producer C
A	3 in. (75 mm)	3 in. (75 mm)	4 in. (100 mm)
B	3 in. (75 mm)	3 in. (75 mm)	3.6 in (90 mm)
C	2 in. (50 mm)	2 in (50 mm)	1.5 in. (40 mm)
G	9 in. (225 mm)	9 in. (225 mm)	3.6 in (90 mm)
L	18 in. (450 mm)	18 in. (450 mm)	12 in. (300 mm)
W	1.5 in. (40 mm)	1.5 in. (40 mm)	0.75 in. (19 mm)

Figure 2: Coupon Geometry

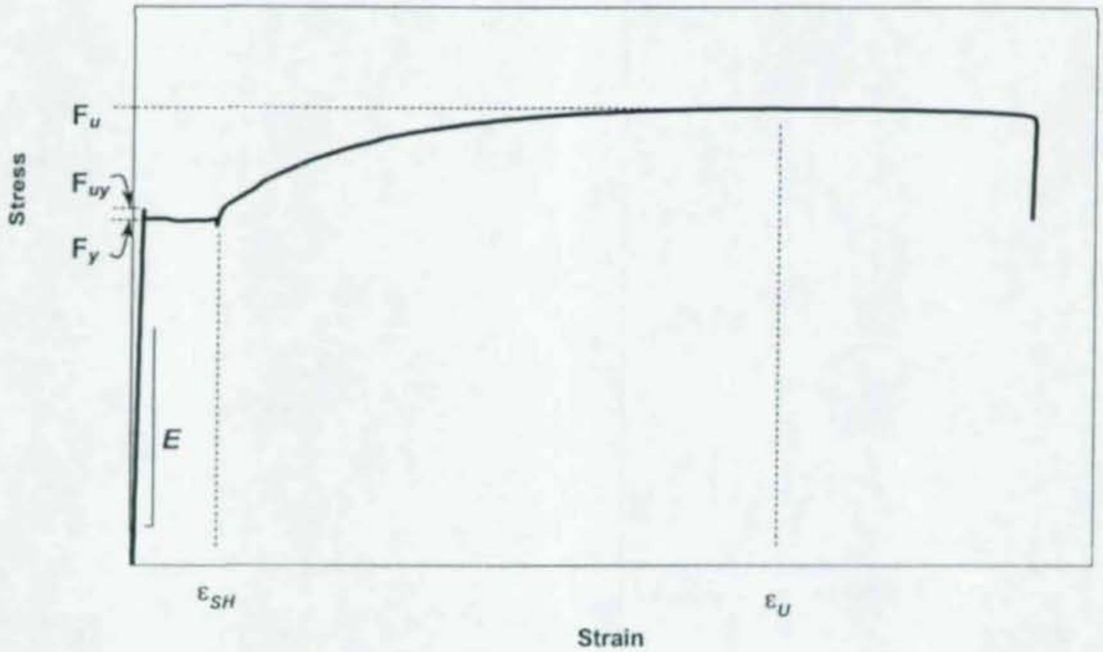

Figure 3: Typical Stress-Strain Curve for Steel

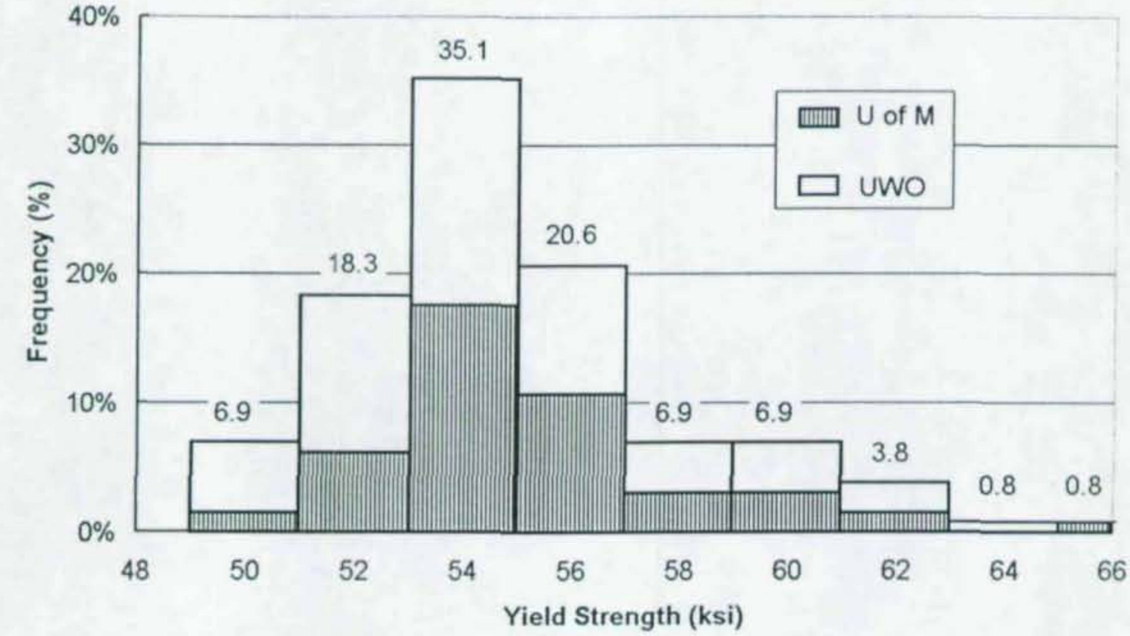

Figure 4: Histogram of Yield Strength Data

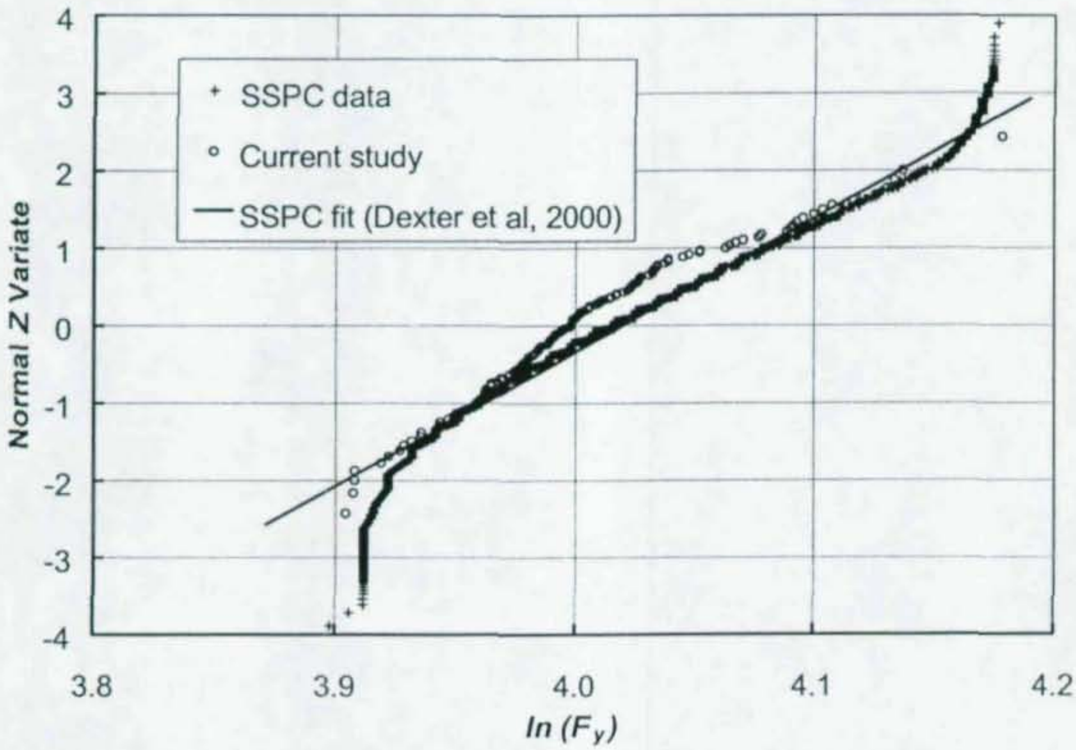

Figure 5: CDF for Yield Strength Data

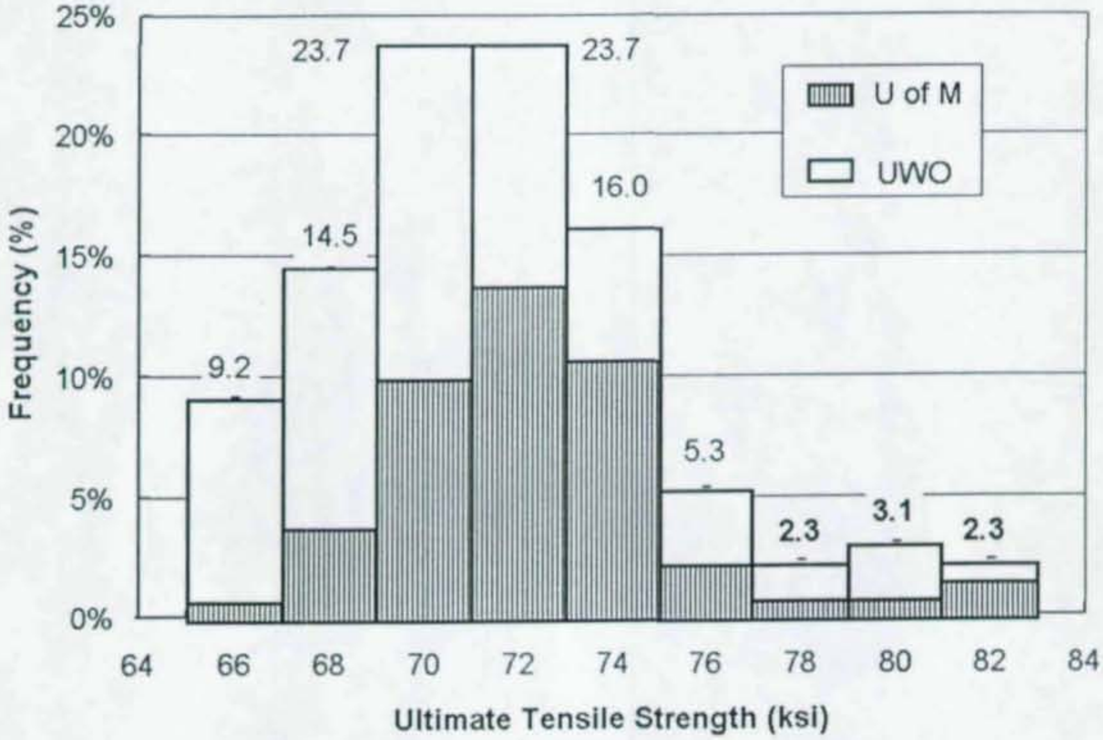

Figure 6: Histogram of Ultimate Tensile Strength Data

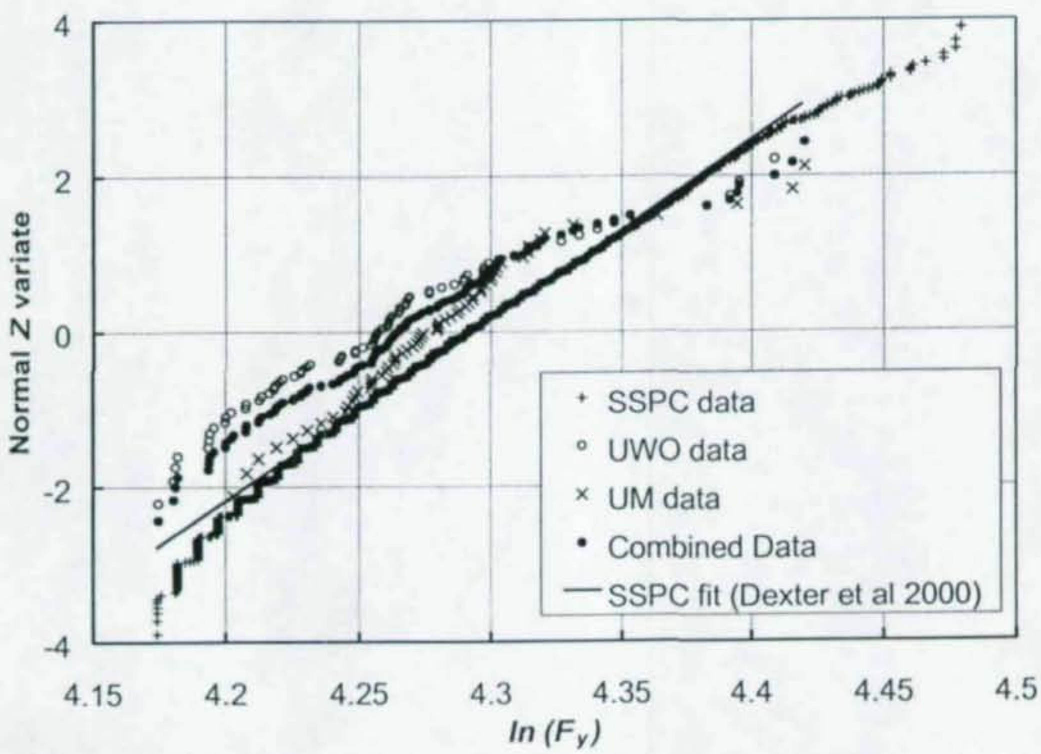

Figure 7: CDF for Ultimate Tensile Strength Data

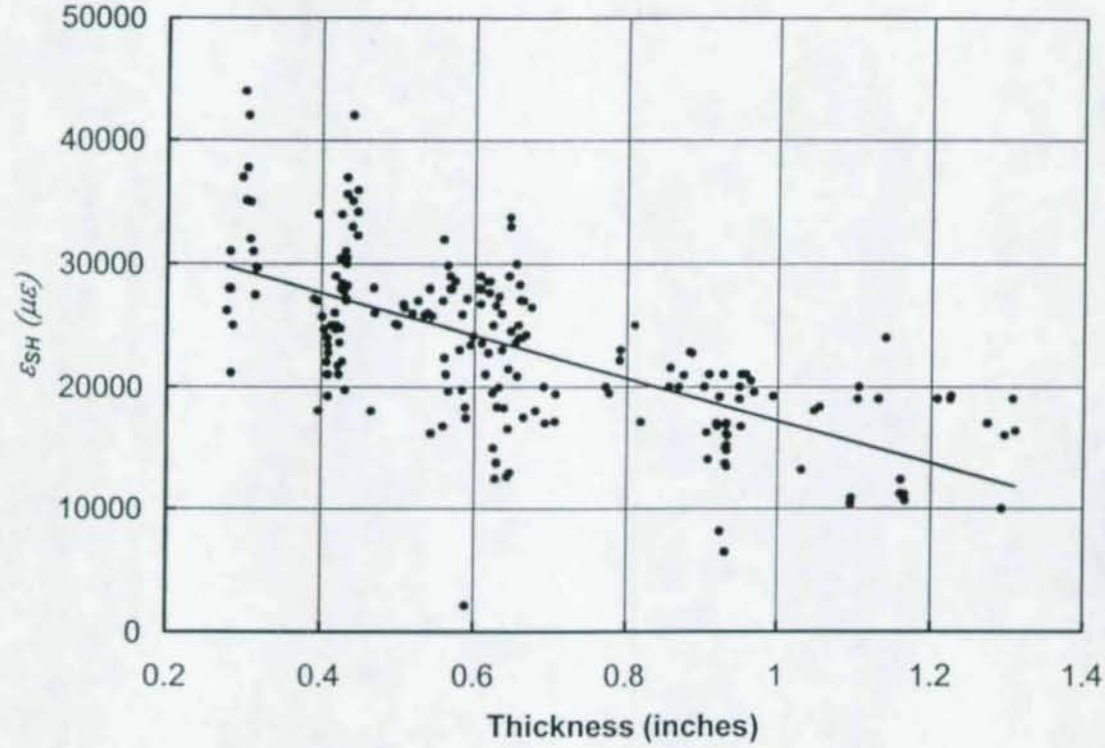

Figure 8: Strain at Onset of Strain Hardening versus Coupon Thickness

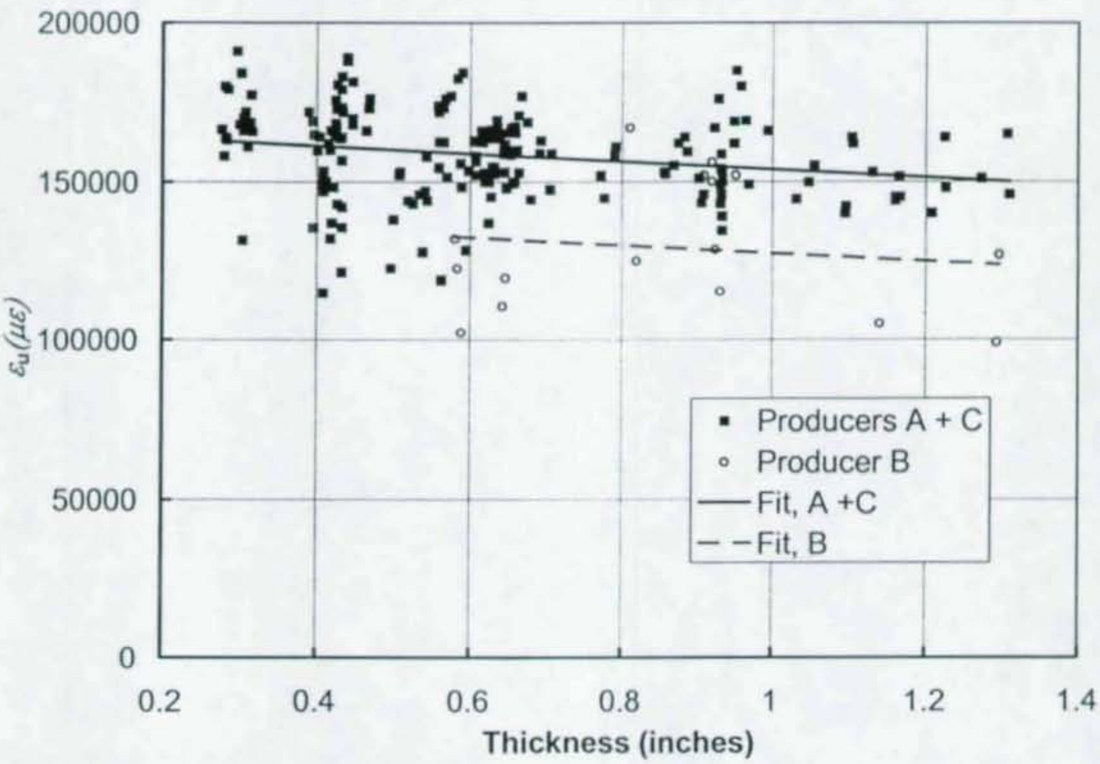

Figure 9: Ultimate Strain versus Coupon Thickness

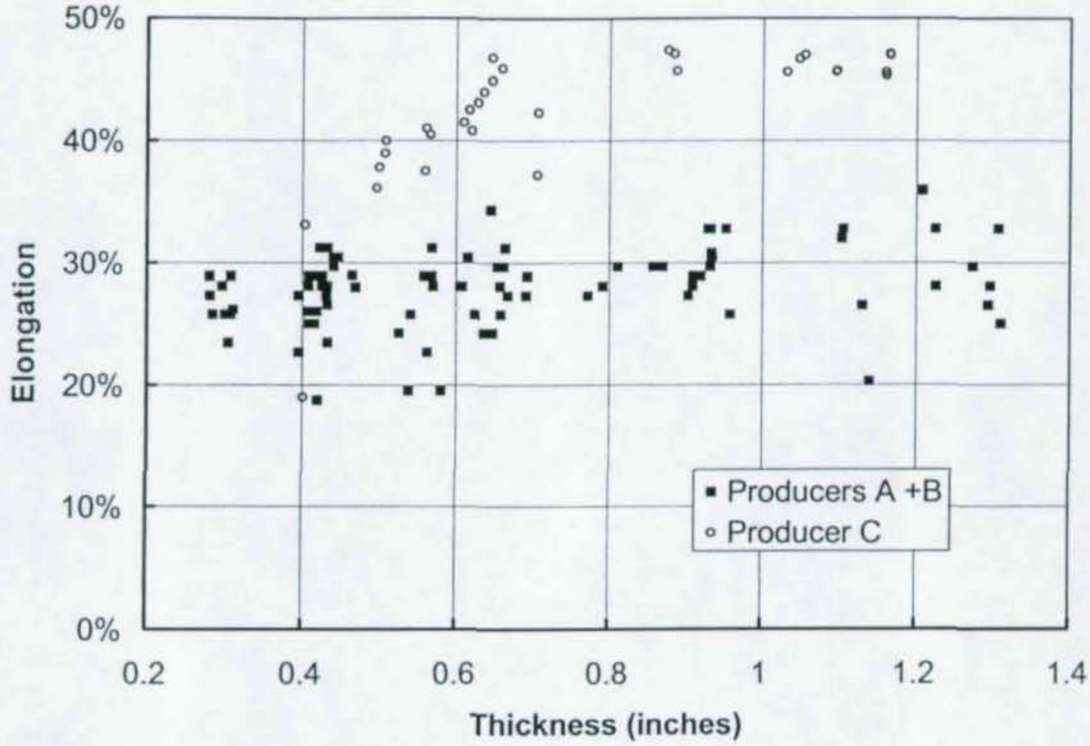

Figure 10: Elongation at Failure versus Coupon Thickness

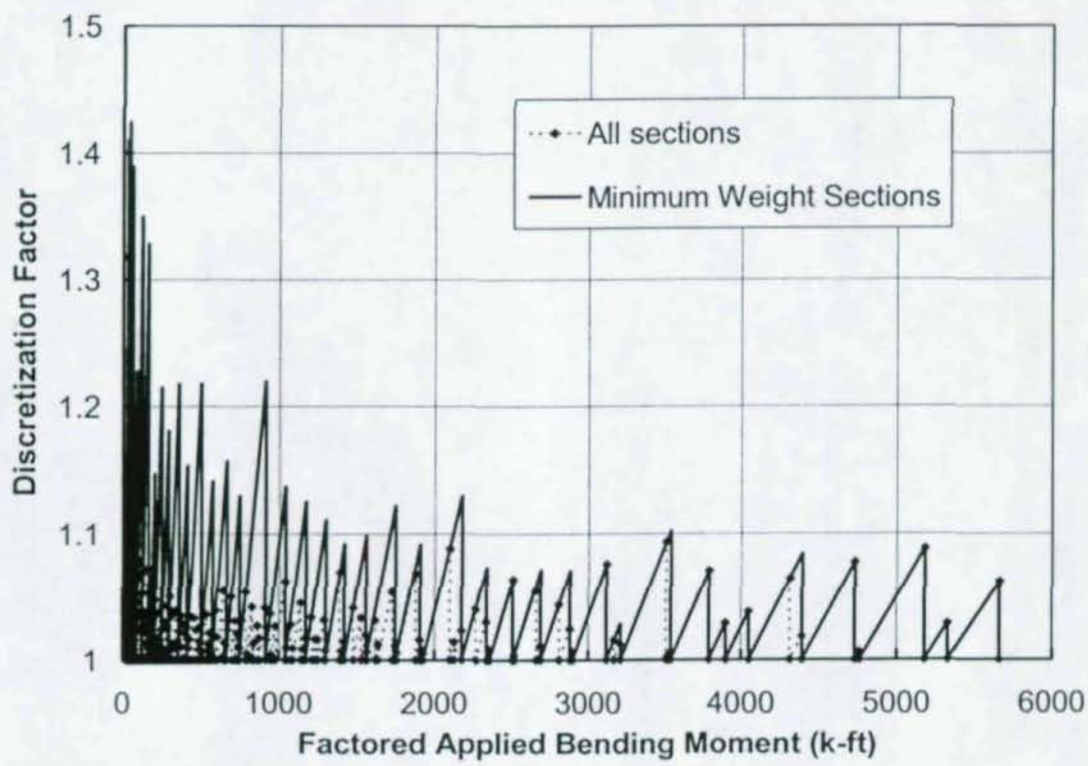

Figure 11: Discretization Factor for Braced Compact Beams

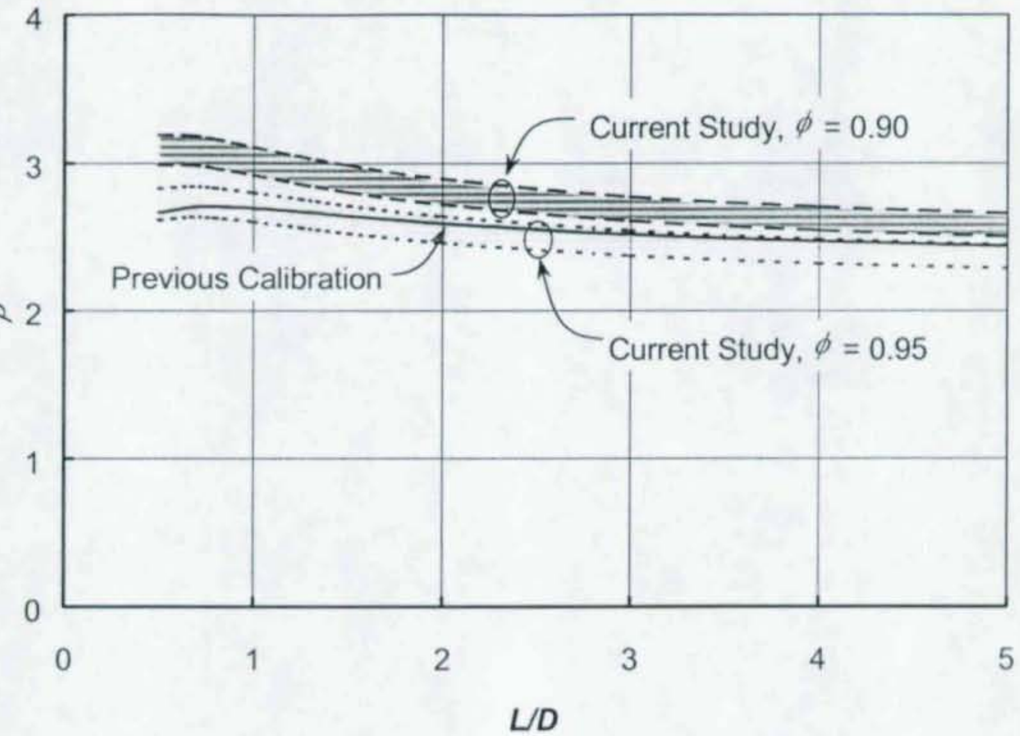

Figure 12: Variation of β with L/D, Braced Compact Beams

APPENDICES

Appendix A: Tabular Summary of All Test Results

The headings and abbreviations in this table are as follows:

- Loc: coupon location, flange (FL) or web (Web)
- Lab: testing lab, Minnesota (M) or Western Ontario (WO)
- t: specimen thickness, full (f) or milled to half thickness (H)
- F_{yu}: upper yield point
- F_y: yield strength (yield plateau stress)
- F_{ys}: yield strength at static rate of loading
- F_{ym}: yield strength reported on mill test certificate
- F_u: ultimate tensile strength
- F_{um}: ultimate tensile strength reported on mill test certificate
- E: elastic modulus
- ε_{sh}: strain at onset of strain hardening
- ε_u: elongation at fracture

Shape	Cpn	Loc.	Lab	t	F_{yu} (ksi)	F_y (ksi)	F_{ys} (ksi)	F_{ym} (ksi)	F_u (ksi)	F_{um} (ksi)	E (ksi)	ε_{sh} ($\mu\varepsilon$)	ε_u ($\mu\varepsilon$)
6x25	D1	FL	M	f	54.1	54.1	48.4	56.3	67.5	68.2	29690	33000	189000
	D2	FL	WO	f	53.9	53.7	—	56.3	65.4	68.2	28270	28443	180548
	D3	FL	WO	f	53.3	52.9	—	56.3	66.3	68.2	28054	35660	173414
	D4	FL	M	f	55.2	54.0	49.3	56.3	68.4	68.2	25082	42000	188000
	D5	Web	M	f	55.2	54.1	48.9	—	68.5	—	34873	37000	191000
	D6	Web	WO	f	55.5	53.0	—	—	66.0	—	30016	35120	184212
6x25	E1	FL	M	f	54.6	53.2	48.6	55.4	66.9	68.3	26881	27000	179000
	E2	FL	WO	f	53.0	51.6	—	55.4	65.0	68.3	29437	32294	181460
	E3	FL	WO	f	53.4	51.9	—	55.4	65.4	68.3	30607	35119	187921
	E4	FL	M	f	54.3	53.7	48.4	55.4	67.2	68.3	23517	34000	173000
	E5	Web	M	f	56.2	55.1	50.7	—	67.9	—	25621	44000	168000
	E6	Web	WO	f	57.7	57.4	—	—	66.7	—	29611	37784	131663

Shape	Cpn	Loc.	Lab	t	F_{yu} (ksi)	F_y (ksi)	F_{ys} (ksi)	F_{ym} (ksi)	F_u (ksi)	F_{um} (ksi)	E (ksi)	ε_{sh} ($\mu\varepsilon$)	ε_u ($\mu\varepsilon$)
6x25	F1	FL	M	f	55.7	55.4	50.3	56.4	69.1	68.9	30479	36000	170000
	F2	FL	WO	f	53.9	51.9	—	56.4	65.5	68.9	28576	34237	167981
	F3	FL	WO	f	—	—	—	56.4	—	68.9	—	—	—
	F4	FL	M	f	56.3	55.8	50.9	56.4	70.1	68.9	22077	37000	183000
	F5	Web	M	f	58.2	57.2	53.0	—	71.8	—	24954	42000	166000
	F6	Web	WO	f	56.8	55.2	—	—	67.4	—	30603	35076	170029
8x31	D1	FL	M	f	55.9	55.1	50.3	54.7	69.9	68.7	23885	25000	162000
	D2	FL	WO	f	55.5	52.5	—	54.7	67.2	68.7	29676	23343	147313
	D3	FL	WO	f	54.2	52.3	—	54.7	66.7	68.7	29119	24730	168355
	D4	FL	M	f	56.1	54.8	49.8	54.7	70.5	68.7	27398	22000	149000
	D5	Web	M	f	56.6	55.6	51.4	—	69.8	—	27114	32000	169000
	D6	Web	WO	f	55.4	51.7	—	—	65.9	—	28252	29732	177390
8x31	E1	FL	M	f	56.1	55.6	51.2	56.1	71.0	69.6	24074	26000	160000
	E2	FL	WO	f	53.5	53.2	—	56.1	68.8	69.6	29545	19229	153277
	E3	FL	WO	f	54.0	54.0	—	56.1	68.0	69.6	29845	23592	164555
	E4	FL	M	f	56.8	55.1	50.8	56.1	72.2	69.6	24374	21000	147000
	E5	Web	M	f	56.2	54.8	50.4	—	70.0	—	22668	31000	161000
	E6	Web	WO	f	55.5	53.1	—	—	66.7	—	30227	29678	165853
8x31	F1	FL	M	f	55.3	54.7	50.5	55.6	70.0	69.7	25676	25000	150000
	F2	FL	WO	f	57.3	55.4	—	55.6	67.9	69.7	29051	22763	148946
	F3	FL	WO	f	53.8	53.1	—	55.6	67.8	69.7	28738	21731	148307
	F4	FL	M	f	54.6	54.2	49.9	55.6	69.7	69.7	23520	24000	151000
	F5	Web	M	f	57.8	56.0	50.9	—	70.3	—	25477	35000	172000
	F6	Web	WO	f	54.6	53.7	—	—	66.0	—	29875	27492	168661
8x31	A1	FL	M	f	57.6	56.5	51.6	57.5	75.1	74.0	24992	21000	166000
	A2	FL	WO	f	57.2	53.5	—	57.5	71.4	74.0	28908	18053	164707
	A3	FL	WO	f	55.3	54.0	—	57.5	71.1	74.0	28719	19731	163655
	A4	FL	M	f	55.4	54.9	49.4	57.5	73.7	74.0	26235	18000	166000
	A5	Web	M	f	56.1	55.4	50.0	—	73.0	—	28614	25000	179000
	A6	Web	WO	f	56.8	53.7	—	—	70.1	—	29208	21140	163271

					F_{yu}	F_y	F_{ys}	F_{ym}	F_u	F_{um}	E	ε_{sh}	ε_u
Shape	Cpn	Loc.	Lab	t	(ksi)	(ksi)	(ksi)	(ksi)	(ksi)	(ksi)	(ksi)	($\mu\varepsilon$)	($\mu\varepsilon$)
8x31	B1	FL	M	f	57.0	56.1	51.0	56.0	71.6	71.0	24743	29000	166000
	B2	FL	WO	f	56.7	53.3	—	56.0	68.4	71.0	28765	27181	171999
	B3	FL	WO	f	53.4	52.7	—	56.0	67.9	71.0	28945	28233	171940
	B4	FL	M	f	56.0	54.5	49.4	56.0	71.1	71.0	21809	26000	176000
	B5	Web	M	f	57.8	57.0	50.9	—	72.1	—	23433	31000	180000
	B6	Web	WO	f	54.9	53.6	—	—	68.7	—	29944	26198	166441
8x31	C1	FL	M	f	55.2	54.6	49.8	53.9	69.4	72.0	27139	27000	169000
	C2	FL	WO	f	54.1	52.6	—	53.9	66.3	72.0	28689	30407	175609
	C3	FL	WO	f	53.5	52.3	—	53.9	66.4	72.0	28428	28052	173230
	C4	FL	M	f	56.2	55.9	51.3	53.9	70.4	72.0	23742	28000	167000
	C5	Web	M	f	56.9	55.5	51.6	—	70.6	—	26276	28000	158000
	C6	Web	WO	f	54.5	52.8	—	—	66.2	—	28925	28005	164046
12x65	A1	FL	M	f	62.9	59.8	55.2	52.5	73.2	69.5	26504	28000	151386
	A2	FL	WO	f	61.5	59.7	—	52.5	72.3	69.5	29059	23376	128437
	A3	FL	WO	f	58.9	56.8	—	52.5	70.0	69.5	28002	24123	153533
	A4	FL	M	f	64.6	61.9	58.0	52.5	75.2	69.5	27706	21000	119000
	A5	Web	M	f	64.2	64.1	59.8	—	75.2	—	32639	21000	115000
	A6	Web	WO	f	62.3	61.7	—	—	72.1	—	29662	24664	132076
12x65	B1	FL	M	f	57.0	55.1	50.1	56.5	71.4	70.5	25669	28000	176000
	B2	FL	WO	f	55.0	53.8	—	56.5	68.6	70.5	28198	28599	177006
	B3	FL	WO	f	55.7	54.0	—	56.5	68.7	70.5	29229	29872	173280
	B4	FL	M	f	56.0	56.0	50.9	56.5	71.8	70.5	25670	29000	176000
	B5	Web	M	f	63.8	63.1	58.8	—	76.5	—	32929	25000	137000
	B6	Web	WO	f	57.9	57.8	—	—	70.9	—	24693	22055	142902
12x65	C1	FL	M	f	54.9	52.6	47.6	55.0	70.7	73.4	30210	32000	172000
	C2	FL	WO	f	51.9	49.8	—	55.0	66.8	73.4	28494	25866	182557
	C3	FL	WO	f	51.9	51.2	—	55.0	67.2	73.4	27343	27191	184365
	C4	FL	M	f	53.6	52.4	47.5	55.0	70.9	73.4	25354	27000	174000

Shape	Cpn	Loc.	Lab	t	F_{yu} (ksi)	F_y (ksi)	F_{ys} (ksi)	F_{ym} (ksi)	F_u (ksi)	F_{um} (ksi)	E (ksi)	ε_{sh} ($\mu\varepsilon$)	ε_u ($\mu\varepsilon$)
12x65	C5	Web	M	f	58.6	57.5	53.3	—	72.9	—	25988	34000	135500
	C6	Web	WO	f	53.0	53.6	—	—	66.1	—	25968	27163	121483
12x65	17-1	FL	WO	f	59.5	57.1	—	53.4	74.3	74.8	29234	22341	162573
	17-2	FL	WO	f	55.3	54.7	—	53.4	74.8	74.8	29597	16776	154406
	17-3	Web	WO	f	59.2	57.1	—		74.2	—	28930	25694	159781
	17-4	Web	WO	f	60.4	56.5	—		73.8	—	30017	24680	164161
	17-5	FL	WO	f	58.5	56.5	—	53.4	75.0	74.8	28727	19632	162383
14x176	A1	FL	M	f	56.7	54.9	51.2	53.0	72.6	72.0	25116	19000	140000
	A2	FL	WO	h	54.4	54.3	—	53.0	70.5	72.0	27110	18001	144434
	A3	FL	WO	h	56.2	54.5	—	53.0	70.5	72.0	29255	19501	150028
	A4	FL	M	f	56.6	53.5	50.7	53.0	72.2	72.0	27480	17000	151000
	A5	Web	M	f	57.3	55.4	51.1	—	72.7	—	26125	20000	153000
	A6	Web	WO	f	56.5	54.3	—	—	70.0	—	29835	21539	152508
14x176	B1	FL	M	f	56.8	54.5	50.7	52.9	73.4	70.0	29257	19000	164000
	B2	FL	WO	h	54.6	53.4	—	52.9	70.5	70.0	29295	18351	163604
	B3	FL	WO	h	53.2	52.9	—	52.9	70.4	70.0	28606	13731	154642
	B4	FL	M	f	56.1	53.8	49.8	52.9	72.2	70.0	25496	19000	165000
	B5	Web	M	f	58.3	56.0	51.4	—	73.4	—	33331	23000	161000
	B6	Web	WO	f	56.0	54.5	—	—	71.1	—	29498	22151	158551
14x176	C1	FL	WO	h	57.6	53.8	—	52.0	70.8	71.0	29111	14951	149823
	C2	FL	M	f	57.2	54.9	51.8	52.0	73.1	71.0	24977	19239	148000
	C3	FL	WO	h	54.8	54.1	—	52.0	71.3	71.0	29849	12425	145252
	C4	FL	M	f	57.2	54.3	50.7	52.0	72.7	71.0	29441	16380	146000
	C5	Web	M	f	57.9	56.2	52.5	—	73.5	—	22921	20000	152000
	C6	Web	WO	f	57.7	55.0	—	—	70.9	—	28517	19470	144757

					F_{yu}	F_y	F_{ys}	F_{ym}	F_u	F_{um}	E	ε_{sh}	ε_u
Shape	Cpn	Loc.	Lab	t	(ksi)	(ksi)	(ksi)	(ksi)	(ksi)	(ksi)	(ksi)	($\mu\varepsilon$)	($\mu\varepsilon$)
14x176	JB1	FL	M	f	63.3	62.6	59.2	61.3	78.5	78.9	24238	16000	127000
	JB2	FL	WO	h	63.8	63.8	—	61.3	77.7	78.9	28227	12585	110790
	JB3	FL	WO	h	62.3	62.2	—	61.3	77.2	78.9	29196	12923	119727
	JB4	FL	M	f	65.2	65.2	61.5	61.3	81.0	78.9	33662	10000	99000
	JB5	Web	M	f	54.4	52.7	48.1	—	68.3	—	30044	25000	167000
	JB6	Web	WO	f	59.5	58.3	—	—	72.5	—	28428	17117	125191
14x176	88-1	FL	WO	f	57.6	55.7	—	54.4	75.7	77.9	29423	18036	149917
	88-2	FL	WO	f	58.4	55.8	—	54.4	76.8	77.9	29684	13186	144586
	88-3	Web	WO	f	60.1	57.7	—	—	76.8	—	28799	19396	158860
	88-4	Web	WO	f	60.3	57.4	—	—	77.3	—	29234	17149	147532
	88-5	FL	WO	f	56.9	56.3	—	54.4	76.2	77.9	28988	18333	155070
14x257	A1	FL	M	h	55.4	53.4	49.6	53.0	73.0	71.5	30076	16000	150000
	A2	FL	WO	h	52.6	52.8	—	53.0	71.2	71.5	28609	13426	134553
	A3	FL	WO	h	53.4	52.4	—	53.0	70.6	71.5	28100	13683	148986
	A4	FL	M	h	52.8	52.7	48.8	53.0	73.9	71.5	27982	14000	146000
	A5	Web	M	f	56.8	53.8	49.9	—	72.4	—	26648	19000	153000
	A6	Web	WO	h	54.3	53.3	—	—	70.4	—	30000	17434	148436
14x257	B1	FL	M	h	53.6	51.6	47.6	50.5	70.8	70.0	26627	17000	154000
	B2	FL	WO	h	51.1	51.0	—	50.5	68.6	70.0	29290	15142	153079
	B3	FL	WO	h	52.4	50.3	—	50.5	68.1	70.0	28780	16124	158720
	B4	FL	M	h	52.8	51.2	47.0	50.5	70.4	70.0	20904	16000	151000

Shape	Cpn	Loc.	Lab	t	F_{yu} (ksi)	F_y (ksi)	F_{ys} (ksi)	F_{ym} (ksi)	F_u (ksi)	F_{um} (ksi)	E (ksi)	ε_{sh} ($\mu\varepsilon$)	ε_u ($\mu\varepsilon$)
	B5	Web	M	f	53.5	50.7	47.0	—	69.5	—	23858	19000	164000
	B6	Web	WO	h	50.4	50.4	—	—	67.9	—	28856	16164	157964
14x257	C1	FL	M	h	55.3	53.4	50.0	55.5	72.8	75.5	25565	17000	146000
	C2	FL	WO	h	53.3	53.1	—	55.5	71.4	75.5	28450	14745	139167
	C3	FL	WO	h	55.0	53.3	—	55.5	70.9	75.5	29672	16880	145381
	C4	FL	M	h	55.6	53.6	49.6	55.5	73.4	75.5	25423	15000	143000
	C5	Web	M	f	54.6	52.7	48.6	—	71.6	—	23322	20000	162000
	C6	Web	WO	h	54.1	52.4	—	—	70.2	—	28934	18302	155677
14x257	89-3	Web	WO	f	58.3	54.5	—	53.1	77.0	78.2	29524	11195	145151
	89-4	Web	WO	f	56.2	54.6	—	53.1	76.9	78.2	29394	12362	143983
14x257	71-3	Web	WO	f	55.3	53.7	—	53.5	76.0	78.2	30873	10417	140035
	71-4	Web	WO	f	56.1	53.0	—	53.5	76.0	78.2	29234	10867	142184
14x257	33-3	Web	WO	f	56.4	52.6	—	49.9	75.2	76.9	29437	10683	145207
	33-4	Web	WO	f	54.9	52.4	—	49.9	75.0	76.9	29075	11158	151544
14x257	JA1	FL	M	f	—	—	—	60.9	—	84.2	—	—	—
	JA2	FL	WO	h	60.5	60.3	—	60.9	81.1	84.2	26328	8182	128600
	JA3	FL	WO	h	61.5	62.4	—	60.9	82.1	84.2	26317	6496	115368
	JA4	FL	M	f	—	—	—	60.9	—	84.2	—	—	—
	JA5	Web	M	f	70.7	70.7	—	—	91.5	—	37286	24000	105000
	JA6	Web	WO	h	67.5	68.8	—	—	87.7	—	28376	2126	102239

Shape	Cpn	Loc.	Lab	t	F_{yu} (ksi)	F_y (ksi)	F_{ys} (ksi)	F_{ym} (ksi)	F_u (ksi)	F_{um} (ksi)	E (ksi)	ε_{sh} ($\mu\varepsilon$)	ε_u ($\mu\varepsilon$)
30x99	C1	FL	M	f	60.9	59.0	55.0	58.0	76.0	75.0	30056	24523	148000
	C2	FL	WO	f	61.6	59.0	—	58.0	73.6	75.0	28520	27354	152486
	C3	FL	WO	f	60.5	57.5	—	58.0	72.9	75.0	28339	20872	149461
	C4	FL	M	f	61.4	60.1	55.0	58.0	74.7	75.0	24534	29000	153000
	C5	Web	M	f	67.0	64.4	60.5	—	78.8	—	25949	26000	128000
	C6	Web	WO	f	64.8	64.4	—	—	74.7	—	29756	25725	144037
30x99	461	FL	WO	f	59.6	56.4	—	55.0	72.0	72.4	29698	26615	166333
	462	FL	WO	f	55.5	54.7	—	55.0	70.9	72.4	29945	23518	162706
	463	Web	WO	f	64.4	60.5	—	—	74.6	—	28683	26759	152118
	464	Web	WO	f	63.3	60.5	—	—	74.6	—	29176	26429	152952
	465	FL	WO	f	58.6	56.7	—	55.0	71.4	72.4	28698	25939	169393
36x150	A1	FL	M	f	55.1	52.7	—	51.0	71.0	66.5	27704	19000	169000
	A2	FL	WO	f	53.9	50.7	—	51.0	67.6	66.5	28213	19978	162009
	A3	FL	WO	f	53.9	50.8	—	51.0	67.5	66.5	29423	19138	166975
	A4	FL	M	f	54.6	52.2	48.0	51.0	69.8	66.5	28223	21000	180000
	A5	Web	M	f	60.0	58.4	54.0	—	72.2	—	24466	29000	158000
	A6	Web	WO	f	61.5	58.4	—	—	70.8	—	27811	26744	152018
36x150	B1	FL	M	f	56.6	56.1	51.9	52.5	73.5	71.5	31244	20000	151000
	B2	FL	WO	f	57.5	53.9	—	52.5	71.2	71.5	26736	16223	143206
	B3	FL	WO	f	57.4	54.6	—	52.5	71.0	71.5	28436	19547	149105
	B4	FL	M	f	59.0	56.0	51.9	52.5	74.0	71.5	26765	20000	155000
	B5	Web	M	f	65.2	62.6	58.5	—	77.3	—	31452	25000	137000
	B6	Web	WO	f	63.2	59.8	—	—	73.1	—	28060	27657	152867
36x150	C1	FL	M	f	53.3	50.5	46.1	50.0	68.7	67.0	24676	21000	185000
	C2	FL	WO	f	52.9	49.8	—	50.0	66.7	67.0	26731	19217	166080
	C3	FL	WO	f	52.6	49.6	—	50.0	66.3	67.0	27749	20481	169312
	C4	FL	M	f	52.5	49.8	46.0	50.0	68.0	67.0	29865	21000	176000
	C5	Web	M	f	58.8	56.5	52.1	—	72.6	—	26045	28000	163000
	C6	Web	WO	f	60.4	56.6	—	—	69.7	—	27420	27969	156343

Shape	Cpn	Loc.	Lab	t	F_{yu} (ksi)	F_y (ksi)	F_{ys} (ksi)	F_{ym} (ksi)	F_u (ksi)	F_{um} (ksi)	E (ksi)	ε_{sh} ($\mu\varepsilon$)	ε_u ($\mu\varepsilon$)
36x150	C1	FL	M	f	53.3	50.5	46.1	50.0	68.7	67.0	24676	21000	185000
	C2	FL	WO	f	52.9	49.8	—	50.0	66.7	67.0	26731	19217	166080
	C3	FL	WO	f	52.6	49.6	—	50.0	66.3	67.0	27749	20481	169312
	C4	FL	M	f	52.5	49.8	46.0	50.0	68.0	67.0	29865	21000	176000
	C5	Web	M	f	58.8	56.5	52.1	—	72.6	—	26045	28000	163000
	C6	Web	WO	f	60.4	56.6	—	—	69.7	—	27420	27969	156343
36x150	JC1	FL	M	f	63.1	60.8	56.9	57.1	82.7	81.5	25839	21000	152000
	JC2	FL	WO	f	62.1	58.4	—	57.1	80.8	81.5	28481	16720	156038
	JC3	FL	WO	f	61.3	59.7	—	57.1	80.1	81.5	29564	16720	151894
	JC4	FL	M	f	62.6	59.9	55.7	57.1	83.1	81.5	29750	17000	150000
	JC5	Web	M	f	72.9	69.8	65.4	—	88.2	—	24892	23000	132000
	JC6	Web	WO	f	71.9	69.7	—	—	86.6	—	27471	19738	122637
36x150	341	FL	WO	f	58.9	56.4	—	56.6	72.7	74.2	28495	22699	159411
	342	FL	WO	f	56.0	55.5	—	56.6	73.0	74.2	27581	20949	162183
	343	Web	WO	f	67.0	62.9	—	—	77.2	—	29118	28551	149973
	344	Web	WO	f	63.9	61.5	—	—	76.2	—	28190	28533	162377
	345	FL	WO	f	62.5	57.3	—	56.6	73.5	74.2	29321	22827	163928
30x99	091	FL	WO	f	63.2	61.3	—	61.3	73.9	74.7	28741	33010	165296
	092	FL	WO	f	61.5	58.2	—	61.3	72.9	74.7	28727	27068	165405
	093	Web	WO	f	70.1	66.0	—	—	78.5	—	28669	25025	138147
	094	Web	WO	f	70.8	68.2	—	—	79.9	—	28553	25112	122816
	095	FL	WO	f	62.9	60.6	—	61.3	73.5	74.7	28727	33768	161753

Appendix B

Updating Standard Shape Material Property Database

for Design and Reliability

A Thesis

Submitted to the Faculty of the Graduate School

of the University of Minnesota By

Mark Daniel Graeser

In Partial Fulfillment of the Requirements

for the Degree of

Master of Science

July 2001

Acknowledgements

I would like to thank my advisor, Professor Robert Dexter for his guidance and patience throughout the project. I also want to thank Professor Theodore Galambos for his assistance. His insight and supervision, particularly regarding the reliability analysis are appreciated. Special thanks goes out to Paul Bergson for his help with the tensile testing equipment and data acquisition system.

This project was conducted as a joint effort between the University of Minnesota and the University of Western Ontario. Professor Michael Bartlett from the University of Western Ontario was instrumental to the success of the project. The efforts of fellow graduate students Brad Schmidt and Jason Jelinek from the University of Western Ontario are also appreciated. Jason Jelinek performed the tensile tests and tabulated the results for the University of Western Ontario tensile test specimens.

The Structural Shape Producer's Council (SSPC) is acknowledged for their input and for allowing the use of the large material property database for this research.

This research project was made possible by the financial support from the American Institute of Steel Construction (AISC).

Abstract

Load and Resistance Factor Design (LRFD) is a probabilistic design approach that requires statistical parameters for the applied loading and the strength of the members to resist the loads. The material properties of steel are important factors that determine the resistance of structural members. In 1978, Galambos and Ravindra established resistance (ϕ) factors according to the variation in steel and an acceptable level of safety. Since then, several changes in steel producers, processes, and specifications have occurred in structural steel. Research was conducted to re-examine the reliability of modern steel. More than 200 tensile tests were conducted at the University of Minnesota and the University of Western Ontario. All test specimens were plate-type coupons taken from the web or flange of A992 W-shapes. The tensile test results were compared to recent tensile property research and material property mill surveys. The tensile test data were processed for statistical analysis and used in a first-order, second-moment reliability analysis to determine current resistance (ϕ) factors. The mean yield stress values for A992 steel were less than the values of the original calibration, however, this effect was offset due to a decrease in variation. As a result, the reliability analysis indicated that the level of reliability for current A992 W-shapes is essentially the same level as the steel of the past.

Table of Contents

Table of Contents (continued)

Chapter 1: Introduction & Background

1.1 Introduction

Load and Resistance Factor Design (LRFD) is a probability-based design approach. This design methodology requires statistical data on the load and resistance variables. Resistance factors are used in steel member design to reduce the nominal strength, therefore, assuring an adequate level of structural safety. The resistance factor is influenced by several parameters: professional, fabrication, and material. The current resistance factor study focuses on the material factor portion of the resistance. The resistance factors in the American Institute of Steel Construction (AISC) LRFD Specification were developed in the 1970's. The current investigation is performed in response to the significant changes that have occurred since then in steel production and specification. The study updates the steel material property database for design and reliability. This information is needed to re-evaluate the resistance (ϕ) factors used in the AISC LRFD Specification. The research concentrates on A992 rolled wide-flange shapes, because A992 W-shapes are more widely used than A572 and A36 W-shapes.

In 1978, Galambos and Ravindra presented the material properties and methodology important to resistance factor development in LRFD (Galambos & Ravindra, 1978). The present AISC LRFD resistance factors are based on data collected in the 1970's from mill tests performed on rolled wide-flange sections. Several changes have taken place since then in the steel producers, processes, and specifications.

Steel production has changed considerably since the original LRFD calibration. One key change is the transition from iron-ore based material to scrap steel. Other changes include the use of continuous casting and the introduction of the electric-arc furnace. These changes in base material and steel production may result in different steel composition and grain structure.

Steel specifications have also changed in response to modern steel production and design. The most significant change involves the new ASTM A992 Specification. This specification is more stringent than A36 and A572 Gr. 50, and it reflects the changes in modern steel.

To re-examine resistance factors, the material properties of modern steel are needed. Structural steel property statistics were collected from past material property surveys and tensile testing. The literature review included mill test data for wide-flange shapes and plates along with laboratory test results for rolled shapes. This database of material properties was compared with laboratory tensile test results.

The University of Minnesota and the University of Western Ontario performed more than 200 tensile tests. Test specimens were obtained from the flanges and the webs of several wide-flange A992 steel shapes. Significant factors relevant to tensile test results were recognized and considered, and all tensile tests were performed according to ASTM A370. Each university laboratory obtained stress-strain curves from the tests. The upper yield point, yield stress, static yield stress, and ultimate tensile strength values were all recorded and compared. Strain, modulus, and percent elongation results were also tabulated. Statistics and histograms are presented for several tensile properties. A reliability analysis was performed based on the tensile test results and past material property surveys.

1.2 LRFD Development

The American Institute of Steel Construction (AISC) first published the Load and Resistance Factor Design (LRFD) Specification in 1986. The safety requirement of the AISC LRFD Specification is given by the formula

$$\Sigma\gamma_i Q_i \quad \phi R_n$$

Q_i = individual load effect — R_n = nominal resistance

γ_i = load factor — ϕ = resistance factor

The left side of the expression includes the summation of the individual load effects multiplied by their appropriate load factors. Examples of load effects include: dead load, live load, and wind load. Similarly, the right side of the expression represents the design strength of the component or system. LRFD is a probability-based assessment of structural safety. It accounts for overload and under strength by using load and resistance factors, respectively. The factors ϕ and γ vary for different load combinations and types of members, however, the resistance factor (ϕ) is always less than unity. The load and resistance factors account for inaccuracies in the theory, variations in the material properties and geometric dimensions, and uncertainties in the loading (AISC, 1993).

The LRFD method evaluates the risk of failure and assures that the probability of occurrence is kept at an acceptable level. The following is a simplified explanation of the probabilistic basis for the load and resistance factor design method. The load effect, Q and the resistance, R are assumed to be statistically independent random variables. The load effect and resistance each have a separate probabilistic distribution with a corresponding mean (Q_m, R_m) and standard deviation. The probability distributions are shown in Figure 1.

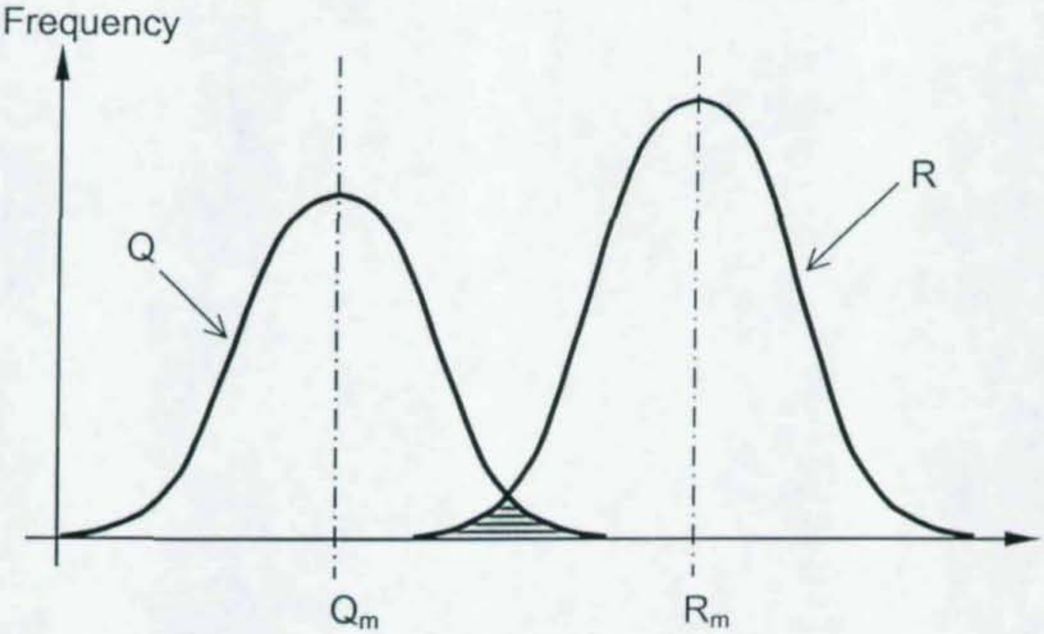

Figure 1: Probability distributions for the load effect, Q and the resistance, R

The structural member or system is safe when the resistance, R is greater than the load effect Q. Since R and Q are random variables, there is some small probability that R may be less than Q. The shaded region shown in Figure 1 represents the potential overlap between the load effect and the resistance. Structural failure may also be examined for ln(R/Q) because the limit state $R < Q$ is equal to the limit state $\ln(R/Q) < 0$. Ln(R/Q) may be treated as a single random variable, and it is simpler than working with two groups of random variables. The result is a single probability distribution, shown in Figure 2, combining the uncertainties of both the resistance, R and load effect, Q. The probability distribution of ln(R/Q) is typically not known, however, the mean values and standard deviations of the many variables involved in the resistance and the load effect can frequently be estimated. The mean values R_m and Q_m and the standard deviations σ_R and σ_Q of the resistance and load can be used in reliability assessment (Salmon & Johnson, 1996). The limit state is violated if ln(R/Q) is negative, and the probability of this happening is represented as the shaded area shown in Figure 2.

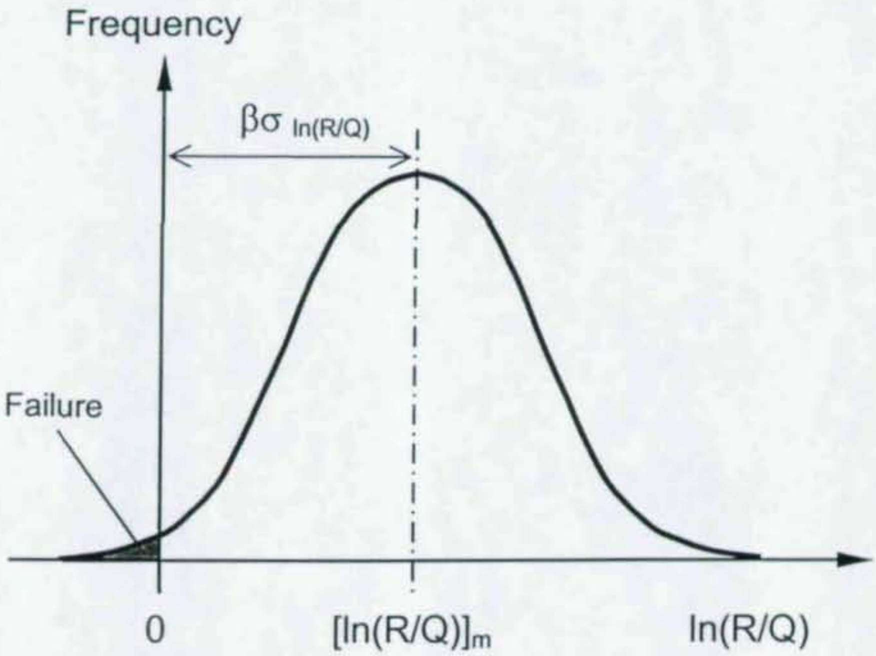

Figure 2: Probability distribution for ln(R/Q)

The margin of safety is illustrated in Figure 2 as the distance from the origin to the mean. This distance is defined as the standard deviation, $\sigma_{\ln(R/Q)}$ multiplied by a factor, β known as the reliability index. The reliability index formula is the following.

$$\beta = \frac{\ln(R_m / Q_m)}{\sqrt{V_R^2 + V_Q^2}}$$

R_m = the mean resistance $\quad$ V_R = the coefficient of variation of the resistance

Q_m = the mean load effect $\quad$ V_Q = the coefficient of variation of the load effect

An advantage of the reliability index is that it can give an indication of the level of safety for various components and systems (Salmon & Johnson, 1996).

Now that the basic probability theory has been introduced, the actual development of the AISC load and resistance factor design criteria will be reviewed. The probability-based LRFD methodology requires statistical data on the load and resistance variables.

The basic requirements include the probability distributions for each load and resistance variable as well as mean and standard deviation estimates (Ellingwood et al., 1982).

The load factors were analyzed and developed for load and resistance factor design by Ellingwood et al. in 1982. The load factors, γ account for the uncertainties in the analysis and the possible deviations in the actual loads from the specified values. These factors were developed from a variety of load statistics collected from previous structural studies. Table 1 summarizes the means, coefficients of variation (COV), and probability distributions of 50 year maximum and arbitrary-point-in-time (APT) load effects used in the LRFD development (Ellingwood et al., 1982). The coefficient of variation, COV is defined as the standard deviation divided by the mean.

Table 1: Summary of statistical data on loads (Ellingwood et al., 1982)

Load Type	Mean / Nominal	COV	Probability Distribution
Dead Load, D	1.05	0.10	Normal
Live Load (max. 50 yrs.)	1.00	0.25	Extreme Value Type I
Live Load (APT)	0.25 – 0.50	0.60	Gamma
Wind Load	0.78	0.37	Extreme Value Type I

As previously shown, the LRFD criterion is defined by the formula

$$\Sigma\gamma_i Q_i \quad \phi R_n$$

The design strength is defined as a resistance factor multiplied by the nominal strength. The resistance factor, ϕ can be determined from the formula

$$\phi = \frac{R_m}{R_n}\exp(-\alpha\beta V_R)$$

Where R_m is the mean resistance, R_n is the nominal resistance, α is a linearizing factor, and β is the reliability index defined earlier. V_R is the coefficient of variation of the resistance, and it is represented by the formula

$$V_R = (V^2_F + V^2_P + V^2_M)^{½}$$

The subscripts F and P are for the uncertainties of the fabrication process and the professional assumptions. Similarly, the M subscript is due to the variability of the material properties (Galambos & Ravindra, 1978). The current resistance factor study addresses this material property portion of the variation and mean resistance.

In 1978, Galambos and Ravindra presented the properties of steel for use in LRFD. The reliability criteria were based on the first-order, second-moment probabilistic design approach. The following material properties were characterized for load and resistance factor design: modulus of elasticity, yield stress, and strain-hardening modulus (Galambos & Ravindra, 1978). Table 2 contains the material property values used in the resistance factor development.

Table 2: Material properties included in the load and resistance factor design development (Galambos & Ravindra, 1978)

Material Property	Mean Value (ksi)	COV
Modulus of elasticity (tension)	29000	0.06
Modulus of elasticity (compression)	29000	0.06
Modulus of elasticity (shear)	11200	0.03
Poisson's ratio	0.30	0.03
Yield stress in flanges	1.05 Fy	0.10
Yield stress in webs	1.10 Fy	0.11
Yield stress in shear	0.64 Fy	0.10
Strain-hardening modulus	600	0.25

Since the resistance factor is the focus of the current study, and yield stress is the principal property affecting the resistance of a steel structure, a more detailed review of the yield stress data is necessary. Table 3 contains a summary of the yield stress data collected for the development of the resistance factors in the AISC LRFD Specification (Galambos & Ravindra, 1978).

Table 3: Yield stress data (Galambos & Ravindra, 1978)

Year Reported	Country	Number of Tests	$F_{y\,nominal}$ (ksi)	$F_{y\,mill}$ / $F_{y\,nominal}$	COV
1957	US	3794	33	1.21	0.09
1972	US	3124	33	1.21	0.08
1958	US	400	36	1.22	0.11
1969	UK	---	36	1.19	0.12
1969	UK	---	50	1.06	0.05
1972	Sweden	19857	32-33	1.23	0.10
1972	Sweden	19217	36-38	1.18	0.10
1972	Sweden	11170	52	1.11	0.06

The data shown in Table 3 were collected in the 1970's from mill tests performed on rolled wide-flange sections. These mill test data were adjusted for use in the early LRFD development. At that time, all mill test coupons were taken from the web. As a result, the mill test yield stress data were reduced by approximately 5% to account for the higher web to flange strength. Another reduction of approximately 4 ksi was included to transform the dynamic mill test results to static values (Galambos, 2000). The dynamic yield stress and static yield stress are defined later in Figure 9. These adjustments resulted in a mean yield stress = 1.05 Fy and COV = 0.10, which were presented in Table 2 for flanges.

The LRFD method was calibrated to typical, representative designs of previous methods. Target reliability levels were established by reviewing the reliability inherent in the 1978 AISC Allowable Stress Design (ASD) Specification (Galambos et al., 1982). Examples of these target reliability levels for the dead, live-load combination (D + L) are shown in Table 4.

Table 4: Summary of target reliabilities (D + L)

(L/D = 1.0) (Galambos et al., 1982)

Member	Reliability, β
Steel tension member, yield (fracture)	2.5 (3.4)
Compact steel beam (L/D = 2.0)	3.1
Steel column, $\lambda = 0.5$	3.1

Target reliabilities, such as in Table 4, along with the statistical information summarized in the previous section, provide the basis for the current AISC LRFD Specification. The AISC LRFD Specification is calibrated to allowable stress design (ASD) at the live to dead load ratio, L/D = 3.0 for braced compact beams in flexure and tension members at yield. The corresponding reliability values are $\beta = 2.6$ for members and $\beta = 4.0$ for connections (AISC, 1993).

1.3 Changes in Steel Production

Many changes have occurred in structural steel production since the calibration of the present resistance factors. In traditional steel production, iron-ore was heated by blast furnaces. The iron-ore exposed to the blast of hot air released heat and gas, which reduced the iron-ore to metallic iron. The hot metal from the blast furnace was then refined further in basic oxygen furnaces to form steel. The molten steel was then poured into molds. After the steel had solidified into an ingot, the mold was removed. The ingots were then reheated and rolled into blooms. (Frank et al., 2000).

Currently, all structural steel shapes produced for use in the United States are continuously cast from electric-arc furnaces (Frank et al., 2000). In addition, scrap steel has replaced iron-ore based steel production. Unlike the basic oxygen furnace, the electric-arc furnace does not need hot metal from a blast furnace. The scrap metal is heated directly by an electric-arc between carbon electrodes, shown in Figure 3. The continuous casting process has replaced ingot casting because it requires less rolling and is more energy efficient. In continuous casting, liquid steel of the desired chemistry and temperature is passed through water-cooled casting molds similar to Figure 4. Steel in direct contact with the mold surface quenches forming a solid shell with a liquid core. After the steel has passed the mold, it is cooled to continue shell thickening (Frank et al., 2000). The continuous casting process, and the resulting near net shape blooms are shown in Figures 5 and 6 respectively.

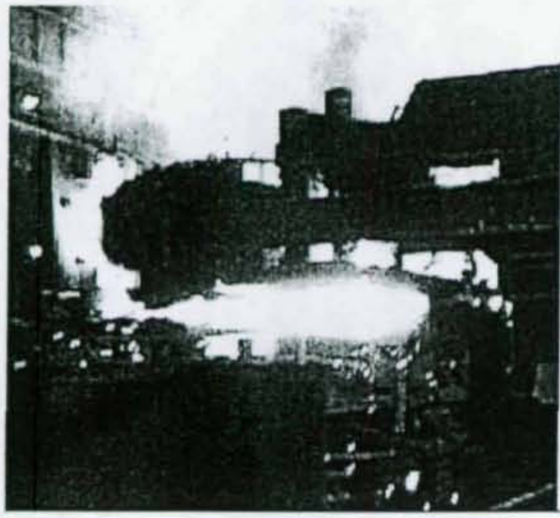

Figure 3: Modern electric-arc furnace

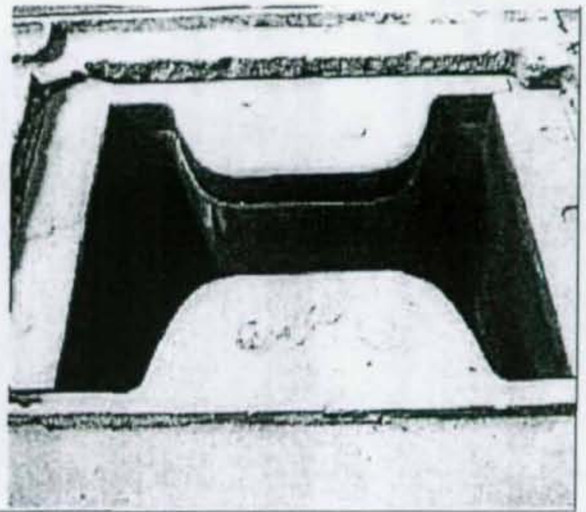

Figure 4: Typical continuous casting mold

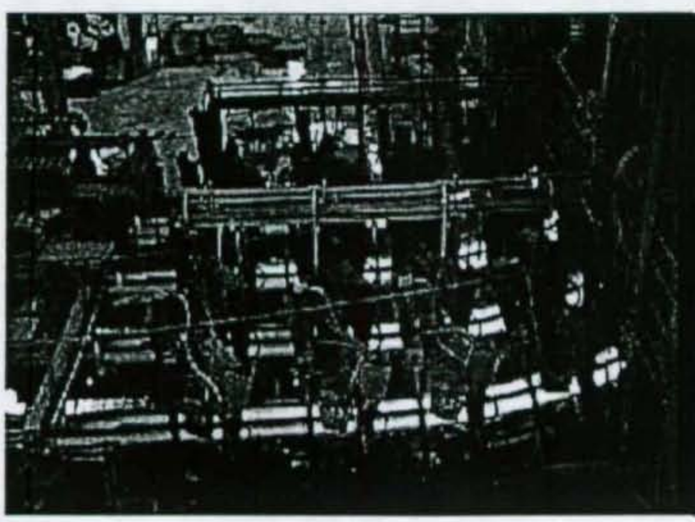

Figure 5: Continuous casting process

Figure 6: Near net shape blooms resulting from continuous casting

1.4 Implications of the New Process

There are several implications of the changes in modern steel production. Steel shapes produced by continuous casting tend to have greater uniformity in composition and properties than shapes made from ingot-casting. This is because the slow solidification rates of ingot-casting can lead to segregation of carbon, sulfur, and phosphorus (Frank et al., 2000). The near net shape casting has also reduced the amount of rolling. Hot rolling is beneficial because it causes the deformed grains to recrystallize into finer grains.

Steel specifications have changed due to modern steel production and design. The most significant change involves the new ASTM A992 "Steel for Structural Shapes for Use in Building Framing" Specification. This specification is more stringent than A36 and A572 Gr. 50, and it reflects the changes in modern steel. The change from predominately iron-ore base material to recycled steel has resulted in more residual elements in modern steel. As a result, the A992 specification tightens previous chemistry limits and sets new limits on residual elements. Other material property trends that have occurred are that the yield strength, F_y has increased substantially, however, the ultimate tensile strength, F_u has not increased as much. Therefore, the yield-to-tensile ratio, Y/T has increased significantly. The modern A992 specification addresses this issue by setting maximum limits on yield strength and the yield-to-tensile ratio. Table 5 compares the specified tensile properties for common ASTM structural steel specifications. Due to the changes in the steel production and specification, A992 W-shapes are more widely used than A572 and A36 W-shapes.

Table 5: Specified tensile properties

ASTM Specification	Yield Strength, Fy (ksi)	Tensile Strength Fu (ksi)	Yield-to Tensile Ratio, Y/T (%)
A36	≥ 36	58 - 80	---
A572 Gr. 50	≥ 50	≥ 65	---
A992	50 - 65	≥ 65	≤ 85

Modern structural steel shapes can no longer be distinguished by one unique specification or grade as a result of the more stringent requirements of the A992 specification. Structural steel shapes are currently produced to meet the modern A992 standard, however, A36 and A572 Gr. 50 steel can still be purchased. A steel heat which satisfies the A992 specification can be sold under several grades and specifications: A992, A572 Gr. 50, or A36. Steel shapes that do not satisfy the A992 specification requirements may still be sold as A572 Gr. 50 steel or A36 steel if it satisfies those specifications. The results of this process are low variability in A992 steel, whereas A36 and A572 Gr. 50 steel are essentially A992 steel with more variability, since the corresponding specifications may include the outliers not satisfying A992 requirements. The changes in steel production as well as the implementation of the modern A992 specification may result in steel considerably different from the past.

Chapter 2: Tensile Testing Considerations & Past Research

2.1 Tensile Testing

The tensile test is a key method in determining the mechanical properties of modern steel. A stress-strain curve reveals tensile properties such as yield strength, ultimate tensile strength, modulus of elasticity, and strain at strain hardening. Figure 7 contains examples of an engineering stress-strain curve and a true stress-strain curve for A992 steel. Engineering stress, σ is defined by the equation

$$\sigma = \frac{P}{A_o}$$

Where, P is the applied tensile load and A_o is the original cross-section before loading. Also, engineering strain, ε is defined by the equation

$$\varepsilon = \frac{\Delta \ell}{\ell_o}$$

Where, Δl is the change in length and l_o is the original gage length. Throughout this report, all stress and strain values will be expressed in engineering stress and strain unless otherwise specified.

Unlike engineering values for stress and strain, true stress and natural strain account for the change in length and cross-sectional area that occurs during loading. True tensile stress can be related to engineering stress before necking by the following equation

$$\sigma_{True} = \sigma_{Eng.}(1 + \varepsilon_{Eng.})$$

Natural strain is related to engineering stress before necking by the following equation

$$\varepsilon_{True} = \ln(1 + \varepsilon_{Eng.})$$

The plastic region of a tensile true stress – natural strain curve for most ductile metals can be approximated by a power function

$$\sigma_{True} = K\varepsilon^{n}_{Natural}$$

K is the strength coefficient, which is the stress at a natural strain equal to one, and n is the strain-hardening exponent. This relationship is a good approximation for the strain-hardening portion of the curve and is shown in Figure 7 for a steel tensile curve. The strain-hardening exponent, n is generally equal to the ultimate strain. As a result, n may be used to characterize the stress-strain properties of a particular material without reference to the actual curve (Ripling & Polakowsky, 1966).

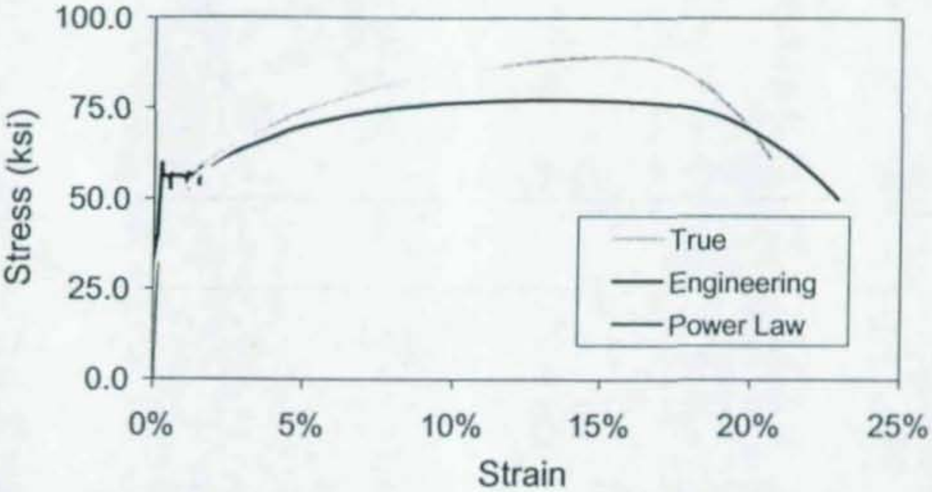

Figure 7: Steel engineering, true stress – strain curves, and fitted power law

2.2 Variables in Tensile Testing

A stress-strain curve reveals several mechanical properties important to steel design. Variation in tensile test results, particularly for yield strength, can be associated with several variables. These may include variation in test methods, selection of samples, or the natural variation in the material. ASTM A370 provides the standard test methods and definitions for mechanical testing of steel products. The most significant factors regarding yield strength are rate of testing, test specimen geometry, location of the test specimen, and the method used to determine yield stress.

Yield point and yield stress values increase with an increase in rate of testing. ASTM A370 specifies tensile test speed ranges for two testing alternatives: rate of crosshead separation of the machine and rate of loading. Machine crosshead separation must not exceed $^{1}/_{16}$ inch per minute per inch of reduced section in determining yield point or yield strength. When determining the tensile strength, the rate of crosshead separation must not exceed $^{1}/_{2}$ inch per minute per inch of reduced section. Also, the minimum speed of testing must not be less than $^{1}/_{10}$ the specified maximum rates for each corresponding region. Similarly for rate of stress or loading, the rate of loading must be between 10 ksi per minute and 100 ksi per minute near the yield strength and tensile strength regions of the curve. Unfortunately, there is not a method to relate load control speeds to crosshead speeds.

Test specimen geometry and location can also influence tensile test results. The two most common test specimen geometries are rounds and plate-type coupons. Rounds, unlike full-thickness plate-type specimens, only represent a small portion of the section. As a result, round test specimens can produce lower or higher results than the whole section depending on where they are taken. The test specimen location for wide-flange shapes is defined in ASTM A6. Test samples taken from webs usually have higher yield stress values than samples taken from flanges of W-shapes. This is because the webs of rolled shapes undergo more rolling and cool more quickly than the flanges.

The ASTM A370 Specification allows several methods for reporting the yield stress. The most common include: drop of the beam, extension under load, and the offset method. The drop of the beam method reports the yield point, and can feature variability due to the upper yield point phenomenon shown in Figure 8.

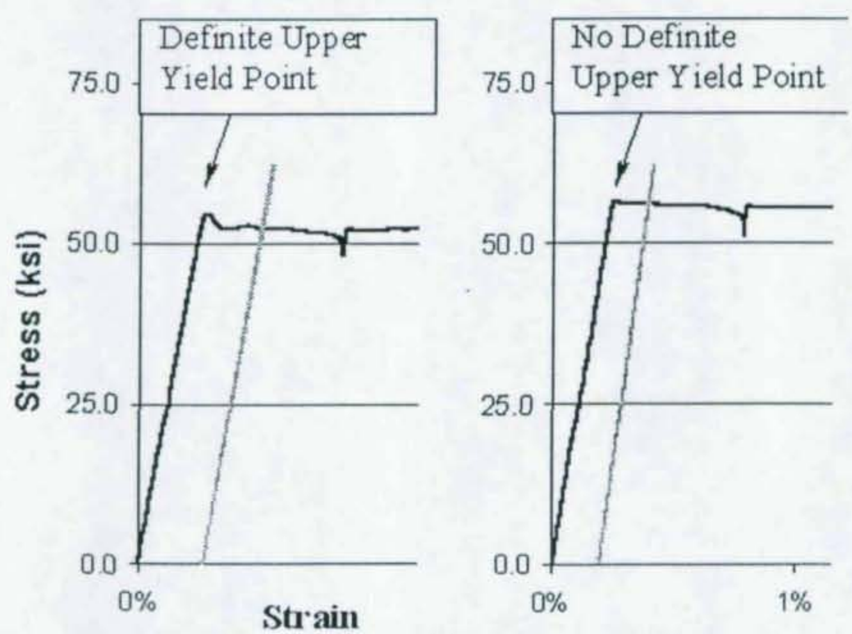

Figure 8: Upper yield point behavior

This can be problematic because not all steels exhibit upper yield point behavior. The 0.5% extension under load and the 0.2% offset methods report the yield strength, and are preferred because measurements are taken at the yield plateau where there is more uniformity between various steel stress-strain curves. Fortunately, similar problems do not occur in the determination of the ultimate tensile strength and percent elongation, because these methods are defined more explicitly in ASTM A370.

Sources of material property data consist primarily of research laboratory tests and steel mill test reports. The ASTM A6 standard specifies what tests are to be conducted and reported by steel producers. Mill test reports must be provided for all steel sold. These mill test reports typically include yield strength, ultimate tensile strength, percent elongation, and chemical composition values. According to ASTM A370, steel mills may report either the yield point (drop of the beam method) or the yield strength (extension under load or offset method) for the yield stress. Methods in determining the yield stress vary according to producer, but all three methods are currently implemented. Mill test strain rates also vary among steel producers, and are typically not known other than that they are within the ASTM A370 specified ranges. Mill tensile tests in the past were only performed on the webs of wide-flange shapes. In 1996, however, the standard test location was changed from web to flange for W-shapes with a width greater than or equal to 6". This portion of the ASTM A6 Specification was changed in order to produce results more representative of section capacity.

Due to the variability encountered in yield strength values, the static yield stress is an important tensile test parameter. Static yield stress is a reliable and consistent measure of steel at yield because it is independent of testing procedures and testing machine behavior (Galambos, 1988). The static yield stress is defined as the average yield stress at zero strain rate. Structural Stability Research Council (SSRC) Technical Memorandum #8 provides the standard method of testing for static yield stress. Figure 9 shows an example of the static yield stress in a typical steel tensile test.

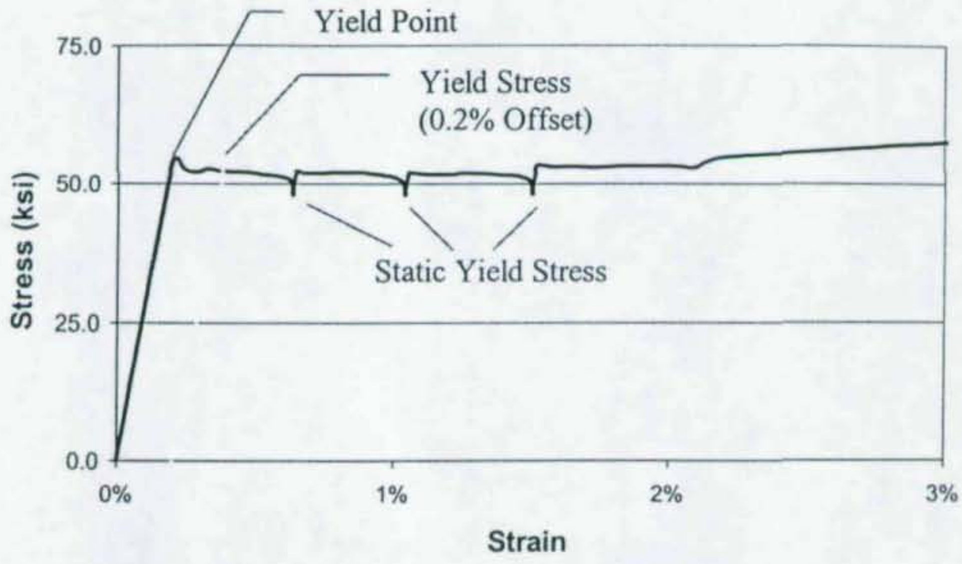

Figure 9: Detailed view of typical steel stress – strain curve

Once the material has entered the yield plateau (and shortly after the 0.2% offset), the crosshead motion of the machine is stopped to record the static yield stress. The static yield stress is recorded when the load has stabilized or after the motion has remained stopped for five minutes. The test is then briefly returned to the standard strain rate, and the process is then repeated. Two or three static yield stress values may be recorded per tensile test.

2.3 Past Material Property Studies

A literature review was conducted to determine past material property studies. Five recent structural steel material property studies were reviewed. Only one study, Dexter et al. 2000, contained tensile data for A992 structural shapes.

2.3.1 Frank and Read Material Property Survey (1993)

In 1993, Frank and Read performed a statistical analysis of tensile data for wide-flange structural shapes. The statistical data were based on 1992 mill test reports provided by six structural steel producers. The study included three steel grades: A36, A572 Gr. 50, and dual grade. Dual grade steel was defined as steel certified in accordance with both A36 and A572 Gr. 50 specifications (Frank & Read, 1993). The distribution of data was the following: 36,570 samples of A36, 7,824 samples of dual grade, and 13,536 samples of A572 Gr. 50. All tensile data for the study were taken from the web of the rolled wide-flange shape. The data were sorted according to ASTM A6 shape group and steel grade. Statistics and histograms were provided for each variable. Frank and Read also concluded that there is not a significant trend in yield strength with web thickness. Table 6 summarizes the 1992 mill test report statistics for dual grade and A572 Gr. 50 steel.

Table 6: Summary of 1992 mill test report data (Frank & Read, 1993)

ASTM Specification	Dual Grade (web)	A572 Gr. 50 (web)
Number of Data	7,824	13,536
Yield Strength (ksi)		
Mean	55.2	57.6
COV	0.066	0.089
Tensile Strength (ksi)		
Mean	73.2	75.6
COV	0.045	0.082
Yield/Tensile Ratio		
Mean	0.754	0.763
COV	0.050	0.063

2.3.2 Rex and Easterling (1999): "Behavior and Modeling of Mild Structural and Reinforcing Steel"

In 1999, Rex and Easterling investigated the stress-strain behavior of A36, A572 Gr. 50, and reinforcing steel. The study involved mill survey data, literature data, and tensile test data. Rex and Easterling developed methods for approximating the full stress-strain behavior along with mean values for the yield stress and tensile strength.

2.3.3 Jaquess and Frank (1999): "Characterization of the Material Properties of Rolled Sections"

In 1999, Jaquess and Frank characterized the geometric properties, tensile properties, toughness properties, and chemical composition of several rolled sections. The study involved 17 wide-flange sections from four different steel mills. Seven different shape sizes were tested, and all sections were A572 Gr. 50 steel.

Section properties were calculated based on several geometric measurements. Flange thickness, web thickness, section depth, and flange width were measured for each section. Flange thickness was the only measurement that exhibited significant variation across the cross-section. Jaquess and Frank accounted for the effect of asymmetric bending due to geometric variation and incorporated it into effective S_x and S_y values. Table 7 summarizes the geometric statistics from Jaquess and Frank.

Table 7: Summary of geometric statistics (Jaquess & Frank, 1999)

Section Property	A	I_x	I_y	$S_{x\,eff}$	$S_{x\,eff}$	Z_x	Z_y
Number of Samples	17	17	17	17	17	17	17
Mean [measured/nominal] (%)	99.0	98.7	98.6	97.5	97.9	98.7	98.4
COV	0.018	0.021	0.031	0.021	0.026	0.019	0.025

Jaquess and Frank analyzed the effect of coupon location as well as sensitivity to coupon type. Tensile tests were performed on coupons taken from the webs and flanges of all sections. The coupons were either full thickness 8-inch gage length plate-type or ½-inch rounds. For most steel producers, the flange yield strength was found to be about 95% of the web yield strength (one producer had widely varying results which increased the overall average to 98%). The Jaquess and Frank tensile tests revealed that the strain hardening modulus, E_{sh} is higher and the strain at strain hardening, ε_{sh} is lower in ½ inch round coupons than in plate-type coupons. The upper yield point, F_{uy} may also be higher for the ½ inch round coupons, but the research results were inconclusive.

Jaquess and Frank investigated several stress-strain parameters. The crosshead test rate was 0.05 inch/minute/inch in the elastic region. The rate was then increased to 0.4

inch/minute/inch after the coupon reached strain hardening. Approximately 65% of the coupons tested exhibited upper yield points. For specimens that exhibited upper yield point behavior, the upper yield point averaged 3% larger then the yield strength value at 0.2% offset. Tables 8 and 9 summarize the web and flange tensile test results for A572 Gr. 50 steel respectively.

Table 8: Summary of flange tensile test results for A572 Gr. 50 steel (Jaquess & Frank, 1999)

	F_{uy} (ksi)	$F_{y\,0.2\%}$ (ksi)	$F_{y\,static}$ (ksi)	$F_{y\,0.2\%}$ / $F_{y\,static}$ (ksi)	$F_{y\,0.2\%}$ / $F_{y\,mill}$ (ksi)	F_u (ksi)	F_u / $F_{u\,mill}$ (ksi)	Elongation (%)
# of Data	41	59	59	59	59	63	63	63
Mean	56.5	54.4	52.0	1.04	0.94	72.5	0.96	31.2
COV	0.080	0.073	0.077	0.010	0.064	0.041	0.042	0.144

Table 9: Summary of web tensile test results for A572 Gr. 50 steel (Jaquess & Frank, 1999)

	$F_{y\,0.2\%}$ (ksi)	$F_{y\,static}$ (ksi)	$F_{y\,0.2\%}$ / $F_{y\,static}$ (ksi)	F_u (ksi)	Elongation (%)
# of Data	42	42	42	43	43
Mean	55.40	52.9	1.05	72.1	29.4
COV	0.077	0.085	0.010	0.055	0.184

2.3.4 Brockenbrough, R. L. (2000): "MTR Survey of Plate Material Used in Structural Fabrication"

In 2000, Brockenbrough conducted a mill test report survey of plate material used in structural fabrication. Two domestic steel plate producers provided 1999 mill test report data. Histograms were generated, and statistics were tabulated for tensile properties, impact properties, and chemical composition. The study consisted of the following ASTM steel designations: A36, A572 Gr. 50, A572 Gr. 60, A588, and A514. The statistics for 50 ksi plate steel most relevant to the scope of the resistance factor research are shown in Table 10.

Table 10: Weighted statistics for 50 ksi plate steel (Brockenbrough, 2000)

Type of Steel	A572 Gr. 50 t<0.5 in.	A572 Gr. 50 t>0.5 in.	Combined A572 Gr. 50
Number of Data	526	1826	2352
Yield Strength (ksi)			
Weighted Mean	57.55	58.39	58.2
Weighted COV	0.086	0.062	0.067
Tensile Strength (ksi)			
Weighted Mean	78.05	83.95	82.63
Weighted COV	0.048	0.049	0.049
Yield/Tensile Ratio			
Weighted Mean	0.736	0.696	0.705
Weighted COV	0.049	0.044	0.045

2.3.5 Dexter et al (2000): SSPC Material Property Survey

The latest material property survey was conducted by Dexter et al. at the University of Minnesota for the Structural Shape Producer's Council (SSPC). The steel survey was exclusively on structural wide-flange shapes sold for construction in the United States in 1998. The data consisted of more than 29,500 mill test reports from five structural steel producers. The scope of work included sorting the mill test report data according to grade and ASTM A6 shape group. Histograms were plotted and summary statistics were evaluated for important tensile, chemical composition, and toughness properties.

Dexter et al. concluded that A992 steel was not significantly different than A572 Gr. 50 steel. A992 and other grade 50 steel were also not significantly different than the 1992 Frank and Read data for web tested dual grade and A572 Gr. 50 steel. In addition, the mean yield strength of the web data was slightly, but not significantly higher than the mean yield strength of the flange data. Statistics of the tensile properties did not vary significantly with shape group or producer. Table 11 summarizes the grade 50 tensile data for both flanges and webs. Figures 10, 11, and 12 are A992 steel histograms of mill test F_y, F_u, and Y/T respectively.

Table 11: Summary of 1998 mill test report data (Dexter et al., 2000)

ASTM Specification	A572 Gr. 50 (flange)	A992 (flange)	A992 (web)
Number of Data	1,052	20,295	4,925
Yield Strength (ksi)			
Mean	60.5	55.8	56.5
COV	0.066	0.058	0.054
Tensile Strength (ksi)			
Mean	76.3	73.3	73.3
COV	0.050	0.044	0.046
Yield/Tensile Ratio			
Mean	0.790	0.760	0.770
COV	0.047	0.040	0.089

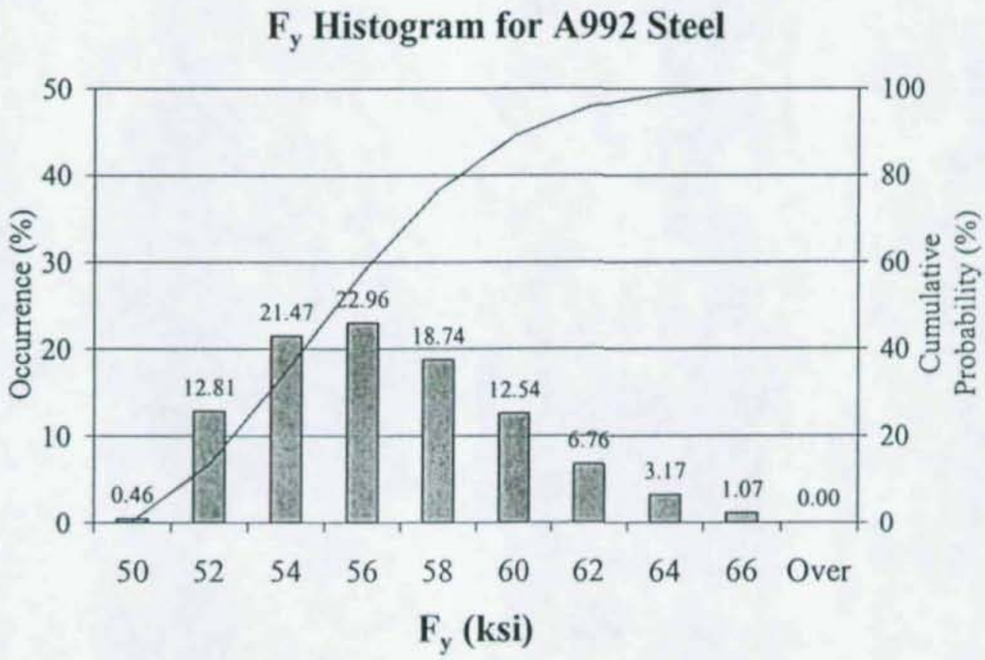

Figure 10: $F_{y\ mill}$ histogram for A992 steel taken from the flange (Dexter et al., 2000)

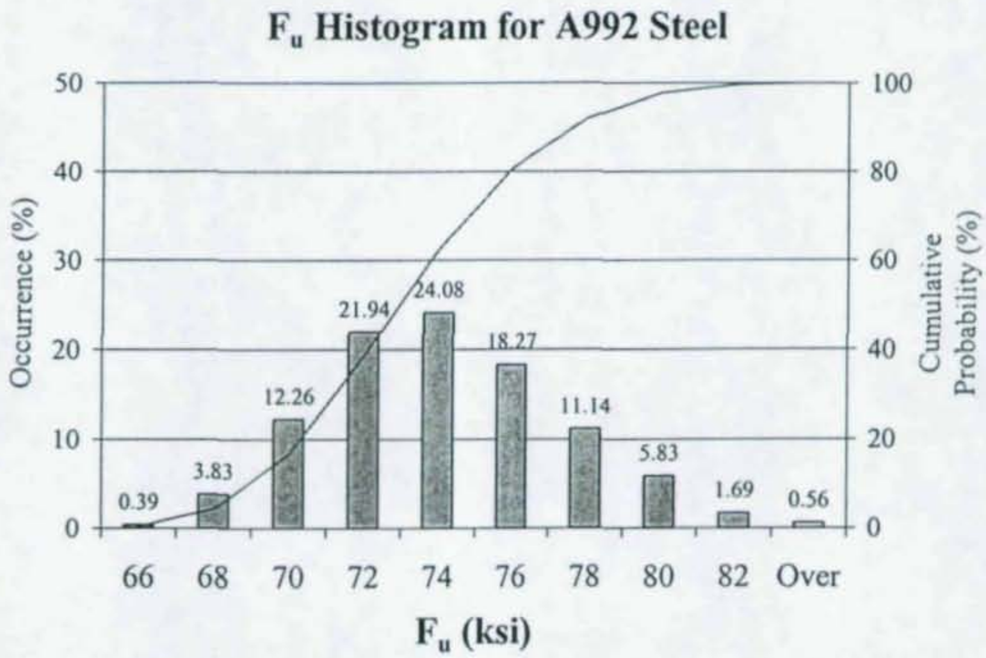

Figure 11: $F_{u\ mill}$ histogram for A992 steel taken from the flange (Dexter et al., 2000)

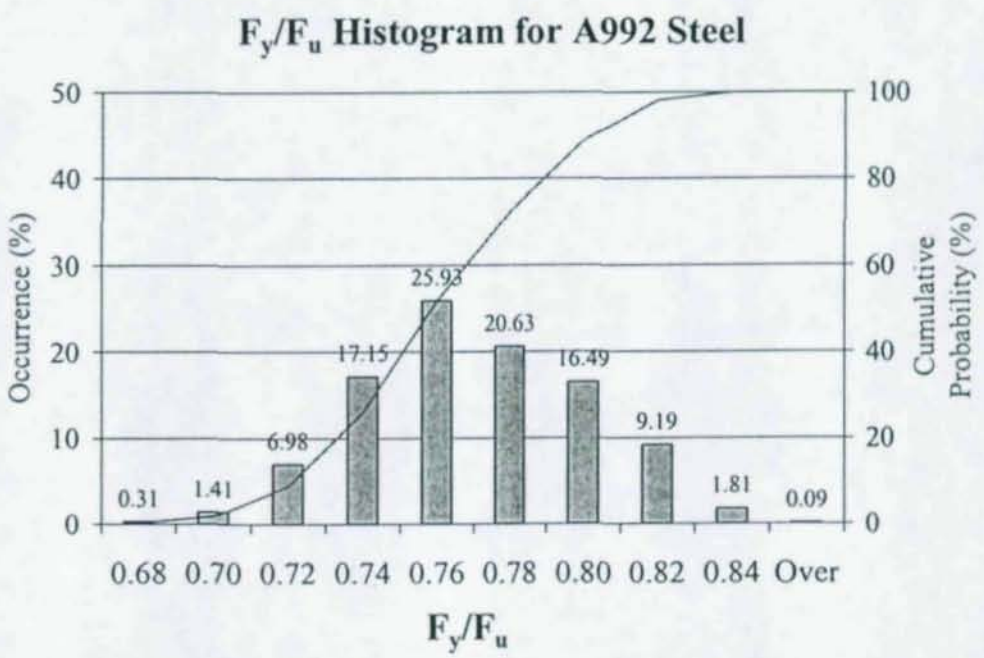

Figure 12: Y/T histogram for A992 steel taken from the flange (Dexter et al., 2000)

Several changes have occurred in steel production and specification. A few of these changes are apparent when comparing the Frank and Reed 1992 mill data with the 1998 Dexter et al. mill data. Unlike the 1992 survey, the 1998 SSPC material property survey includes the new A992 specification steel as well as the change in tensile test location from the web to the flange. Each data point in the SSPC survey represented a single heat of steel, however, most structural steel shapes meet several specifications and grades within specifications. As a result, Dexter et al. developed a consistent method to assign only one specification and grade to each heat (Dexter et al., 2000). The steel heat classification scheme used in the survey is summarized below.

1) If the producer assigned the heat to one and only one grade, then the steel was assigned to that grade only.
2) If the steel was not classified by the producer to a unique grade and the heat met A992 specifications, then it was classed as A992.
3) If the heat did not meet A992, but met A572 Gr. 50 specifications, it was classed as A572 Gr 50.
4) If the heat was not classified yet by the above criteria, and it met the A36 specification, it was classed as A36.

This classification resulted in a significant portion of the data, 85%, classified as A992 steel. The A992 steel also satisfies both A572 Gr. 50 and A36 specifications, but it was not included in those groups because it would overwhelm the small number of data that only met A36 or A572 and not A992 (Dexter et al., 2000). The resistance factor calibration for modern steel is concerned with the material properties of A992 steel. Therefore, the classification scheme incorporated in the SSPC report is still appropriate for this research. The Dexter et al. report for SSPC represents the most recent mill test report survey of tensile properties for A992 structural steel. These mill data will be used subsequently for comparison and correlation with laboratory tensile test results.

Chapter 3: Testing Procedure & Results

3.1 Tensile Testing Procedure

More than 200 tensile tests were performed on A992 steel coupons taken from several wide-flange shapes. The tests were performed at the University of Western Ontario and the University of Minnesota. The test coupons were equally distributed between laboratories so that there could be a direct comparison of results. The University of Western Ontario tested the samples with a Tinius Olsen Universal Testing Machine, model #120 D, with a capacity of 120 kips. The University of Minnesota performed all tests with a 600 kip MTS machine.

Steel sections were provided by three major structural steel producers. The sections represented several W-shape sizes and heats of A992 steel. The shapes tested are listed in Table 12.

Table 12: W-shapes tested

W6x25	W14x257
W8x31	W24x76
W12x65	W30x99
W14x176	W36x150

Test coupons were taken from the web and flange of each section. The coupon test locations are shown as the shaded regions in Figure 13.

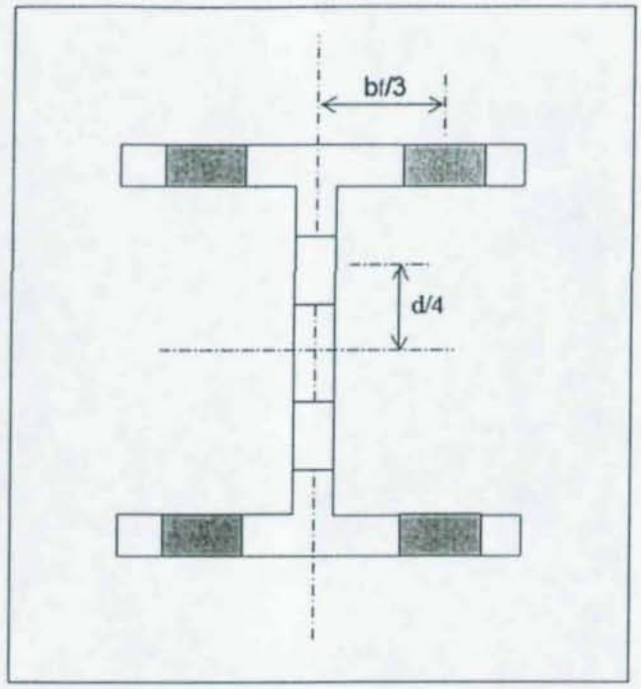

Figure 13: Tensile test locations

Two types of coupons were machined for testing, and are illustrated in Figures 14 and 15.

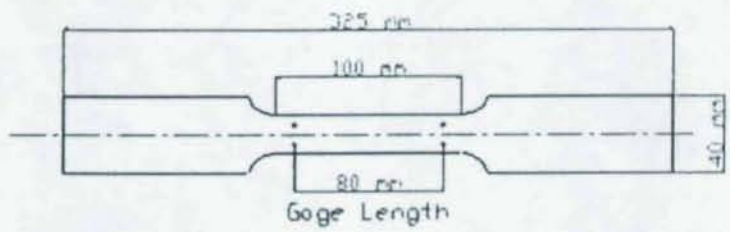

Figure 14: European standard test coupon

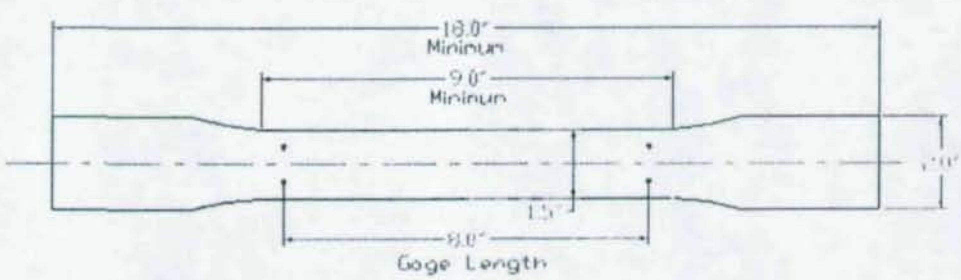

Figure 15: ASTM A370 plate-type coupon

Most coupons were machined as full-thickness 8-inch gage length plate-type coupons according to ASTM A370. A few large specimens were milled down to ½ thickness due to limitations in capacity of the test equipment. Other coupons were also machined full-thickness, but in accordance to the European Standard: EN 10 002-1:1990. This coupon type was selected because it is a standard test coupon size utilized by European mills.

The tensile tests were performed according to ASTM A370. The test specimens were loaded at a constant crosshead separation of 0.0175 inches per minute per inch of reduced section in the elastic region. After the specimen reached the yield plateau, static yield stress readings were performed according to the SSRC procedure detailed earlier. After the last static yield stress reading, the crosshead separation was then increased to 0.275 inches per minute per inch of reduced section for the strain-hardening region of the stress-strain curve. The tensile test setup is shown in Figure 16.

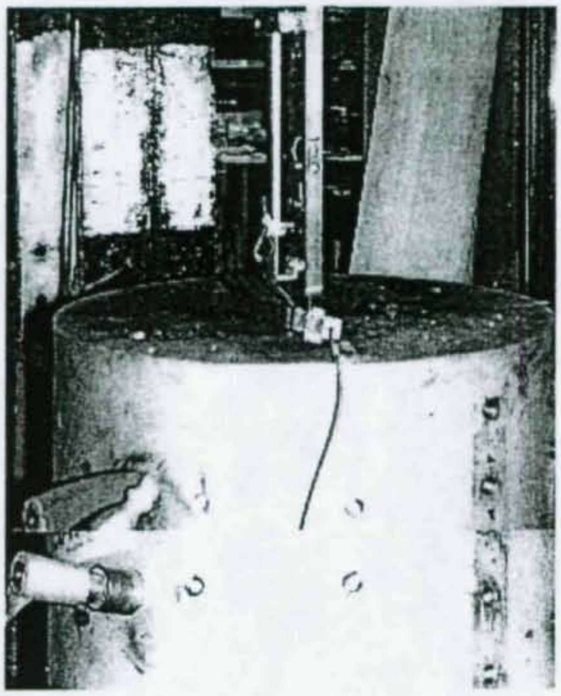

Figure 16: Tensile test setup

Each laboratory acquired the tensile test data digitally for each test specimen. The data were then plotted to obtain stress-strain curves. The yield stress was determined by the

0.2% offset method. After the test was completed, total elongation was measured from putting the pieces of the test coupon back together.

The laboratory results from both universities were compared. The test results for most material properties were considered the same for each laboratory. Material properties such as, strain at strain-hardening, elastic modulus, and yield stress were consistent between laboratories.

The yield stress values for each laboratory were only approximately 0.5 ksi apart. However, the distribution of the University of Minnesota data were consistently higher then the University of Western Ontario data, so the results are conservatively presented separately due to this bias. The ultimate tensile strength values featured the largest disparity between the two laboratories. This was because several University of Western Ontario tests were abbreviated due to instrumentation. The elongation of the test specimen was often greater than the displacement range of the strain instrumentation. As a result, the ultimate tensile strength results were typically underestimated because the data stopped short of the actual ultimate tensile strength. Therefore, the University of Western Ontario ultimate strength and percent elongation results are not included in the analysis.

The University of Western Ontario lab equipment was not capable of performing static yield stress readings. Therefore, all static yield test results are from the University of Minnesota.

3.2 Tensile Test Results

3.2.1 *Overview*

Important stress statistics from the A992 steel laboratory tensile tests are summarized in Tables 13 and 14.

Table 13: University of Minnesota tensile test results and corresponding mill data.

University of Minnesota (A992 flange data)							
	F_{uy} (ksi)	$F_{y\,0.2\%}$ (ksi)	$F_{y\,static}$ (ksi)	$F_{y\,mill}$ (ksi	F_u (ksi)	$F_{u\,mill}$ (ksi)	Y/T
Samples	58	58	57	60	58	60	58
Average	56.9	55.3	51.0	54.9	72.4	71.8	0.764
Min.	52.5	49.8	46.0	50.0	66.9	66.5	0.714
Max.	65.3	65.3	61.5	61.3	83.1	84.2	0.823
COV	0.054	0.054	0.061	0.049	0.045	0.055	0.036

University of Minnesota (A992 web & flange data)				
	E_{sh} (ksi)	ε_{sh} (%)	ε_u (%)	Elongation (%)
Samples	88	88	88	87
Average	323	2.5	15.8	27.9
Min.	209	1.0	9.9	18.8
Max.	497	4.4	19.1	35.9
COV	0.182	0.267	0.111	0.115

Table 14: University of Western Ontario tensile test results and corresponding mill data

U. of Western Ontario (A992 data)				
		flange		web & flange
	F_{uy} (ksi)	$F_{y\,0.2\%}$ (ksi)	$F_{y\,mill}$ (ksi	ε_{sh} (%)
Samples	73	73	75	119
Average	56.5	54.8	55.2	2.2
Min.	51.1	49.6	50.0	0.2
Max.	63.8	63.8	61.4	3.8
COV	0.059	0.057	0.050	0.300

Histograms of frequency of occurrence for several important material properties were created. The laboratory test results were also compared to past material property surveys and mill data.

The test results were primarily compared with the SSPC mill survey data analyzed by Dexter et al. 2000 because this data consists of A992 wide-flange steel shapes. A572 Gr. 50 studies are also included for comparison of A992 material properties with past steel properties.

3.2.2 *Upper Yield Point, F_{uy}*

The upper yield point (F_{uy}) phenomenon is common in structural steel. The yield point determined from the drop of the beam method is reported as the yield stress value (F_y) by some steel mills. The upper yield point value can be more than 5% larger than the yield stress determined from the offset method ($F_{y\,0.2\%}$). Therefore, it is important to characterize this behavior. Figures 17 and 18 are histograms for the upper yield point. Figure 17 includes all flange-tested data, and Figure 18 includes the upper yield point divided by the corresponding yield stress. The upper yield point phenomenon occurred in 64% of the tensile test specimens. Any test specimen without a definite upper yield point, F_{uy} was reported as the peak yield stress immediately before the yield plateau.

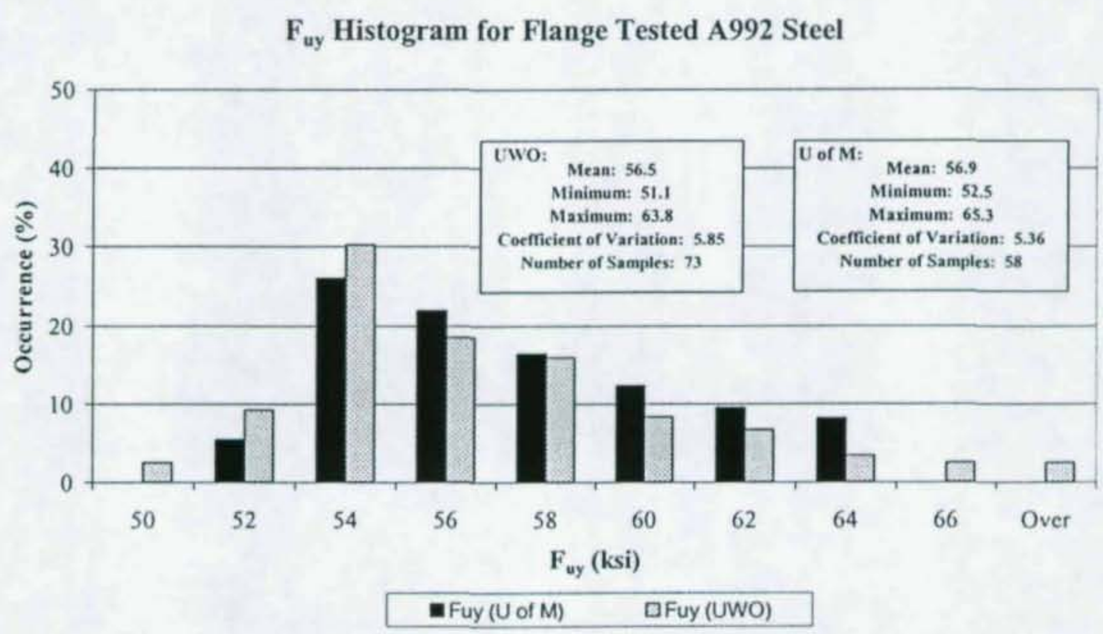

Figure 17: Upper yield point, F_{uy} histogram for all flange tested A992 steel

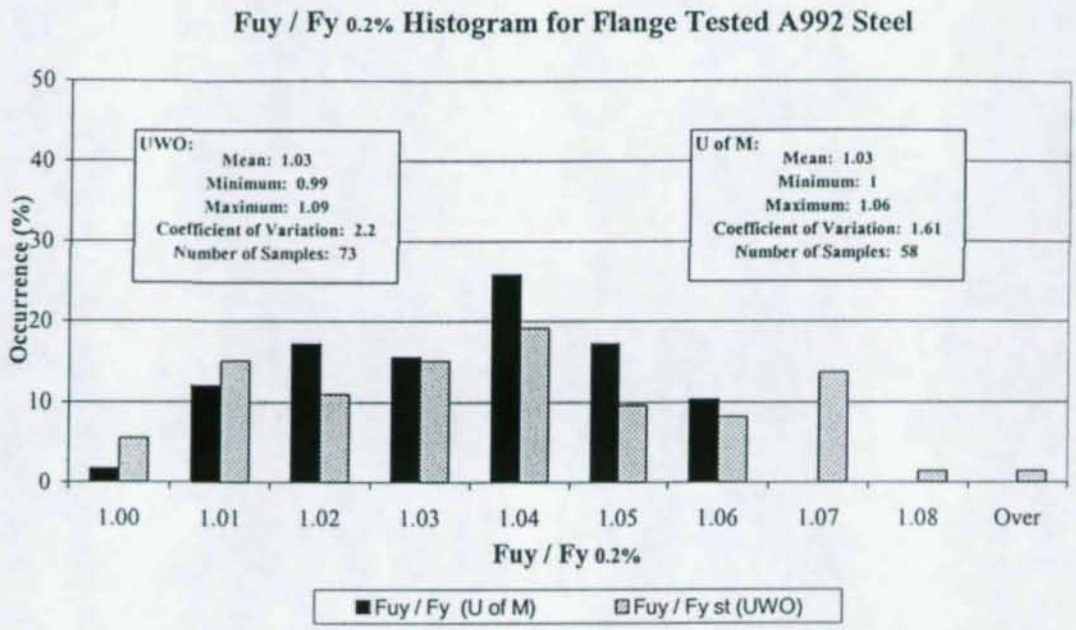

Figure 18: Upper yield point divided by yield stress, F_{uy} / $F_{y\ 0.2\%}$ histogram for flange tested A992 steel

The F_{uy} / $F_{y\ 0.2\%}$ histogram indicates that there is not a strong relation between the upper yield point and the yield stress. This is most likely because not all steel specimens exhibited a definite upper yield point.

The 1999 study by Jaquess & Frank investigated upper yield point behavior for A572 Gr. 50 steel. The A992 tensile test results and the A572 Gr. 50 results are included in Tables 15 and 16, respectively.

Table 15: A992 Upper yield point laboratory test results

	University of Minnesota			University of Western Ontario		
Source	Lab Tests			Lab Tests		
Steel	A992			A992		
Type	Flange			Flange		
Property	F_{uy} (ksi)	F_{uy} / $F_{y\,0.2\%}$	$F_{uy}/F_{y\,mill}$	F_{uy} (ksi)	F_{uy} / $F_{y\,0.2\%}$	$F_{uy}/F_{y\,mill}$
Samples	58	58	58	73	73	73
Mean	56.9	1.03	1.04	56.5	1.03	1.03
Min.	52.5	1.00	0.96	51.1	0.99	0.94
Max.	65.3	1.06	1.23	63.8	1.09	1.17
COV	0.054	0.016	0.051	0.059	0.022	0.050

Table 16: A572 Gr. 50 upper yield point test results from Jaquess & Frank, 1999

	Jaquess & Frank, 1999		
Source	Lab Tests		
Steel	A572 Gr. 50		
Type	Flange		
Property	F_{uy} (ksi)	F_{uy} / $F_{y\,0.2\%}$	$F_{uy}/F_{y\,mill}$
Samples	41	27	41
Mean	56.5	1.03	0.98
Min.	48.0	1.01	0.92
Max.	64.5	1.06	1.04
COV	0.080	0.019	0.031

The University of Minnesota and the University of Western Ontario A992 test results correlate very well. The only differences are due to slightly higher upper yield point values for the University of Minnesota when compared to the University of Western Ontario.

The Jaquess and Frank mean upper yield point value is consistent with the A992 test results. The F_{uy} / $F_{y\ mill}$ ratio = 0.98, however is considerably lower than the mean ratios for the A992 steel which range from 1.02 to 1.04.

3.2.3 *Yield Stress, Fy*

The yield stress is a very significant parameter in structural steel design. Steel member and connection design criteria are based on yield stress data. All yield stress values from laboratory tests were obtained by the 0.2% offset method. Figure 19 is a comparison between the laboratory yield stress test results and the A992 SSPC mill test data from the Dexter et al. 2000 survey.

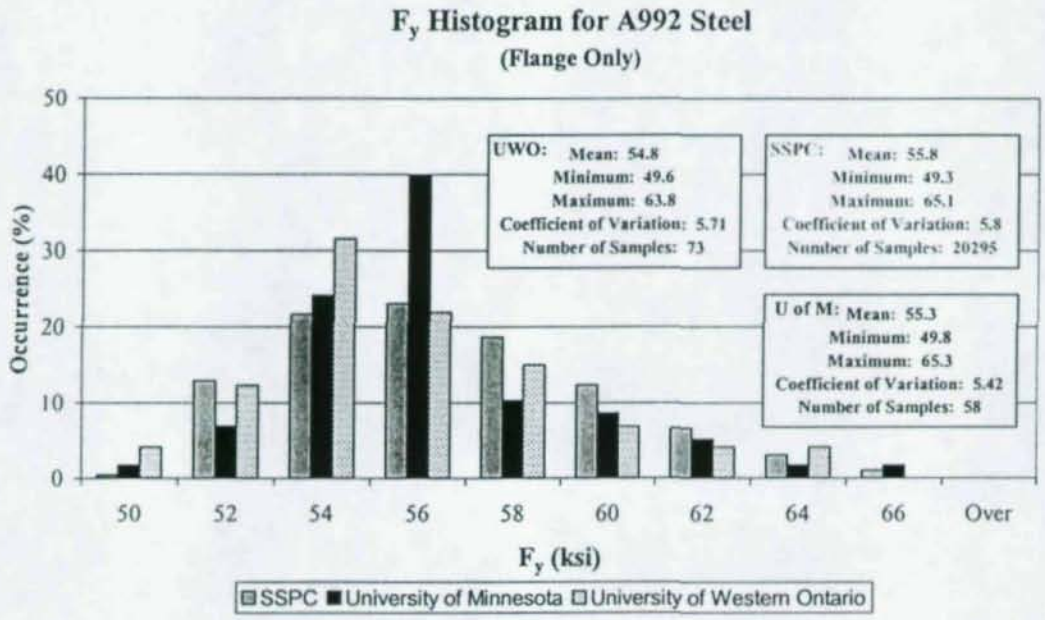

Figure 19: Yield stress, F_y histogram for A992 flange data

The current A992 test data from both laboratories (U of M & UWO) correlate very well with the SSPC A992 mill test data. The mean values, coefficient of variation, and the distribution of data shown in the histogram are consistent between all three sources.

A statistical breakdown of yield stress data for A992 steel and A572 Gr. 50 steel is included in Tables 17 and 18, respectively.

Table 17: Yield stress comparison for A992 steel

	University of Minnesota			University of Western Ontario			Dexter et al., 2000
Source	Lab Tests			Lab Tests			SSPC Mill Data
Steel	A992			A992			A992
Type	Flange	Web	Flange	Flange	Web	Flange	Flange
Property	$F_{y\ 0.2\%}$ (ksi)	$F_{y\ 0.2\%}$ (ksi)	$F_{y\,0.2\%}$ / $F_{y\ mill}$	$F_{y\ 0.2\%}$ (ksi)	$F_{y\ 0.2\%}$ (ksi)	$F_{y\,0.2\%}$ / $F_{y\ mill}$	F_y (ksi)
Samples	58	30	58	73	46	73	20295
Mean	55.3	58.5	1.01	54.8	57.5	0.99	55.8
Min.	49.8	50.7	0.95	49.6	50.4	0.91	49.3
Max.	65.3	70.7	1.18	63.8	69.7	1.14	65.1
COV	0.054	0.085	0.044	0.057	0.084	0.043	0.058

The yield stress test results for both the University of Minnesota and the University of Western Ontario are very similar. The mean web and flange yield stress results from the University of Minnesota are approximately 0.5 and 1 ksi higher respectively, than the results from the University of Western Ontario. The two laboratories had essentially the same level of variation. The laboratory results are also essentially the same as the SSPC A992 mill data in the Dexter et al. 2000 survey. The A992 steel test results and mill data are summarized in Table 17.

The tested yield stress to mill test ratios for both laboratories were essentially 1.0 (1.01 & 0.99). It is apparent from the yield stress comparison between the laboratory test results and the SSPC mill data that the mill tests are not performed at the maximum strain rate. This statement was affirmed at a meeting with SSPC members.

Table 18 summarizes data for A572 Gr. 50 steel. The Frank and Read web mill data for A572 Gr. 50 steel is very similar to the Brockenbrough, 2000 plate data for A572 Gr. 50 steel. The A992 yield stress results for the web are also similar to these A572 Gr. 50 results.

Table 18: Yield stress comparison for A572 Gr. 50 steel

	Jaquess & Frank, 1999			Frank & Read, 1993	Brockenbrough, 2000
Source	Lab Tests			Mill Data	Mill Data
Steel	A572 Gr. 50			A572 Gr. 50	A572 Gr. 50
Type	Flange	Web	Flange	Web	Plate
Property	$F_{y\ 0.2\%}$ (ksi)	$F_{y\ 0.2\%}$ (ksi)	$F_{y\,0.2\%}$ / $F_{y\ mill}$	F_y (ksi)	F_y (ksi)
Samples	59	42	59	13536	2352
Mean	54.5	55.4	0.94	57.6	58.2
Min.	48.0	47.4	0.75	50.0	25.0
Max.	64.0	65.7	1.03	79.5	82.9
COV	0.073	0.077	0.064	0.089	0.067

Jaquess and Frank reported a test yield stress to mill yield stress ratio for flanges = 0.94, whereas, this ratio was near 1.00 for the current A992 test results. The average mill test report yield stress for the Jaquess and Frank data was considerably higher than the SSPC mill values. The A572 Gr. 50 mill tests may have been performed at higher strain rates or the mills may have reported yield point values from the drop of the beam method.

3.2.4 *Static Yield Stress, $F_{y\ static}$*

The static yield stress is another significant material property. Unlike yield stress and yield point, the static yield stress is similar to the actual loading rate of most structures, and it is independent of strain rate and test equipment. The static yield test is not performed at steel mills, so comparison can only be made with research laboratory results. Figure 20, and Figure 21 contain static yield stress histograms of A992 flange specimens tested at the University of Minnesota.

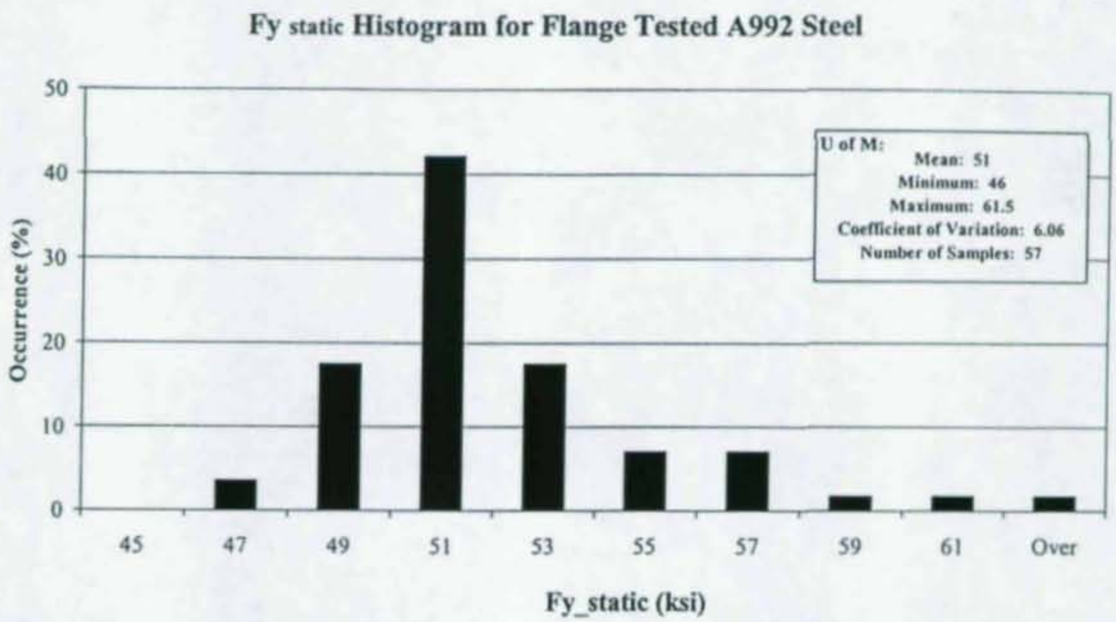

Figure 20: $F_{y\,static}$ histogram of A992 flange specimens tested at the University of Minnesota.

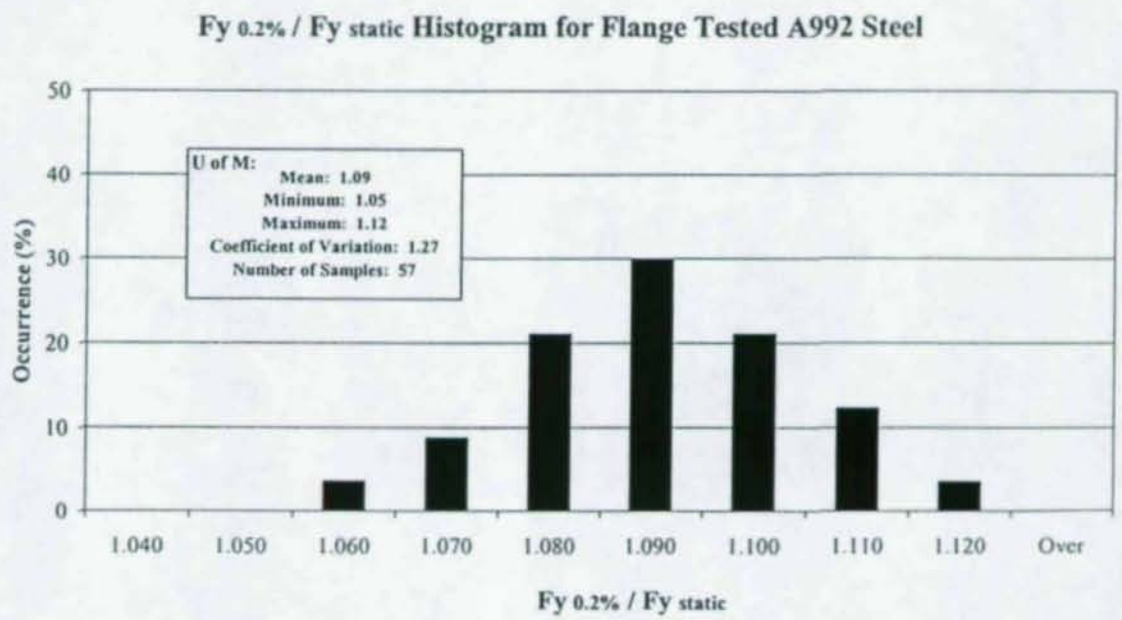

Figure 21: $F_{y\,0.2\%}$ / $F_{y\,static}$ histogram of A992 flange specimens tested at the University of Minnesota.

The static yield stress data in Figure 20 appear to fit a lognormal distribution. Tables 19 and 20 contain a comparison of the A992 University of Minnesota static yield stress data with the A572 Gr. 50 Jaquess and Frank test data.

Table 19: University of Minnesota static yield stress data

	University of Minnesota				
Source	Lab Tests				
Steel	A992				
Type	Flange	Flange	Web	Flange	Web
Property	$F_{y\ static}/F_{y\ mill}$	$F_{y\ 0.2\%}$ / $F_{y\ static}$	$F_{y\ 0.2\%}$ / $F_{y\ static}$	$F_{y\ statuc}$ (ksi)	$F_{y\ statuc}$ (ksi)
Samples	57	57	29	57	29
Mean	0.93	1.09	1.08	51.0	53.6
Min.	0.86	1.05	1.06	46.0	47.0
Max.	1.11	1.12	1.12	61.5	65.4
COV	0.051	0.013	0.012	0.061	0.084

Table 20: Jaquess & Frank static yield stress data

	Jaquess & Frank, 1999				
Source	Lab Tests				
Steel	A572 Gr. 50				
Type	Flange	Flange	Web	Flange	Web
Property	$F_{y\ static}/F_{y\ mill}$	$F_{y\ 0.2\%}$ / $F_{y\ static}$	$F_{y\ 0.2\%}$ / $F_{y\ static}$	$F_{y\ statuc}$ (ksi)	$F_{y\ statuc}$ (ksi)
Samples	62	59	42	59	42
Mean	0.90	1.04	1.05	52.0	52.9
Min.	0.71	1.01	1.03	45.5	45.4
Max.	1.00	1.08	1.07	62.0	63.8
COV	0.067	0.010	0.010	0.077	0.085

The mean $F_{y\ static}$ / $F_{y\ mill}$ ratios ranged from 0.93 for A992 steel to 0.90 for A572 Gr. 50 steel. The mean ratio values for the $F_{y\ 0.2\%}$ / $F_{y\ static}$ are different, but the coefficients of variation are the same. The difference in mean ratio values may be due to strain rate effects.

3.2.5 *Ultimate Tensile Strength, F_u*

The ultimate tensile strength material property is used in steel connection design. Figure 22 is a histogram of the ultimate tensile strength of A992 steel.

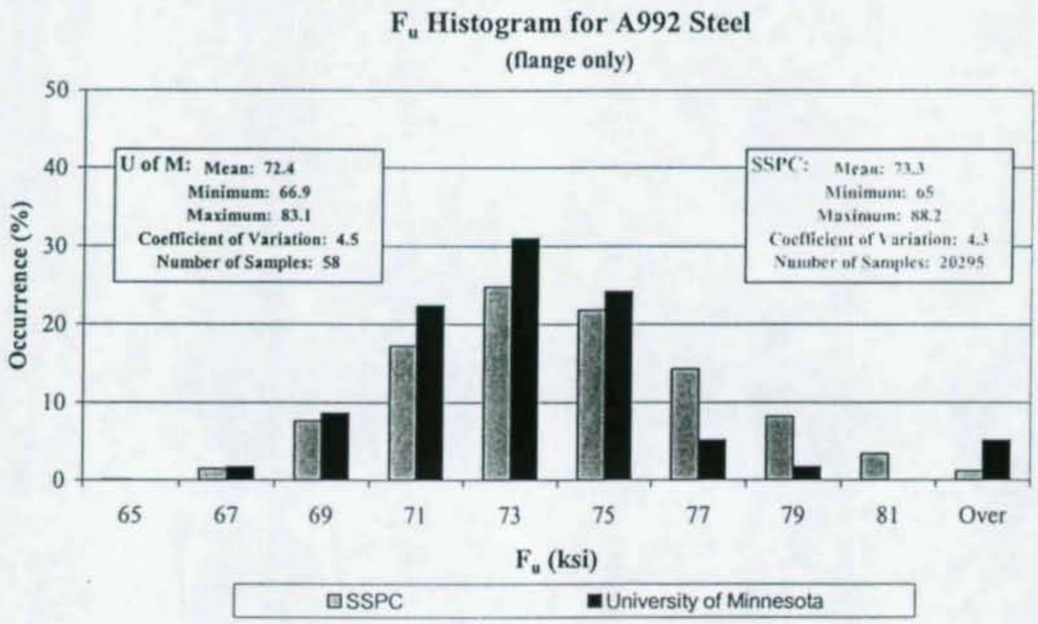

Figure 22: F_u histogram comparison for A992 steel

The University of Minnesota lab results once again correlate well with the SSPC mill data. The distributions of both data sets and the coefficients of variations are essentially the same. The A992 flange statistical data for ultimate strength is included in Table 21.

Table 21: Ultimate tensile strength data for A992 steel

	University of Minnesota		Dexter et al., 2000
Source	Lab Tests		SSPC Mill Data
Steel	A992		A992
Type	Flange		Flange
Property	F_u (ksi)	$F_u/F_{u\ mill}$	F_u (ksi)
Samples	58	58	20295
Mean	72.4	1.02	73.3
Min.	66.9	0.96	65.0
Max.	83.1	1.08	88.2
COV	0.045	0.026	0.043

Ultimate tensile strength data is summarized in Table 22 for A572 Gr. 50 steel.

Table 22: Ultimate tensile strength data for A572 Gr. 50 steel

	Jaquess & Frank, 1999			Frank & Read, 1993	Brockenbrough, 2000
Source	Lab Tests			Mill Data	Mill Data
Steel	A572 Gr. 50			A572 Gr. 50	
Type	Flange	Web	Flange	Web	Plate
Property	F_u (ksi)	F_u (ksi)	$F_u/F_{u\ mill}$	F_u (ksi)	F_u (ksi)
Samples	63	43	63	13536	2352
Mean	72.5	72.1	0.96	75.6	82.6
Min.	66.0	64.9	0.85	65.0	50.0
Max.	77.5	81.6	1.03	104.0	109.0
COV	0.041	0.055	0.042	0.082	0.049

The mean ultimate tensile strength for plates is significantly higher than for rolled shapes. The wide-flange shape ultimate strength statistics are similar for A992 and A572 Gr. 50 steel.

3.2.6 Yield-to-Tensile Ratio, Y/T

The yield-to-tensile ratio, Y/T is a particularly important material property in connection design. Steels with high Y/T ratios are more likely to fail by fracture than by yielding. This failure mechanism is more unpredictable and is typically avoided when possible. The Y/T histogram comparison for flange A992 steel is illustrated in Figure 23.

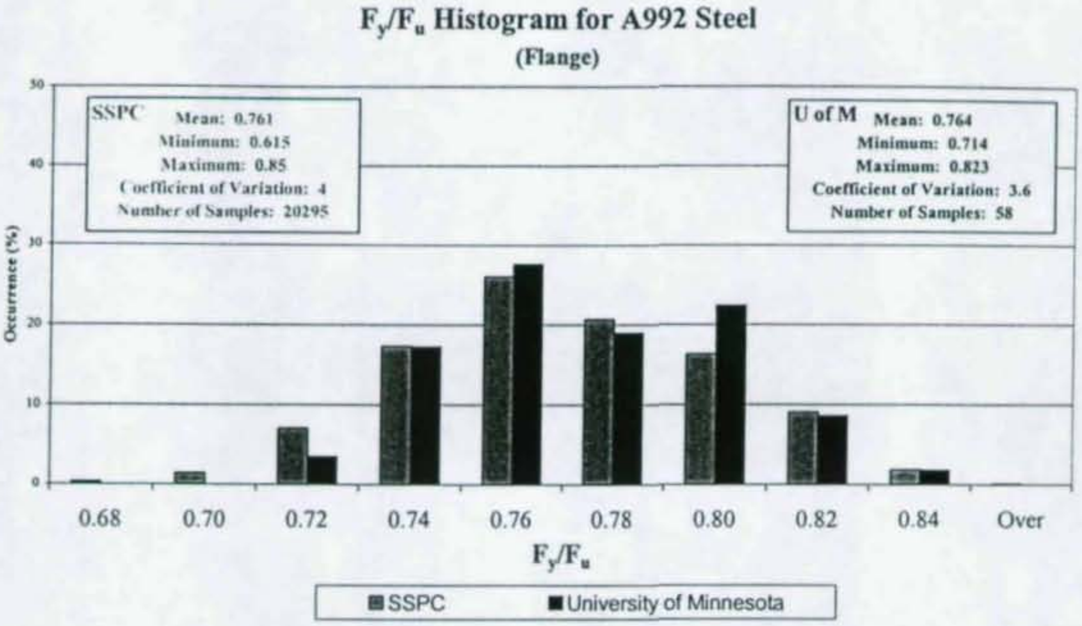

Figure 23: Y/T histogram comparison for A992 steel

The yield-to-tensile ratio data for A992 and A572 Gr. 50 steel are included in Tables 23 and 24.

Table 23: A992 Y/T data

	University of Minnesota	Dexter et al., 2000
Source	Lab Tests	SSPC Mill Data
Steel	A992	A992
Type	Flange	Flange
Property	Y/T	Y/T
Samples	58	20295
Mean	0.764	0.761
Min.	0.714	0.615
Max.	0.823	0.850
COV	0.036	0.040

Table 24: A572 Gr. 50 Y/T data

	Jaquess & Frank, 1999	Frank & Read, 1993	Brockenbrough, 2000
Source	Lab Tests	Mill Data	Mill Data
Steel	A572 Gr. 50	A572 Gr. 50	A572 Gr. 50
Type	Flange	Web	Plate
Property	Y/T	Y/T	Y/T
Samples	59	13536	2352
Mean	0.752	0.763	0.705
Min.	0.688	0.618	0.500
Max.	0.839	0.954	0.882
COV	0.044	0.063	0.045

The Y/T values for plates are lower than for W-shapes due to the significantly higher ultimate strength values. Once again, the University of Minnesota laboratory results are essentially the same as the A992 SSPC mill data. The mean yield-to-tensile ratio values are similar for A992 and A572 Gr. 50 rolled shapes. The range in Y/T values and consequently the COV is smaller for A992 steel than for A572 Gr. 50 steel. This is most likely due to the new restriction found in the A992 specification.

3.2.7 Percent Elongation

Percent elongation is a parameter, which accounts for ductility. Tables 25 and 26 summarize the percent elongation for grade 50 steel. Percent elongation values are dependant on coupon dimensions. As a result, only the ASTM A370 coupon percent elongation test results are presented. Also, only the University of Minnesota percent elongation test results are included because most tensile tests at the University of Western Ontario were not performed all the way to failure.

Table 25: Percent elongation data for A992 steel

	University of Minnesota		Dexter et al., 2000
Source	Lab Tests		SSPC Mill Data
Steel	A992		A992
Type	Web & Flange	Flange	Web & Flange
Property	Elongation (%)	$El._{test} / El._{mill}$	Elongation (%)
Samples	87	57	24847
Mean	27.9	1.19	24.2
Min.	18.8	0.99	18.0
Max.	35.9	1.51	51.0
COV	0.115	0.105	0.082

Table 26: Percent elongation data for A572 Gr. 50 steel

	Jaquess & Frank, 1999			Brockenbrough, 2000
Source	Lab Tests			Mill Data
Steel	A572 Gr. 50			572 Gr. 50
Type	Flange	Web	Flange	Plate
Property	Elongation (%)	Elongation (%)	$El._{test} / El._{mill}$	Elongation (%)
Samples	63	43	12	2319
Mean	31.2	29.4	1.11	22.3
Min.	25.0	22.0	0.95	10.0
Max.	44.0	43.0	1.26	45.0
COV	0.144	0.184	0.081	0.120

The A992 and A572 Gr. 50 laboratory results both featured mean percent elongation values larger than the mill percent elongation values. Mill test percent elongation values for plates and rolled shapes were consistently less than laboratory test values.

3.2.8 Strain Properties

Table 27 includes strain properties for A992 tested steel. Test results from the University of Minnesota and the University of Western Ontario were essentially the same for these material properties and are presented together. The corresponding statistical data for A572 Gr. 50 steel from research by Jaquess and Frank are included in Table 28.

Table 27: Strain tensile test results for A992 steel

(combined University of Minnesota & University of Western Ontario results)

U. of Minnesota & U. of Western Ontario		
Source	Lab Tests	
Type	Web & Flange	
Property	ε_{sh} (%)	ε_u* (%)
Samples	207	88
Mean	2.3	15.8
Min.	0.2	9.9
Max.	4.4	19.1
COV	0.289	0.111

* University of Minnesota data only

Table 28: Strain tensile test results for A572 Gr. 50 steel

(Jaquess & Frank, 1999)

Jaquess & Frank, 1999		
Source	Lab Tests	
Steel	A572 Gr. 50	
Type	Flange	
Property	ε_{sh} (%)	ε_u (%)
Samples	38	59
Mean	1.5	14.9
Min.	0.7	11.8
Max.	2.4	20.2
COV	0.333	0.133

3.3 Trends and Notable Behavior

Notable trends and behavior observed from the tensile tests were investigated. Correlations between various material properties with ASTM group, material thickness, and producer were all considered. A few trends were observed from the tensile test results.

3.3.1 *Web & Flange Yield Stress Comparison*

For wide-flange shapes, the yield stress in the web is typically higher than in the flange. The effect of the coupon test location was investigated. Initial analysis of the test data revealed a significantly larger yield stress in the web when compared to the flange. Figures 24 and 25 compare the web and flange yield stress values for each laboratory.

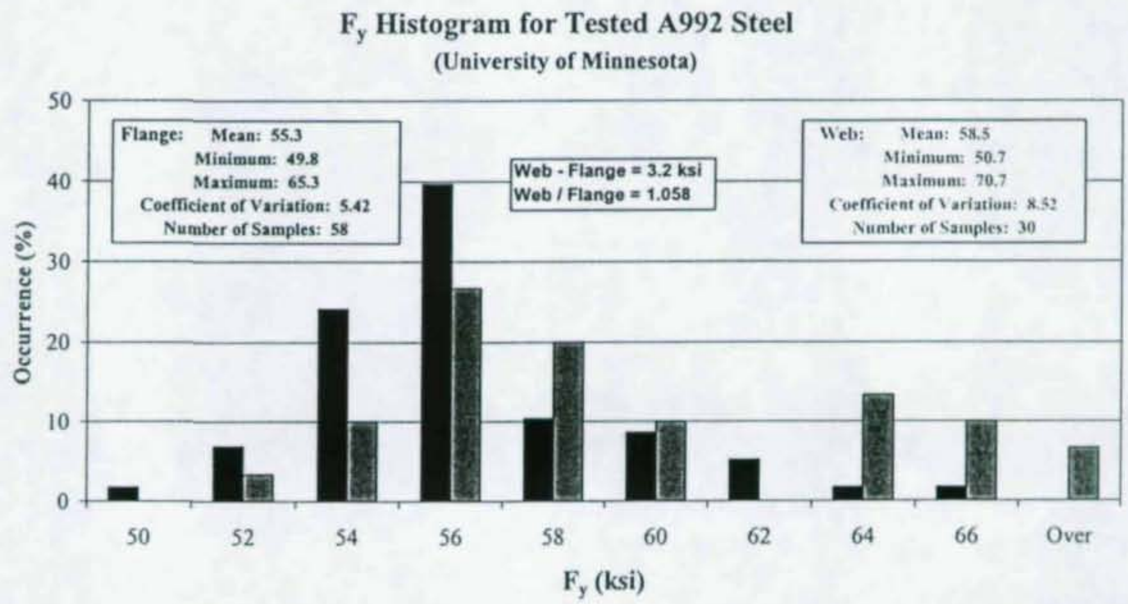

Figure 24: $F_{y\,0.2\%}$ histogram comparison between web and flange for the University of Minnesota tensile test results

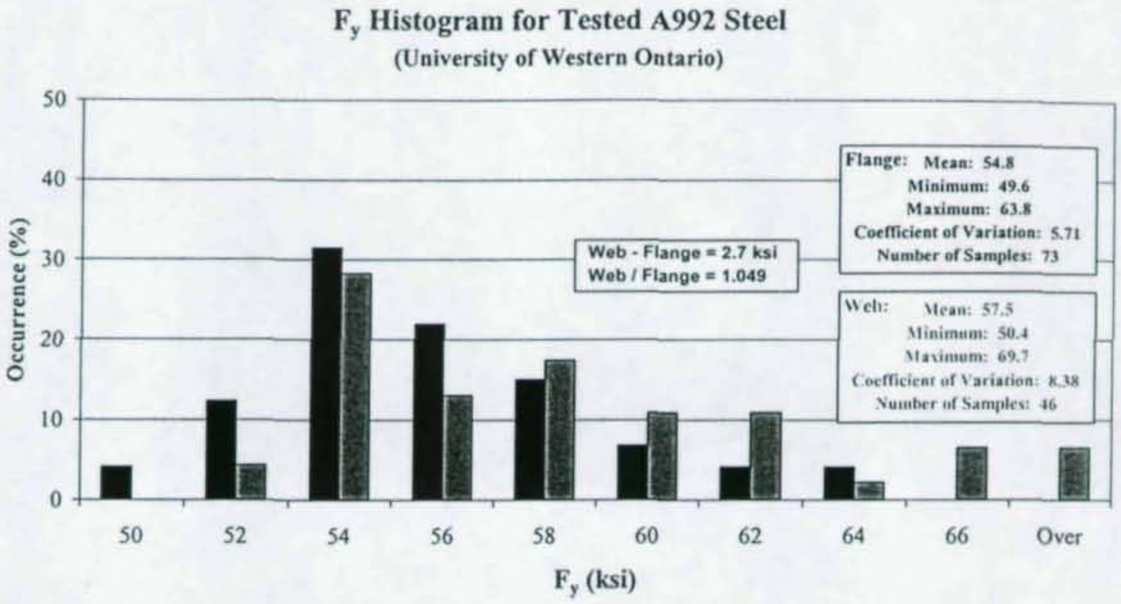

Figure 25: $F_{y\,0.2\%}$ histogram comparison between web and flange for the University of Western Ontario tensile test results

The histograms indicate that the yield stress values for the flange and web have the same distribution of data, but the specimens tested in the web are about 3 ksi higher than the flange tested specimens. This significant difference between the flange and web tested specimens was not observed in other tensile properties.

The data were separated into ASTM shape group to determine if the web-flange effect followed a trend with shape size. Table 29 is a comparison between web and flange for each ASTM shape group.

Table 29: Yield stress comparison between web and flange for all ASTM shape groups tested.

	U of Minnesota $F_{y\,0.2\%}$ Data				U of Western Ontario $F_{y\,0.2\%}$ data			
ASTM Group	Flange	Web	web/flange	web-flange	Flange	Web	web/flange	web-flange
1	54.9	55.6	1.01	0.71	53.0	53.8	1.02	0.82
2	55.8	62.0	1.11	**6.22**	55.2	60.8	1.10	**5.60**
3	56.7	55.1	0.97	-1.64	56.1	56.2	1.00	0.10
4	52.7	57.0	1.08	4.33	54.5	56.3	1.03	1.79

ASTM shape group 2 specimens exhibited the largest disparity between web and flange. This result is consistent between both labs so it is not due to laboratory test error or irregularity.

The wide-flange shapes tested were investigated further to determine if the Group 2 phenomenon was associated with one shape, or several shapes. Table 30 shows the shapes tested along with their associated ASTM shape group.

Table 30: W-shapes tested according to ASTM group

ASTM Group 1	ASTM Group 2	ASTM Group 3	ASTM Group 4
W6x25	W12x65	W14x176	W14x257
W8x31	W24x76		
	W30x99		
	W36x150		

Table 30 indicates that several different shapes from ASTM group 2 were tested, so this behavior is not due to one shape size. More data is needed to reach a conclusion regarding this difference in yield stress between the web and the flange. Since, ASTM shape group relates to the size of the section, the ratio of web thickness / flange thickness was also investigated, but no correlation was found.

3.3.2 Strain at Strain-Hardening

The strain at strain-hardening for large sections initially appeared small when compared to smaller sections. This property was analyzed further to determine if there was a notable trend. Figure 26 is a plot of the strain at strain-hardening data for each ASTM shape group tested.

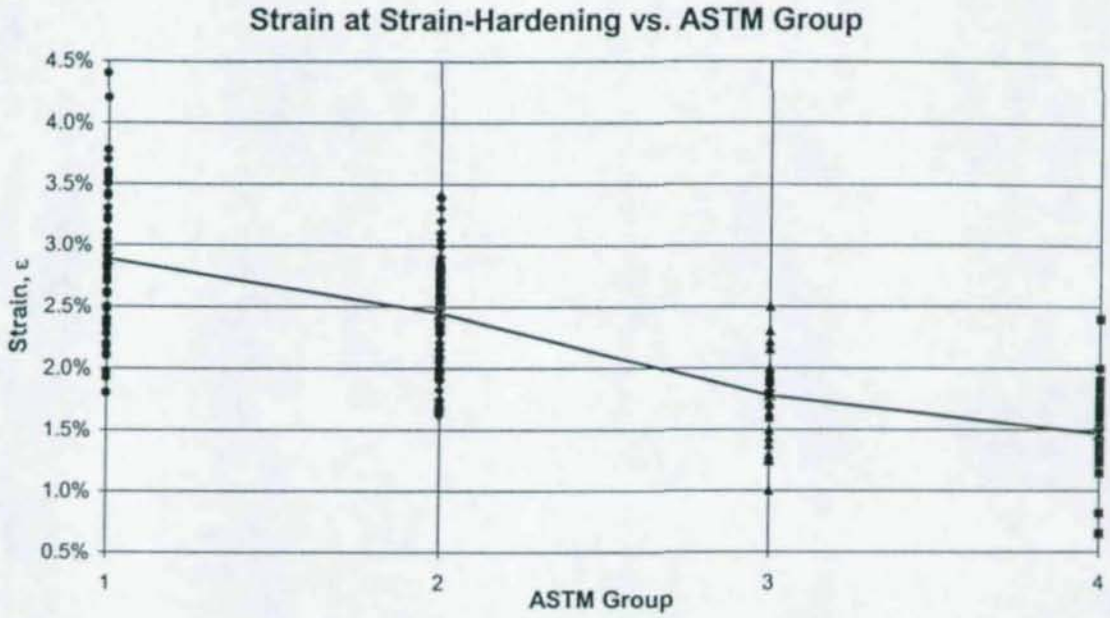

Figure 26: Strain at strain-hardening for each ASTM shape group tested

The line in Figure 26 passes through the mean value at each ASTM group tested. From this figure, it does appear that strain at strain-hardening does decrease with section size. The strain at strain-hardening was then plotted as a function of material thickness. The scatter plot and fitted linear regression are shown in Figure 27. There is a weak correlation (r^2 only = 0.53) between member thickness and strain at strain-hardening.

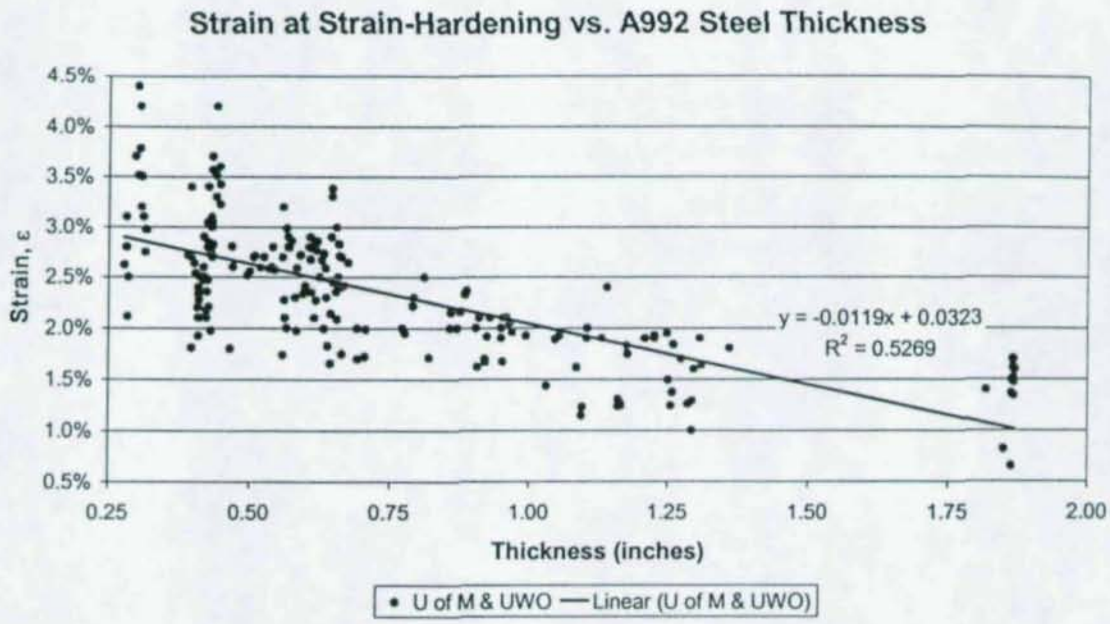

Figure 27: Scatter plot and fitted linear regression for strain at strain-hardening verse steel thickness

3.3.3 Power Function

The strain-hardening portion of the true stress-natural strain curve for mild steel can be approximated by a power function.

$$\sigma_{True} = K\varepsilon_{Natural}^{n}$$

In this approximation, the exponent (n) is generally equal to the ultimate strain. The power law approximation was investigated for several stress-strain curves to see if A992 steel could also be modeled by this function. Figure 28 is a typical A992 true stress-natural strain curve with fitted power law.

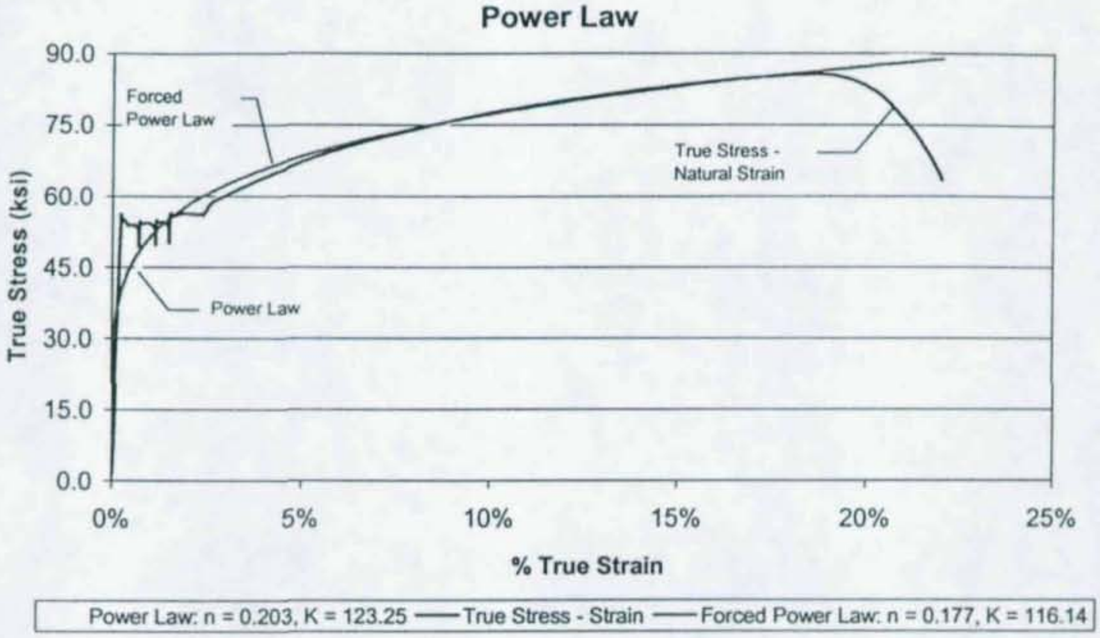

Figure 28: A992 true stress-natural strain curve with fitted power law functions

The dotted line represents the fitted power law, which features an exponent of n = 0.203. This power law fits the curve well, however the exponent is much larger than the actual ultimate strain value of 0.177. This actual value was used for the exponent, and the corresponding "forced power law" distribution is illustrated in Figure 28 as the gray line. In general, the exponent was greater than the actual ultimate strain. Therefore, A992 steel is not as accurately approximated by the power law function. This may be due to the changes in A992 steel compared to mild steel of the past.

3.4 Geometric Measurements and Properties

Along with tensile tests, geometric measurements were also taken. A992 steel geometric properties were necessary for determining the fabrication factor, F in reliability analysis. The dimensions of several wide-flange sections were measured. The section depth (d), flange width, (b_f), flange thickness (t_f), and web thickness (t_w) were all measured at various locations. The cross-sectional measurements and geometric property statistics were then tabulated and compared to past research results. The variability along the length of the member was investigated by taking two sets of measurements for each section. Summary statistics including the measured-to-nominal values for the geometric properties are shown in Table 31 for the sections tested. Tables 32 and 33 contain geometric property statistics from Jaquess & Frank and Schmidt respectively. The plastic modulus, Z_x statistics will be used in the reliability analysis of compact beams.

Table 31: Measured and geometric statistics for A992 steel W-shapes (Current Investigation)

	t_f	t_w	b_w	d	Z_x
Mean *	0.981	1.002	1.010	1.004	0.999
COV	0.041	0.039	0.007	0.006	0.018

Table 32: Measured and geometric statistics for A572 Gr. 50 steel W-shapes (Jaquess & Frank, 1999)

	t_f	t_w	b_w	d	Z_x
Mean *	0.977	1.010	1.000	1.000	0.988
COV	0.025	0.030	0.004	0.010	0.019

Table 33: Measured and geometric statistics for A992 steel W-shapes (Schmidt, 2000)

	t_f	t_w	b_w	d	Z_x
Mean *	1.020	1.040	1.000	1.000	1.03
COV	0.038	0.038	0.008	0.004	0.034

* measured value divided by nominal value

The geometric statistics for all three sources are very similar. The measured values are essentially the same as the nominal values (mean* ~1.0). The coefficients of variation, COV are also similar, and the level of variation is quite small.

Chapter 4: Reliability Analysis

4.1 Reliability Parameters

4.1.1 Overview

A reliability analysis was performed for the plastic moment capacity of a compact beam under uniform moment. This beam type and loading were the basis for the resistance factor ($\phi = 0.9$) in the AISC LRFD Specification (Galambos, 2000). The theory and background behind the AISC resistance factors was reviewed earlier. The load and resistance parameters used in the original resistance factor ($\phi = 0.9$) derivation are included in Table 34.

Table 34: Load and resistance factor parameters used in the original derivation of $\phi = 0.9$ for a compact beam under uniform moment

Load & Resistance Parameters in the Original Derivation ($\phi = 0.9$)	
$L_n/D_n = 3$	live to dead load ratio
$D_{bar} = 1.05*D_n$, $COV_D = 0.1$ *(Normal Distribution)*	mean to nominal dead load relation, & coefficient of variation
$L_{bar} = L_n$, $COV_L = 0.25$ *(Extreme Type 1 Distribution)*	mean to nominal live load relation, & coefficient of variation
$M_{bar} = 1.05$, $COV_M = 0.10$ *(Lognormal Distribution)*	mean material factor, & coefficient of variation
$F_{bar} = 1.00$, $COV_F = 0.05$	mean fabrication factor, & coefficient of variation
$P_{bar} = 1.02$, $COV_P = 0.06$	mean professional factor, & coefficient of variation

The original load parameters and type of distribution shown in Table 34 for live and dead load were retained and incorporated in the reliability analysis.

4.1.2 Material Factor, M

The A992 SSPC mill data from the Dexter et al., 2000 study correlated well with the laboratory tensile test results. Therefore, this larger data set was the basis for the reliability analysis. The original resistance factor development was based on a lognormal yield stress distribution. Figure 29 includes the A992 yield stress histogram for the SSPC mill data. The lognormal distribution included in Figure 29 appears to fit the data very well. As a result, the lognormal material strength assumption was also adopted for the A992 steel reliability analysis.

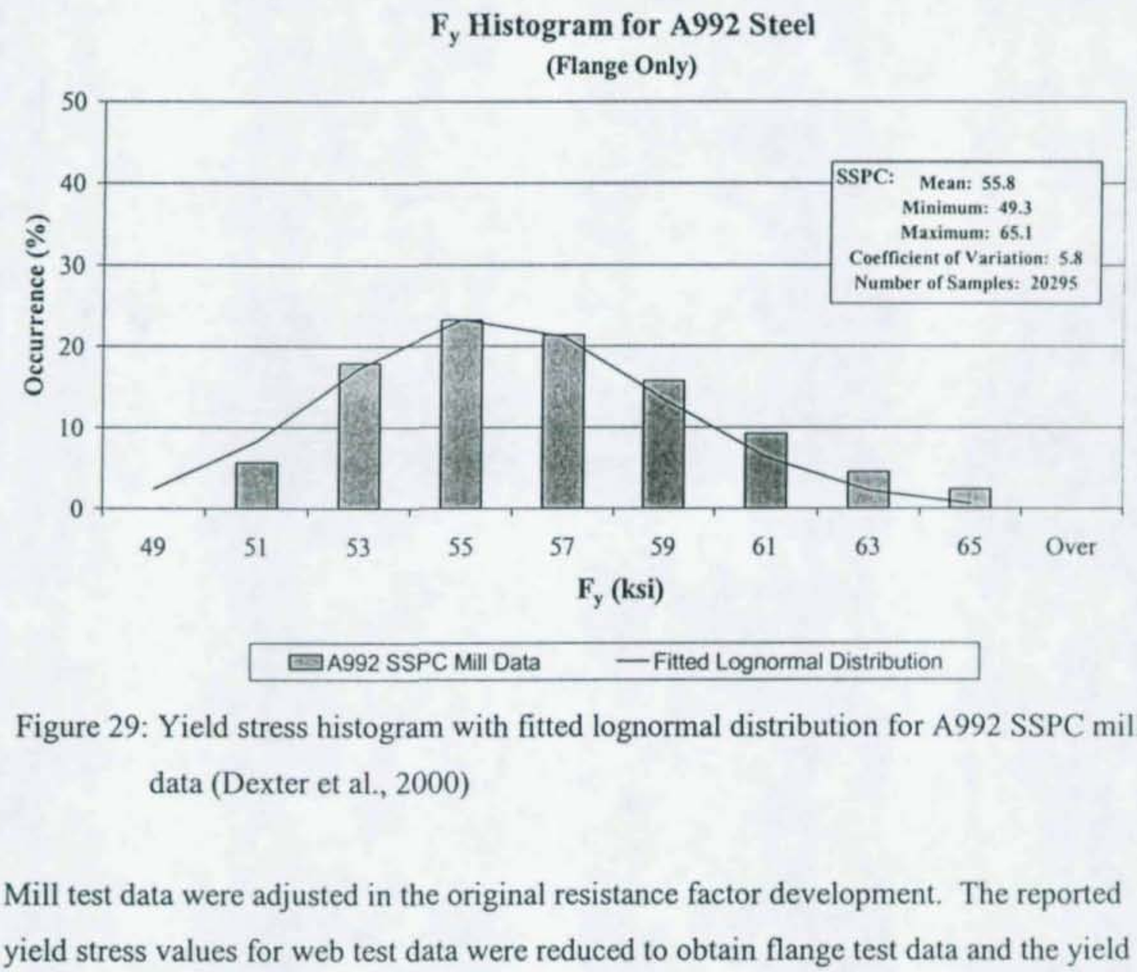

Figure 29: Yield stress histogram with fitted lognormal distribution for A992 SSPC mill data (Dexter et al., 2000)

Mill test data were adjusted in the original resistance factor development. The reported yield stress values for web test data were reduced to obtain flange test data and the yield stress was reduced further to obtain static yield stress values. Due to the change in ASTM A6, steel mill tests are now predominately taken from the flange rather than the web. The availability of flange mill test data means that there is one less adjustment. Galambos and Ravindra reduced the mill data by 4 ksi to transform the dynamic yield stress values to static yield stress values. The University of Minnesota average difference between the mill test yield stress ($F_{y\ mill}$ = 54.94) and the corresponding average tested static yield stress ($F_{y\ sstatic}$ = 50.99) was 3.95 ksi. Therefore, the 4 ksi adjustment incorporated by Galambos and Ravindra was also justified for A992 steel. Utilizing this 4 ksi adjustment, the A992 SSPC mill test data mean yield stress of 55.8 ksi was reduced to 51.8 ksi, resulting in a mean (static mill/nominal) value = 1.036. The material effect was changed from 1.05 to 1.036, and the material variation was changed from 0.10 to 0.058.

4.1.3 Fabrication Factor, F

For a compact beam under uniform moment, $\phi M_n = \phi Z_x F_y \geq \gamma M_u$

The most important parameters are the plastic modulus and the yield stress. For this situation, the fabrication parameter is based on the plastic modulus, Z_x. The mean fabrication parameter was kept at 1.00, but the COV was changed from 0.05 to 0.02 based on the geometric results presented earlier.

4.1.4 Professional Factor, P

The professional factor, P was not changed from its original values (Mean, P = 1.02 and COV_P = 0.06). There are a few reasons for not changing this reliability parameter:

1.) The focus of the current study is the impact of changes in steel material properties. This parameter has undergone the most change since the resistance factor development.

2.) Any change in the professional factor would require a more detailed investigation, which is outside the scope of this research.

3.) Current design philosophies and practice have not changed significantly, and the original professional parameters would error on the conservative side.

4.2 Analysis & Results

A first-order, second-moment reliability analysis for a compact beam was performed. The results were then verified by Monte-Carlo simulation. The results of this analysis are plotted in Figures 30, 31, and 32. The graphs compare the original AISC parameters to the current material parameters determined from this study. Comparisons using the current resistance factor ($\phi = 0.9$) are made in two figures. Figure 30 includes the new material parameter values, and Figure 31 also includes new fabrication values.

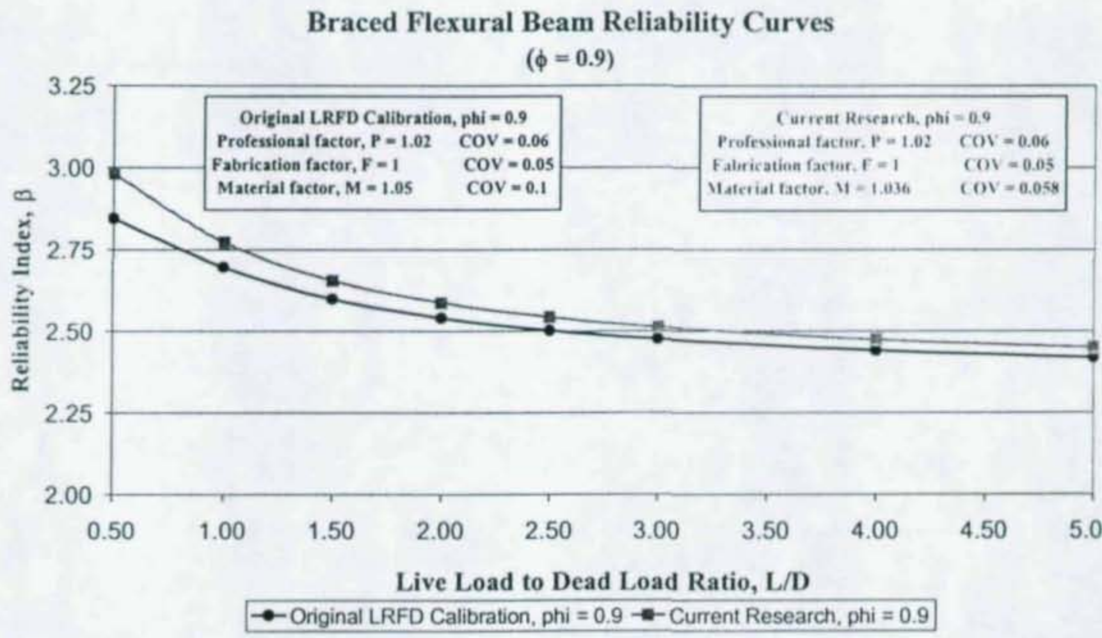

Figure 30: Reliability curves for the original LRFD calibration and parameters based on current research parameters (M changed from 1.05 to 1.036 & corresponding COV changed from 0.10 to 0.058)

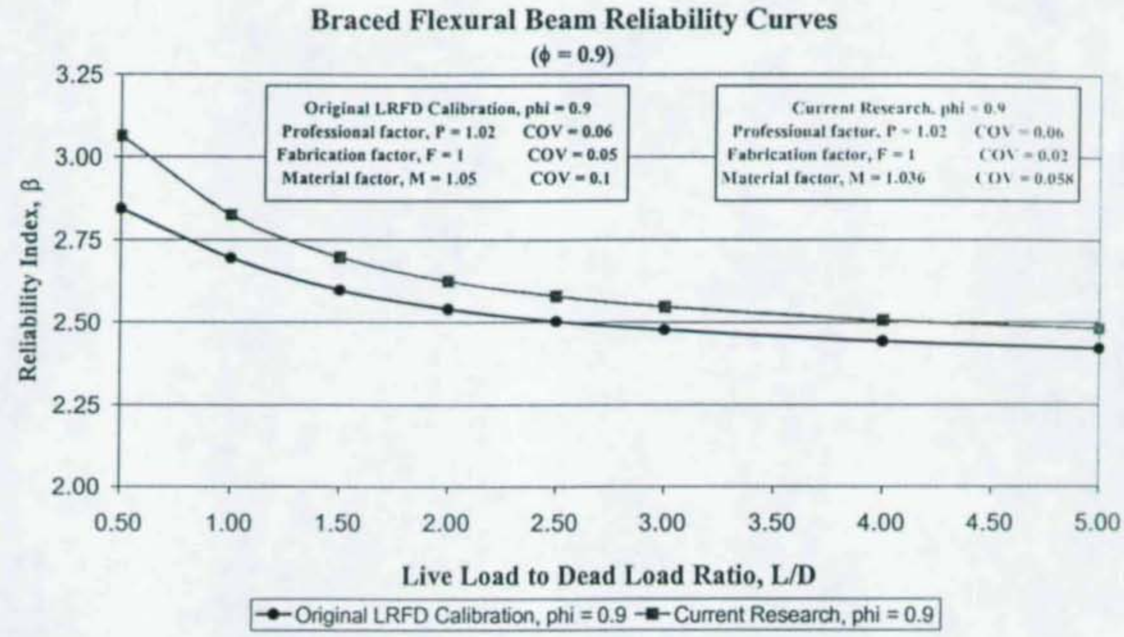

Figure 31: Reliability curves for the original LRFD calibration and parameters based on current research parameters (M & F changed)

Figures 30 and 31 indicate that current A992 steel has a slightly higher level of reliability than that of the original LRFD development. This is because the mean value for the material parameter, M is less, however, there is considerably less variation in the material and fabrication parameters. Due to this slight increase in reliability, a resistance factor of 0.95 was investigated. The results and comparison of this new value are illustrated in Figure 32.

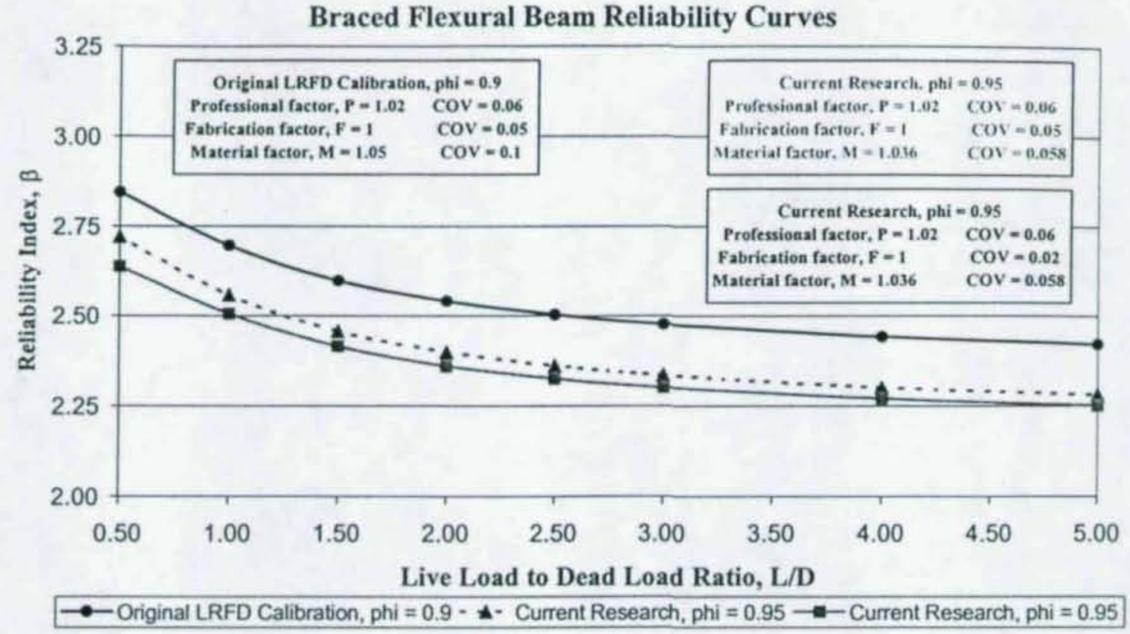

Figure 32: Reliability curves for the original LRFD calibration ($\phi = 0.9$) and parameters based on current research parameters with a $\phi = 0.95$ (M & F changed).

Figure 32 clearly indicates that A992 steel does not obtain the desirable level of reliability for a resistance factor = 0.95. The level of reliability is very good for a resistance factor = 0.90, however, any change in resistance factor by less than 0.05 would be unpractical.

Due to essentially the same level of reliability for both the original AISC parameters and the current research parameters, there is no need for further investigation beyond this beam example. The current resistance factor ($\phi = 0.9$) is still appropriate because the variation, COV has decreased significantly, but the mean has also decreased slightly. The result is a slightly higher level of reliability, but not enough of an increase to be significant.

Chapter 5: Conclusions

Tensile tests were performed on several A992 wide-flange shapes. Tensile specimens were taken from the web and the flange. The tests were performed at two laboratories: the University of Minnesota and the University of Western Ontario to compare results. The tensile test results were also compared with A992 and A572 Gr. 50 laboratory and mill test data. A992 comparison data consisted of 1998 SSPC mill test report data analyzed by Dexter et al., 2000. A572 Gr. 50 wide-flange shape data were from the Frank and Read analysis of 1992 web mill test report data and the 1999 Jaquess and Frank web and flange laboratory tensile test results. A reliability analysis was performed to determine the current level of reliability of A992 wide flange shapes. The conclusions from this research are summarized below.

1. In general, the tensile test results for A992 steel are similar to the A572 Gr. 50 steel statistics from the literature review. The mean yield stress, ultimate tensile strength, and Y/T values for the tested A992 steel are very similar to A572 Gr.50 steel; however, the variation is less for A992 steel. This may be due to changes in steel production and the new requirements in the A992 ASTM steel specification. The Y/T values for A992 steel had a much tighter range compared to A572 Gr. 50 steel data of past material property studies. This is most likely due to the new Y/T maximum limit featured in the A992 steel specification.

2. The A992 tensile test results are very similar to the A992 SSPC mill test data presented by Dexter et al., 2000. The mean A992 flange tensile test results from the University of Minnesota were 55.3 ksi, 72.4 ksi, and 0.764 for the yield stress, ultimate tensile strength, and Y/T respectively. Similarly, the University of Western Ontario mean yield stress was 54.8 ksi. The laboratory static yield stress averaged 4 ksi lower than the corresponding mill yield stress value. The laboratory tensile test results from both laboratories were essentially the same as the mill test report values. This is because the steel mill tests are currently performed at the mid-range speed, not at the maximum speed.

3. The tensile test data were further analyzed for notable trends. Yield stress was the only material property, which demonstrated a distinct difference between web and flange results. Group 2 ASTM shapes exhibited the largest disparity (6 ksi) between web and flange. It is unclear why this shape group featured the largest difference. Overall yield stress for web test specimens was 3 ksi higher than flange specimens. The strain at strain-hardening exhibited a weak correlation with steel thickness. The trend featured a decrease in strain at strain-hardening with an increase in steel thickness.

4. A first-order, second-moment reliability analysis was performed for a compact beam under uniform moment. The material parameters were changed from the original LRFD development with a bias factor of M = 1.05, $COV_M = 0.10$ to M = 1.036, $COV_M = 0.058$. Where the material bias factor (M) is defined as the mean static yield stress for mill data divided by the nominal yield stress, and the coefficient of variation (COV) is defined as the mean divided by the standard deviation. The fabrication parameters were also changed from a bias factor of F = 1.00, $COV_F = 0.05$ to F = 1.00, $COV_F = 0.02$ based on geometric measurements taken from the A992 steel test sections. The fabrication bias factor for a compact beam is defined as the measured plastic modulus divided by the nominal value in the code.

5. The mean yield stress values are less than the values of the past, however, this effect is offset due to a decrease in variation. As a result, the level of reliability for current A992 W-shapes is essentially the same as the steel of the past. The AISC LRFD Specification resistance factors are more than adequate for current steel production and design.

References

1. AISC (1993), *Load and Resistance Factor Design Specification for Structural Steel Buildings*, American Institute of Steel Construction, Chicago, IL.

2. Brockenbrough, R. L. (2000) "MTR Survey of Plate Material Used in Structural Fabrication," Final Report to American Institute of Steel Construction, R. L. Brockenbrough & Associates, Inc., Pittsburgh, PA.

3. Dexter. R. J., et al. (2000), "Structural Shape Material Property Survey," Final Report to Structural Shape Producer's Council, University of Minnesota, Minneapolis, MN.

4. Dexter, R. J, et al. (2001), "Evaluation of the Design Requirements for Column Stiffeners and Doublers and the Variation in Properties of A992 Shapes," *Proc. Annual Technical Session*, NASCC, Ft. Lauderdale, FA.

5. Ellingwood, B., Galambos, T. V., MacGregor, J. G., and Cornell, C. A. (1982), "Probability Based Load Criteria: Assessment of Current Design Practice," *Journal of the Structural Division*, ASCE, Vol. 108, No. ST5, pp. 959 – 977.

6. Frank, K. H. and Read, D. R. (1993), "Statistical Analysis of Tensile Data for Wide-Flange Structural Shapes," Final Report to Structural Shape Producer's Council, University of Texas at Austin, Austin, TX.

7. Frank, K. H., et al. (2000), "State of the Art Report Base Metals and Fracture," Final Report to SAC Joint Venture, University of Texas at Austin, Austin, TX.

8. Galambos, T. V. and Ravindra, M. K. (1978), "Properties of Steel for Use in LRFD," *Journal of the Structural Division*, ASCE, Vol. 104, No. ST9, pp. 1459 – 1468.

9. Galambos, T. V., Ellingwood, B., MacGregor, J. G., and Cornell, C. A. (1982), "Probability Based Load Criteria: Load Factors and Load Combinations," *Journal of the Structural Division*, ASCE, Vol. 108, No. ST5, pp. 978 – 997.

10. Galambos, T. V. (1985), "Reliability of Connections, Joints, and Fasteners," Structural Engineering Report No. 85-05.

11. Galambos, T. V. (2000), "The Effect of Material Properties on the Stability Design Criteria of Steel Structures," *Proc. Annual Technical Session*, Structural Stability Research Council, Memphis, TN.

References (continued)

12. Galambos, T. V., Hajjar, J. F., and Earls, C. J. (1997), "Required Properties of High-Performance Steels," National Institute of Standards Technology, Report No. 6004.

13. Galambos, T. V. ed. (1988), *Guide to Stability Design Criteria for Metal Structures,* 4th ed., Wiley, New York, NY.

14. Gentilcore, M. L. (1996), "Ductile Tearing of High-Toughness Steel Members." Doctoral Thesis, Lehigh University, Bethlehem, PA.

15. Jaquess, T. K. and Frank, K. H. (1999), "Characterization of the Material Properties of Rolled Sections," Final Report SAC Joint Venture, University of Texas at Austin, Austin, TX.

16. Kassar, M. and Yu, W. W. (1992), "Effect of Strain Rate on Material Properties of Sheet Steels," *Journal of the Structural Division*, ASCE, Vol. 118, No. 11, pp. 3136 - 3150.

17. Kennedy, D. J. L. and Gad Aly, M. (1980), "Limit States Design of Steel Structures – Performance Factors," *Canadian Journal of Civil Engineering,* Vol. 7, pp. 45 –77.

18. Mahadevan, S. and Haldar, A. (1991), "Stochastic FEM-Based Validation of LRFD," *Journal of the Structural Division*, ASCE, Vol. 117, No. 5, pp. 1393 – 1411.

19. Mazzolani, F. M., Mele, E., and Piluso, V. (1993), "Statistical Characterization of Constructional Steels for Structural Ductility," *Construzioni Metalliche,* No. 2, p. 89.

20. Nowak, A. S. and Collins, K. R. (2000), *Reliability of Structures,* McGraw-Hill, New York, NY.

21. Phelps, R. H., ed. (1950), *Theory of Flow and Fracture of Solids,* McGraw-Hill, New York, NY, pp. 70 – 88.

22. Rex and Easterling (1999), "Behavior and Modeling of Mild Structural and Reinforcing Steel," Virginia Tech University, Blacksburg, VA.

References (continued)

23. Ripling, E. J., and Polakowsky, N. H., (1966). *Strength and Structure of Engineering Materials,* Prentice-Hall, Englewood Cliffs, New York, NJ.

24. Rosowsky, D. V., Hassan, A. F., and Phani Kumar, N. V. V. (1994), "Calibration of Current Factors in LRFD for Steel," *Journal of the Structural Division*, ASCE, Vol. 120, No. 9, pp. 2737 – 2746.

25. Salmon, C. G. and Johnson, J. E. (1996). *Steel Structures: Design and Behavior,* 4th ed., Harper Collins Publishers Inc, New York, NY.

26. Schmidt, B. J. (2000), "Review of the Resistance Factor for Steel", Master's Thesis, The University of Western Ontario, London, Ontario.

27. Soroushian, P. and Ki-Bong Choi (1987), "Steel Mechanical Properties at Different Strain Rates," *Journal of the Structural Division*, ASCE, Vol. 113, No. 4, pp. 663 – 671.

Western
Engineering Science

The University of Western Ontario
Department of Civil and Environmental Engineering

APPENDIX C

Mechanical Properties of A992 Steel

Prepared By:

J. J. Jelinek & F. M. Bartlett, Ph.D., P.Eng.

Contents

Page

List of Figures **Page**

List of Tables

Page

1.1 Introduction

This report has been written for the American Institute of Steel Construction (AISC) and compliments a parallel study conducted at the University of Minnesota (UM). It presents the material properties of structural steel produced in 1999 and 2000 in accordance with the ASTM A992 "Steel for Structural Shapes for Use in Building Framing" specification.

The current resistant factor used for the design of structural steel in CAN/CSA-S16.1-94, ϕ, was developed more than 20 years ago (Kennedy & Gad Aly, 1980). There have since been significant changes in both the material and the production practices of structural steel. The ASTM A992 specification was implemented to limit the impact these changes have on both the strength of the steel and its chemical composition.

The most significant change in the material to occur in the past 20 years is the switch to recycled steel. Almost all of the rolled shapes currently produced in the U.S. originate from recycled material (Jaquess & Frank, 1999). The original calibration of ϕ was based on steel produced directly from iron ore. When using recycled material to produce new steel, both inherent chemical variabilities and impurities are introduced. The impact of these on the material properties of the finished product and the resistance factor used for design is not known.

A second recent change in the production of structural steel is the elimination of ingots and the adoption of a continuous casting process with near net shape blooms. The outcome is a slightly different chemical composition in the material. Although the process is much more energy efficient, the use of near net shapes may reduce the yield strength of the final product because it requires much less rolling than a traditional ingot and so may have less strength enhancement due to work hardening.

To investigate the material properties of modern structural steel, produced according to ASTM A992, tensile tests of 217 coupons obtained from 38 specimens representing 8 different shapes have been conducted at the University of Western Ontario (UWO) and UM. The results obtained by UWO are presented in this report.

The specific objectives of this study are:

1. To test tensile specimens representing ASTM A992 structural steel and analyze the data to report a statistical summary of the upper yield point, F_{uy}, yield strength, F_y, ultimate strength, F_u, modulus of elasticity, E, strain at strain hardening, ε_{sh}, strain at ultimate, ε_u, and elongation at failure.
2. To investigate replicate tensile tests conducted at UM and determine the reproducibility and repeatability for results of different laboratories.
3. To determine if a tensile coupon from a thick element that has been milled to half-thickness displays the same strengths, F_y and F_u, as the full-thickness coupon.
4. To investigate dependence between F_{uy}, F_y, and F_u and the thickness.
5. To quantify the yield to ultimate strength ratio, Y/T, for comparison to that prescribed by ASTM A992.
6. To quantify the difference between F_{uy} and F_y.
7. To quantify the relative strengths of flanges and webs.
8. To compare the material properties of ASTM A992 steel from different producers.
9. To compare the material properties measured in the lab to the values reported on mill certificates.

There are three sections in this report. Section 2 describes the testing program, including the materials, methods, and apparatus used. Section 3 summarizes the tensile testing results and subsequent data analysis. Section 4 gives a summary and states the conclusions.

In this report, all mechanical properties are presented in SI (metric) units, consistent with Canadian practice. In the text, equivalent values in inch-pound units are also presented, to facilitate comparison with data from the parallel investigation conducted at the University of Minnesota. In the tables and figures, however, only SI units are provided. To convert these values to equivalent inch-pound units, the relevant conversion factors are:

- millimetres (mm)/25.4 = inches
- kiloNewtons (kN)/4.448 = kips
- MegaPascals (MPa)/6.895 = kips per square inch (ksi).

2.1 Test Program

The mechanical properties of structural steel produced according to the ASTM A992 specification are to be investigated. The minimum material property requirements specified by this designation are given in Table 2.1.1.

Three U.S. steel producers provided 38 structural steel samples representing 8 different W shapes conforming to the A992 specification for this study. The producers will simply be identified as Producer A, Producer B, and Producer C throughout this report. Table 2.1.2 lists the designations, ASTM Shape Size Group, and number of specimens supplied by each producer.

A total of 207 tensile coupons were machined from the 38 samples, typically two from each flange and two from the web as shown in Fig. 2.1.1. Each coupon was assigned an identification number of the general form [Sample ID] [Location ID], where the Sample ID is shown in Table 2.1.3 and the Location ID is as shown in Fig. 2.1.1. Coupons from Producers A and B with location identification numbers 2, 3, and 6, and all coupons from Producer C, a total of 119 specimens, were tested at UWO. The remaining 88 specimens were tested at UM.

At UWO, the capacity of the testing machine limited the maximum coupon thickness to 25.4 mm (1 in). Thicker coupons were milled on one side to one half of the original thickness. The UM testing machine capacity did not impose a limit on the coupon thickness. Table 2.1.4 lists the half-thickness coupons tested at UWO and the corresponding full-thickness coupons tested at UM.

Fig. 2.1.2 gives the dimensions of the coupons tested. Coupons from Producers A and B were machined at the UWO machine shop to the ASTM A370 standard for plate-type coupons, with longer-than-minimum grip lengths as permitted by the standard. Producer C provided coupons already milled to consistent sizes that did not conform to ASTM A370.

Mill certificates were provided, stating the mechanical properties of all the sections supplied. Producers A and B supplied mill certificates for flange coupons from a section produced in the same heat. Producer C reported material properties of the coupon from location 6, shown in Fig. 2.1.1, for each section supplied.

A Tinius Olsen Deluxe Super "L" Model 120 Universal Testing Machine with a capacity of approximately 530 kN (120 k), was used to test coupons at UWO. An MTS extensometer, Model #634.25E-54 with a gauge length of 50.8 mm (2 in) recorded strains. A Novotechnik Model TRS100 LVDT with a travel of 100 mm (4 in), tracked the movement of the crossheads on the Tinius Olsen machine. All of the data was recorded by a Sciemetric Instruments Inc. Series 7000 data logger.

The coupons were all tested at loading rates ranging from 42.1 $\mu\varepsilon$/s to 170.6 $\mu\varepsilon$/s with an average rate of 103.5 $\mu\varepsilon$/s. These rates fall below the ASTM A370 maximum of 1/16 in per min per inch of reduced section which corresponds to approximately 292 $\mu\varepsilon$/s.

All yield strengths were determined using the 0.2% offset method (ASTM A370). The upper yield point was taken as the highest value from the stress strain curve before the yield plateau. The modulus of elasticity was found by regressing a line onto the upper elastic portion of the stress strain curve. The ultimate strength was taken as the area of the sample divided by the maximum load attained. The strain at strain hardening was taken as the value of strain where the slope of the stress strain curve begins to increase again after the yield plateau. The strain at ultimate was taken as the value of strain that corresponds to the ultimate load.

The extensometer was removed prior to fracture, but after the maximum load was reached, for the majority of the coupons to prevent damage. As a result, there are no strain data after the ultimate load for a large number of coupons. The % elongation at fracture was captured for four coupons, allowing a relationship to be derived between the % elongation and ε_u. Using this relationship, the % elongation was the estimated for the remaining coupons from the observed ε_u values. For Producer C, the extensometer was not removed from the coupons before fracture and the % elongation at fracture was measured.

When the dynamic effects of the loading on the yield strength wish to be considered, Eq. [1] (Rao et al, 1966) will be applied. The SI equivalent of Eq. [1] is given by Eq. [2] (Schimdt, 2000), where $\frac{d\varepsilon}{dt}$ is measured in $\mu\varepsilon$/s.

$$F_{yd}\text{-}F_{ys} = 3.2+0.001\frac{d\varepsilon}{dt} \quad [1]$$

$$F_{yd}\text{-}F_{ys} = 22.1+0.007\frac{d\varepsilon}{dt} \quad [2]$$

Table 2.1.1: Minimum Requirements Specified In ASTM A992

Material Property	Requirement
Yield Strength, F_y	345 – 450 MPa
Ultimate Strength, F_u	450 MPa (minimum)
Yield to Ultimate Ratio, Y/T	0.85 (maximum)
Elongation in 50.8 mm	21% (minimum)

Table 2.1.2: Sections List

Metric Designation	Imperial Designation	Shape Size Group	# Provided By Producer A	B	C	*Total*
W150x37	W6x25	1	3	0	0	3
W200x46	W8x31	1	6	0	0	6
W310x97	W12x65	2	3	0	1	4
W360x262	W14x176	3	3	1	1	5
W360x382	W14x257	4	3	1	3	7
W610x113	W24x76	2	3	0	0	3
W760x147	W30x99	2	3	0	2	5
W920x223	W36x150	2	3	1	1	5
Total			27	3	8	**38**

Table 2.1.3: Section Identification Numbers

Source	Sample ID #	Shape Designation	# of Flange Coupons To UWO	# of Web Coupons To UWO	# of Flange Coupons To UM	# of Web Coupons To UM
A	625D	W150x37	2	1	2	1
	625E	W150x37	2	1	2	1
	625F	W150x37	1	1	2	1
	831D	W200x46	2	1	2	1
	831E	W200x46	2	1	2	1
	831F	W200x46	2	1	2	1
	8A	W200x46	2	1	2	1
	8B	W200x46	2	1	2	1
	8C	W200x46	2	1	2	1
	12A	W310x97	2	1	2	1
	12B	W310x97	2	1	2	1
	12C	W310x97	2	1	2	1
	141A	W360x262	2	1	2	1
	141B	W360x262	2	1	2	1
	141C	W360x262	2	1	2	1
	142A	W360x382	2	1	2	1
	142B	W360x382	2	1	2	1
	142C	W360x382	2	1	2	1
	24A	W610x113	1	1	2	1
	24B	W610x113	2	1	2	1
	24C	W610x113	2	1	2	1
	30A	W760x147	2	1	2	1
	30B	W760x147	2	1	2	1
	30C	W760x147	2	1	2	1
	36A	W920x223	2	1	2	1
	36B	W920x223	2	1	2	1
	36C	W920x223	2	1	2	1
B	JA	W360x382	2	1	0	1
	JB	W360x262	2	1	2	1
	JC	W920x223	2	1	2	1
C	606589	W360x382	0	2	0	0
	615871	W360x382	0	2	0	0
	616117	W310x97	3	2	0	0
	617633	W360x382	0	2	0	0
	623446	W760x147	3	2	0	0

Table 2.1.3: Section Identification Numbers Continued

Source	Sample ID #	Shape Designation	# of Flange Coupons To UWO	# of Web Coupons To UWO	# of Flange Coupons To UM	# of Web Coupons To UM
C	624388	W360x262	3	2	0	0
	626534	W920x223	3	2	0	0
	626709	W760x147	3	2	0	0
Total			73	46	58	30
			UWO Total = 119		***UM Total =*** 88	

Table 2.1.4: List of Milled Coupons

	UWO		UM	
Coupon	$t_{original}$ (mm)	t_{milled} (mm)	Corresponding Coupon	t (mm)
141A2	34.08	17.27	141A1	30.68
141A3	31.00	15.85	141A4	32.34
141B2	32.17	16.00	141B1	31.12
141B3	32.40	15.98	141B4	33.20
141C1	32.88	15.88	141C2	31.13
141C3	32.56	15.95	141C4	33.27
142A6	28.96	14.96	142A5	28.71
142B6	28.08	13.79	142B5	28.02
142C6	28.13	14.94	142C5	28.07
JA6	29.00	14.96	JA5	28.96
JB2	33.50	16.22	JB1	32.93
JB3	33.70	16.43	JB4	32.85

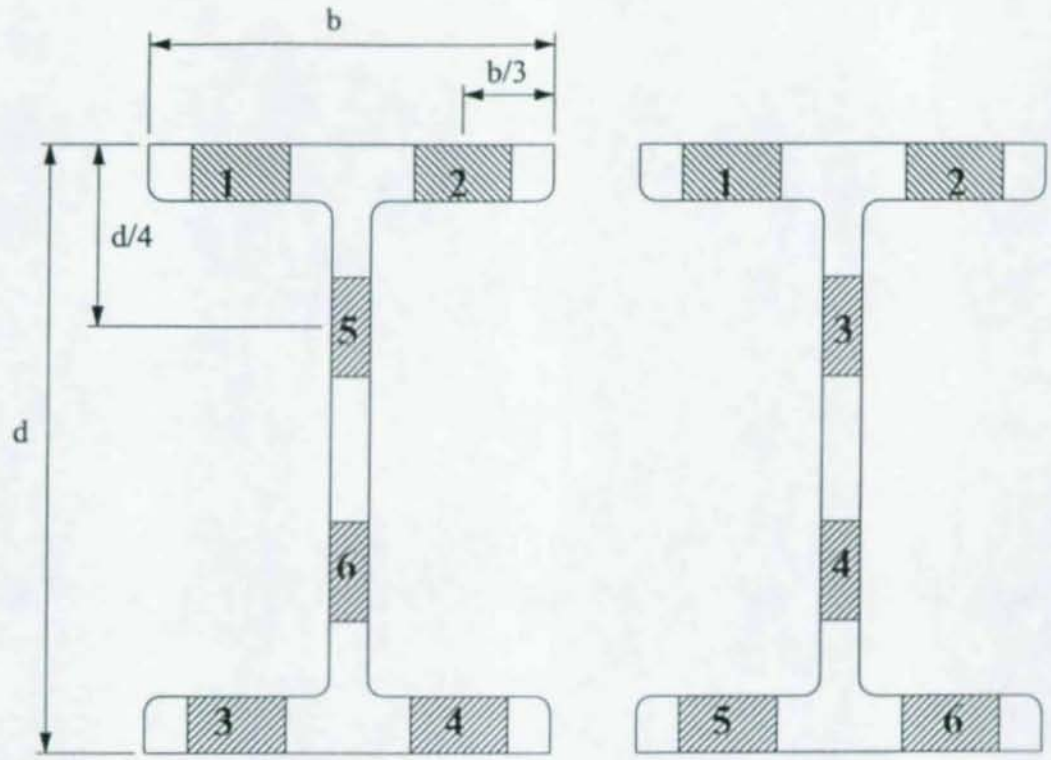

a. Producers A and B Location Numbers *b. Producer C Location Numbers*

Fig. 2.1.1: Location Indicator Key

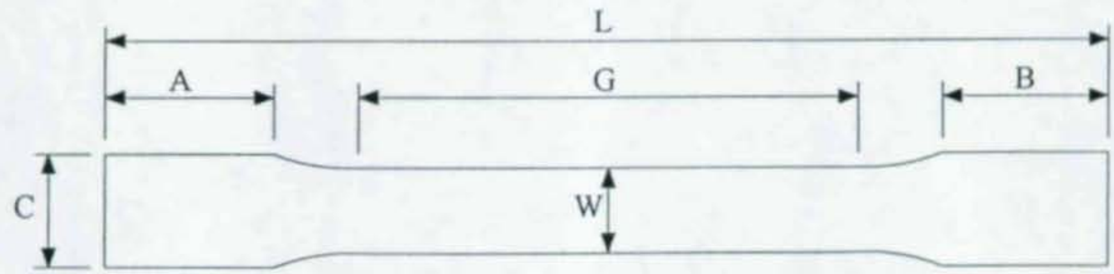

Dimension	Producer A	Producer B	Producer C
A	125 mm	125 mm	100 mm
B	125 mm	125 mm	90 mm
C	50 mm	50 mm	40 mm
G	225 mm	225 mm	90 mm
L	550 mm	550 mm	300 mm
W	40 mm	40 mm	19 mm

Fig 2.1.2: Coupon Dimensions

3.1 Basic Statistics

This section presents histograms and summary statistics for the observed material properties of ASTM A992 structural steel that were generated using the combined populations of all 3 producers and include the data for both flange and web specimens tested at UWO. Differences in the properties of flange and web coupons, taken from the same section, will be further investigated in Section 3.4. The data for half-thickness coupons listed in Table 2.1.4, have been included in this population. It will be shown in Section 3.3 that there are no significant effects on the material properties caused by milling to half-thickness. Table 3.1.1 summarizes the statistics found for F_{yu}, F_y, F_u, E, ε_{sh}, ε_u, and total elongation at failure. Fig. 3.1.1, Fig. 3.1.2, Fig. 3.1.3, Fig. 3.1.4, Fig. 3.1.5, Fig. 3.1.6, and Fig. 3.1.7 give the histograms and summary statistics for the F_{yu}, F_y, F_u, E, ε_{sh}, ε_u, and total elongation at failure respectively.

3.2 Laboratory Comparison

This portion of the study was conducted to determine the reproducibility of results in different labs for coupons that should have identical material properties.

Coupons tested at UM consistently demonstrated a higher yield strength than the corresponding coupons tested at UWO. This is shown by the plot of UM Yield Strength vs UWO Yield Strength in Fig. 3.2.1, where the majority of the data points lie above the 45° line. On average, UM yield strengths were approximately 9.0 MPa (1.3 ksi), or 1.023 times higher than the UWO yield strengths. Fig. 3.2.2 gives a comparative histogram for the combined Producer A and B yield strength data for each university. A summary of the yield strength statistics is given for Producer A and B data, Producer A data only, and Producer B data only in Table 3.2.1.

Coupons tested at UM demonstrated a higher ultimate strength than the corresponding coupons tested at UWO in all cases but one. This is shown by the plot of UM Ultimate Strength vs UWO Ultimate Strength in Fig. 3.2.3, where all but one of the data points lie above the 45° line. On average, the UM ultimate strengths were approximately 18.3 MPa (2.7 ksi), or 1.038 times higher than the UWO ultimate strengths. Fig. 3.2.4 gives a comparative histogram of the combined Producer A and B data for each university. A summary of the ultimate strength statistics is given for the entire data set, Producer A data only, and Producer B data only in Table 3.2.2.

Ideally there should have been a smaller difference between the UM and UWO results. The coupons that were compared were cut from the same sections and from the same flange or web. Similar techniques for area measurement and applied rates of load were used. The difference in results may arise from slight mis-calibration of the load sensors in one or both of the testing machines. The UWO Tinius Olsen testing machine was calibrated for loads up 220 kN (50 k) with no significant error. However, the coupon test loads were in excess of 500 kN (110 k), for which the associated error is not known. No information about the calibration history of the tensile testing machine at UM was available.

The stress difference, σ_{UM}-σ_{UWO}, at both yield and ultimate load levels, between the two labs is plotted versus the corresponding UWO load in Fig. 3.2.5. There is more variability in the stress difference at the lower load levels.

An interlaboratory precision study was conducted in accordance with ASTM E691. A summary of the repeatability statistic, k, is given in Table 3.2.3. It was found that the results obtained at UWO had better repeatability for both yield and ultimate strengths than the results obtained by UM. The repeatability for UWO results improved when going from ultimate strengths to yield strengths when the reverse trend was seen for UM. There were not enough laboratories participating in the study to obtain a meaningful reproducibility statistic, h. However, as already noted, UM results were deemed to be consistently higher than UWO results for both yield and ultimate strengths.

The coefficients of variation for repeatability, V_r, and reproducibility, V_R, for the yield and ultimate strengths calculated as prescribed by ASTM E8 are reported in Table 3.2.4.

3.3 Milling Effects

Coupons listed in Table 2.1.4 were milled to approximately one half of their original thickness to accommodate to UWO equipment constraints. If there is a symmetric distribution of material strength through the thickness of the coupons, as shown schematically in Fig. 3.3.1a, the average strength of the full-thickness coupon would equal the average strength of the half-thickness coupon, as shown in Fig. 3.3.1b. Table 3.3.1 lists the yield strengths for the half-thickness UWO coupons, $F_{y\text{-}UWO}$, full-thickness UM coupons, $F_{y\text{-}UM}$, the difference between them, $F_{y\text{-}UM}-F_{y\text{-}UWO}$, and the ratio between them, $F_{y\text{-}UM}/F_{y\text{-}UWO}$. On average, the half-thickness coupons had yield strengths 4.3 MPa (0.6 ksi) less than the yield strengths of the full-thickness coupons. In the laboratory comparison above, it was observed that the full-thickness and half-thickness UWO coupons yield strengths averaged 9.0 MPa (1.3 ksi) lower than the UM yield strengths. If only full-thickness coupons tested at UWO are considered, the yield strength difference increases to 9.8 MPa (1.4 ksi).

Table 3.3.2 lists the ultimate strengths for the half-thickness UWO coupons, $F_{u\text{-}UWO}$, the corresponding full-thickness UM coupons, $F_{u\text{-}UM}$, the difference between them, $F_{u\text{-}UM}-F_{u\text{-}UWO}$, and the ratio between them, $F_{u\text{-}UM}/F_{u\text{-}UWO}$. On average, the half-thickness UWO coupons ultimate strengths 14.6 MPa (2.1 ksi) less than the full-thickness UM coupons. In the laboratory comparison conducted in Section 3.2 it was observed that the full-thickness and half-thickness UWO coupons ultimate strengths average 18.3 MPa (2.7 ksi) lower than the full-thickness UM coupons. If only full-thickness coupons are compared, the difference in the ultimate strengths increases 18.9 MPa (2.7 ksi).

Fig. 3.3.2 shows the distribution of the yield stress difference in the two labs for both half-thickness and full-thickness coupons. It has been assumed that both distributions are normal. It can be seen that the mean values of the 2 distributions do not coincide but large portions of the distributions overlap each other. A Student's t-test indicates that the two means are not statistically different for a probability level of 88%. Thus the difference between the full-thickness and half-thickness yield strengths will be considered insignificant.

Fig. 3.3.3 shows the distribution of the ultimate stress difference in the two labs for both half-thickness and full-thickness coupons. It has been assumed that both distributions are normal. Again, there is a large overlap of the 2 distributions. A Student's t-test indicates that the two means are not statistically different for a probability level of 88%. Thus the difference between the full-thickness and half-thickness ultimate strengths will be considered insignificant.

3.4 Correlation With Thickness

The more the steel is rolled during production, the more it experiences the strength enhancing effects of work hardening. For a given chemical composition, it would be expected that as the thickness increases, the strength would decrease. Typically, F_y is more sensitive to the change in thickness than F_u. In Fig. 3.4.1, Fig. 3.4.2, and Fig. 3.4.3 respectively, F_{uy}, F_y, and F_u are plotted against the thickness, t. There is a slight tendency for F_{uy} and F_y to decrease as the thickness increases but F_u remains relatively constant across all thicknesses. It is common for steel producers to change the chemical composition of the material they supply to nullify significant strength variation with thickness (Schmidt, 2000).

3.5 Yield to Ultimate Ratio

The yield to ultimate strength ratio, Y/T, represents the fraction of a tension member's total capacity consumed once yield occurs. The enhancements to structural steel in the past 20 years have had a greater effect on the yield strength than the ultimate strength. Increasing the yield strength without increasing the ultimate strength proportionally decreases the margin between ductile failures and brittle failures.

The mean value of the ratio of the ultimate strength to yield strength, $\overline{Y/T}$, was found to be 0.778 with a coefficient of variation, $V_{Y/T}$, of 0.045. A histogram is shown in Fig. 3.5.1 for the distribution of Y/T. The maximum value Y/T observed was 0.862. There were a total of 5 instances of Y/T having values greater than the limit of 0.85 prescribed by ASTM A992 out of the 119 coupons tested. However, all occurrences were for web samples from different sections.

A plot of Y/T versus the thickness is given in Fig. 3.5.2. It can be seen in this figure that Y/T has a tendency to decrease as the thickness increases. This is the trend that would be expected. Typically, F_y decreases as the thickness increases while F_u is less sensitive to the change in thickness and remains relatively constant.

3.6 Upper Yield Strength and Yield Strength Difference

There are several accepted methods for defining the yield strength including the drop of beam method, 0.2% offset method, and the 0.5% absolute strain method. Each method can produce significantly different yield strengths. Therefore it becomes important to know which method is used to define the yield strength and how the strengths generated with each method relate to one another. In this study the difference between F_{uy} and F_y, generated by the 0.2% offset method, was investigated. The mean difference, $\overline{F_{uy} - F_y}$, was 13.4 MPa (1.9 ksi) and the mean ratio, $\overline{F_{uy}/F_y}$, was 1.034. Histograms of F_{uy}-F_y, and F_{uy}/F_y, are given in Fig. 3.6.1 and Fig. 3.6.2 respectively. In Figs. 3.6.1 and 3.6.2, F_{uy}-F_y and F_{uy}/F_y are plotted against the thickness. Neither figure shows any dependence on the thickness

3.7 Web Versus Flange Comparison

Kennedy and Gad Aly (1980) assumed that the static yield strength of webs was 5% higher than the static yield strength of flanges taken from the same section. Since webs are generally thinner than the flanges it would be expected that they would demonstrate higher yield strengths than the flanges as they would be exposed to more rolling during production.

On average, the web dynamic yield strengths were 21.2 MPa (3.1 ksi), or 1.056 times higher than the corresponding flange values, which confirms the assumptions made by Kennedy and Gad Aly. To correct for the dynamic effects of testing on the yield strength, equivalent static strengths are derived using the relationship proposed by Rao et al. (1966). In this case, the average difference remains 21.2 MPa (3.1 ksi) but the ratio increases to 1.063, but can still be considered to agree with Kennedy and Gad Aly's assumptions. A plot of the flange yield strength, $F_{y\text{-}fl}$, versus the corresponding web yield strength, $F_{y\text{-}web}$, is given in Fig. 3.7.1. For data from coupons representing Producers A and B, two flange yield strengths are plotted for each web yield strength. For data from Producer C, 3 flanges samples are plotted for each average of the 2 web samples taken from the section.

The web ultimate strength average 8.7 MPa (1.3 ksi), or 1.017 times higher than the corresponding flange. A similar plot to Fig. 3.7.1 is given for the ultimate strengths in Fig. 3.2.2, where $F_{u\text{-}fl}$ is the flange ultimate strength and $F_{u\text{-}web}$ is the web ultimate strength. Table 3.7.1 gives a more detailed break down of the differences in flange and web strengths for the different producers.

3.8 Producer Comparison

As previously stated, there were a variety of sections provided by 3 U.S. steel producers. All three provided ASTM A992 grade steel. As a means of determining if the material strengths are producer-dependent, the yield and ultimate strength data for each producer's set of coupons was analyzed individually.

Table 3.8.1 presents the statistics for each producer's yield strengths. Table 3.8.2 presents the statistics for each producer's ultimate strengths. It was found that for both the case of yield strength and ultimate strength that Producer B's coupons demonstrated the highest values and Producer A's coupons demonstrated the lowest values. On average, Producer B, Producer C, and Producer A's yield strengths were 86.9 MPa, 51.4 MPa, and 29.8 MPa respectively (13.0 ksi, 7.5 ksi, and 4.3 ksi, respectively) higher than the minimum specified yield strength of 345 MPa (50 ksi). On average, Producer B, Producer C, and Producer A's ultimate strengths were 106.2 MPa, 67.4 MPa, and 28.5 MPa respectively (15.4 ksi, 9.8 ksi, and 4.1 ksi, respectively) higher than the minimum specified ultimate strength of 450 MPa (65 ksi).

It should also be noted that there were 3 flange coupons that had yield strengths lower than the specified minimum yield strength and 1 flange coupon that had an ultimate strength less than the minimum specified ultimate strength. There were also 4 web coupons which had yield strengths higher than the maximum specified yield strength of 450 MPa (65 ksi).

Since there was such a large discrepancy between the yield and ultimate strengths of the different producers, the data were re-analyzed by dividing it up into its respective Shape Size Groupings (ASTM A6, 1997). The same trends are seen again. Mean values and coefficients of variation for yield strengths by Shape Size Grouping are presented in Table 3.8.3 and in Table 3.8.4 for ultimate strengths.

3.9 Mill Certificate Comparison

The coupons provided by both Producer A and B were accompanied by mill certificates which reported a yield strength, ultimate strength, and an elongation at fracture for a flange coupon that was tested by the mill from the same heat of steel. The coupons that were provided by Producer C were accompanied by mill certificates that gave a yield strength, ultimate strength, and an elongation at fracture for a flange coupon at Location 6 tested by the mill.

Fig. 3.9.1 shows the mill yield strength, $F_{y\text{-mill}}$, versus the UWO yield strength, $F_{y\text{-UWO}}$, for flange coupons. Slightly more than half the data lie above the 45° line, indicating that the mill generally reports slightly higher yield strengths. On average, the yield strength reported by the mill certificate was 2.6 MPa (0.4 ksi) or 1.008 times higher than the yield strength achieved by UWO. This inconsistency could easily be attributed to the more rapid rate of loading used by the mill. A detailed break down of the statistics is given in Table 3.9.1 for the difference between the mill reported yield strength and the UWO yield strength, $F_{y\text{-mill}}$-$F_{y\text{-UWO}}$, and the ratio between the mill reported yield strength and the UWO yield strength, $F_{y\text{-mill}}/F_{y\text{-UWO}}$.

Fig. 3.9.2 shows the mill ultimate strength versus the UWO ultimate strength for flange coupons. In this case, the majority of the data lies above the 45° line, indicating that the mill almost always reports slightly higher ultimate strengths. On average, the ultimate strength reported on the mill certificate was 9.9 MPa (1.4 ksi) or 1.021 times higher than the UWO ultimate strength. Each producer's reported ultimate strengths were consistently higher than the UWO ultimate strengths. A more detailed break down of the statistics of the mill versus as tested data for the ultimate strengths is given in Table 3.9.1 where $F_{u\text{-mill}}$ is the ultimate strength reported by the mill and $F_{u\text{-UWO}}$ is the ultimate strength achieved by UWO.

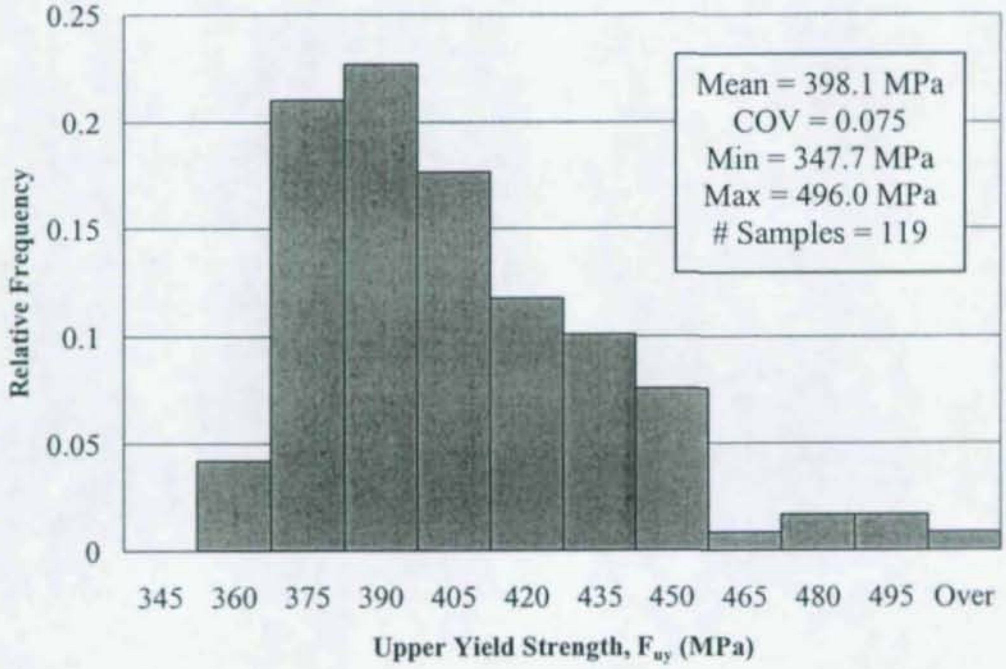

Figure 3.1.1: Histogram of F_{uy} For UWO Data

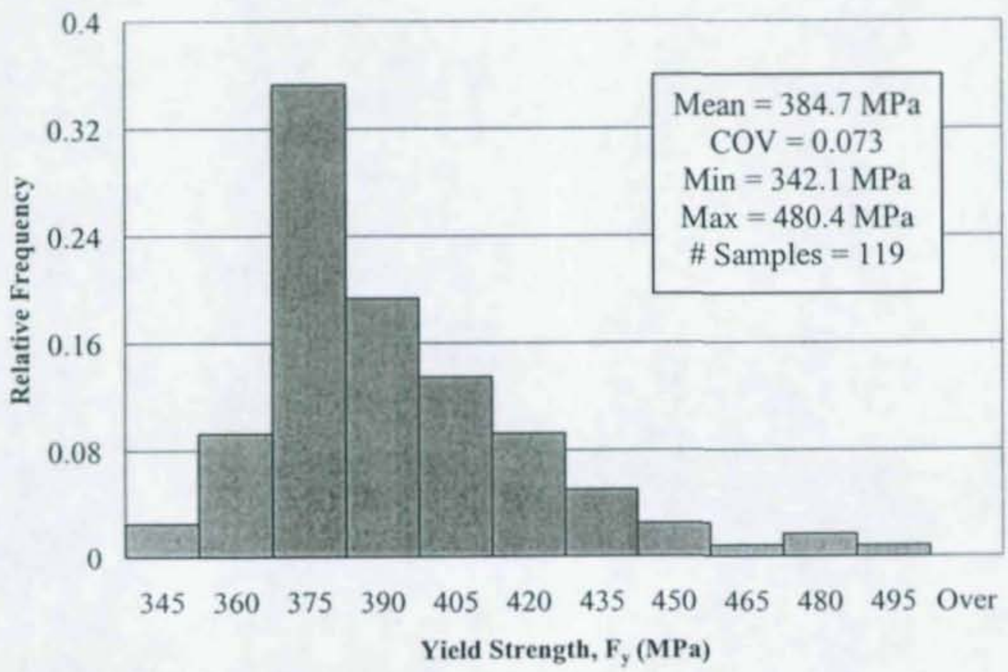

Figure 3.1.2: Histogram of F_y For UWO Data

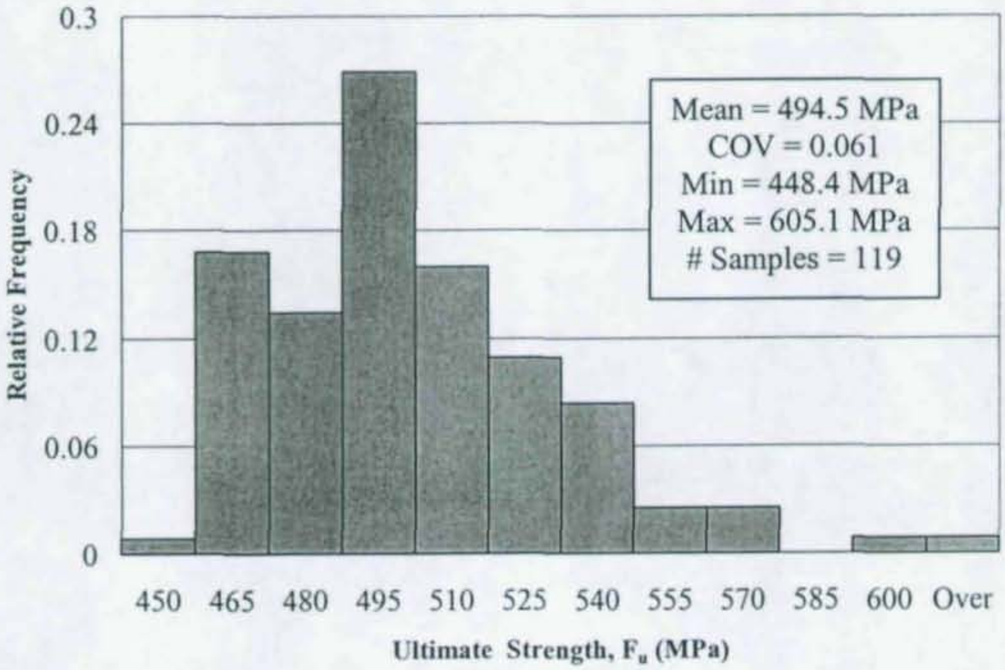

Figure 3.1.3: Histogram of F_u For UWO Data

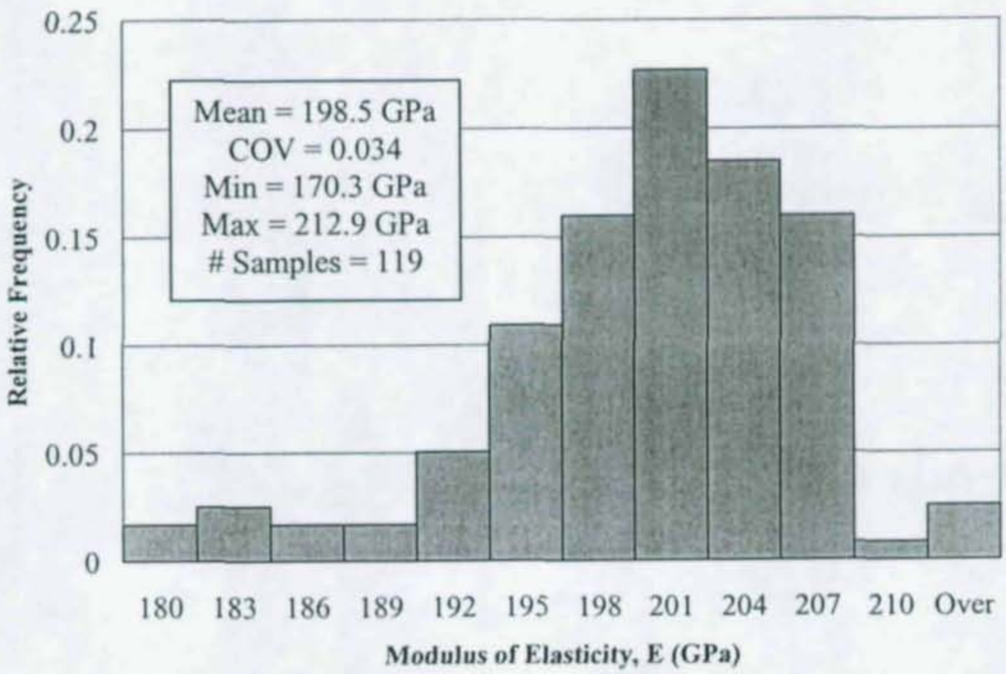

Figure 3.1.4: Histogram of E For UWO Data

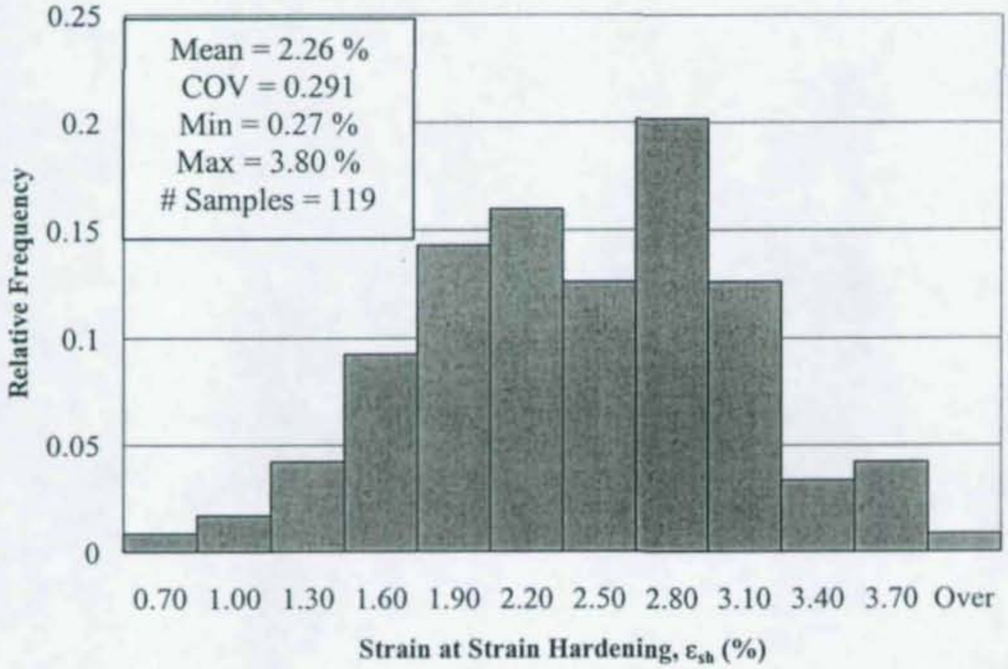

Figure 3.1.5: Histogram of ε_{sh} For UWO Data

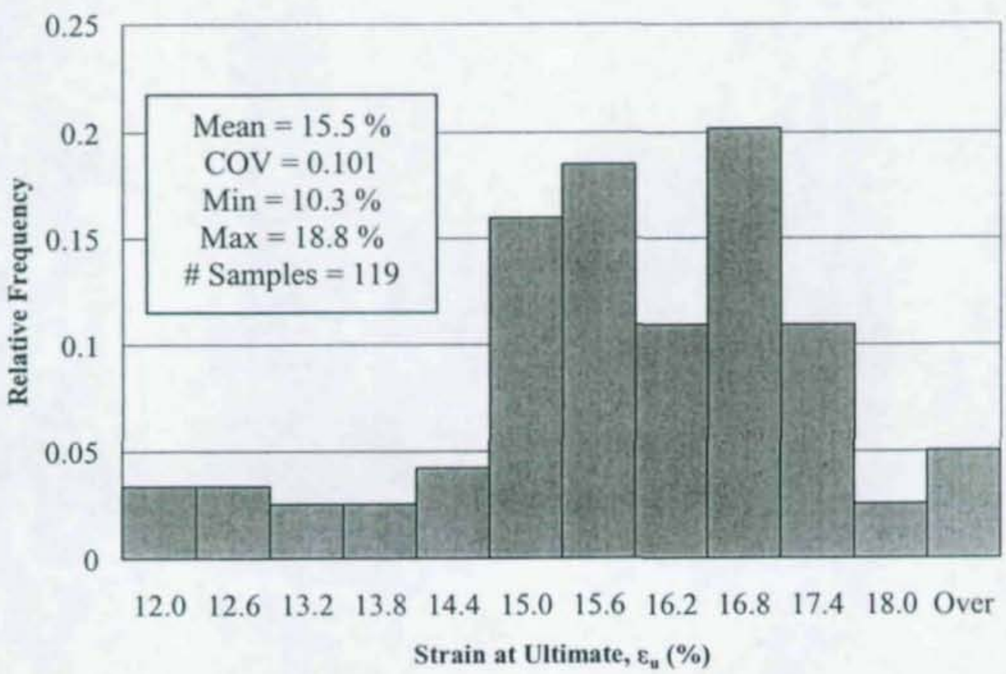

Figure 3.1.6: Histogram of ε_u For UWO Data

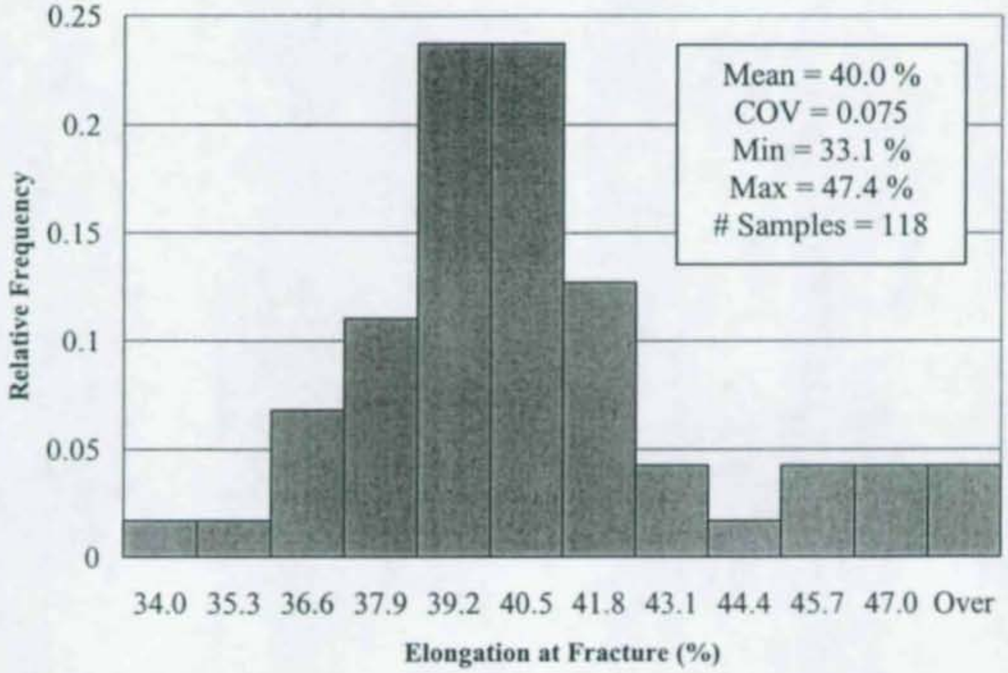

Figure 3.1.7: Histogram of % Elongation at Fracture For UWO Data (50.8 mm Gauge Length)

Table 3.1.1: Summary of Material Property Statistics for UWO Data

Statistic	F_{uy}	F_y	F_u	E	ε_{sh}	ε_u	Elong.
Mean	398.1 MPa	384.7 MPa	494.5 MPa	198.5 GPa	2.26%	15.5%	40.0%
COV	0.075	0.073	0.061	0.034	0.291	0.101	0.075
Min	347.7 MPa	342.1 MPa	448.4 MPa	170.3 GPa	0.27%	10.3%	33.1%
Max	496.0 MPa	480.4 MPa	605.1 MPa	212.9 GPa	3.80%	18.8%	47.4%
Number	119	119	119	119	119	119	118

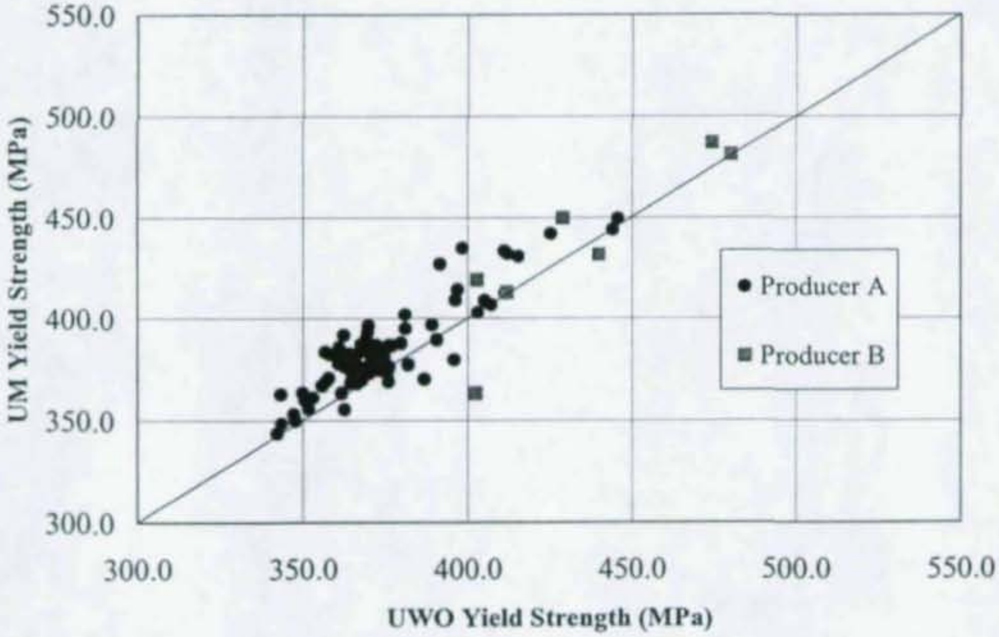

Figure 3.2.1: Comparison of UWO and UM Yield Strengths

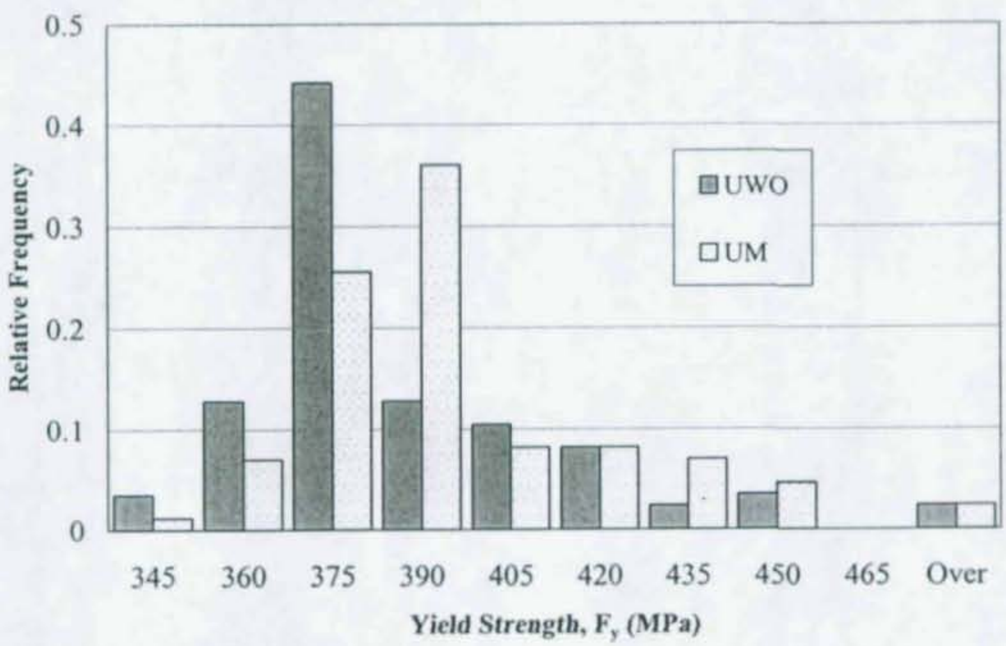

Figure 3.2.2: Histogram of F_y For Each Laboratory

Table 3.2.1: Comparative Summary of Statistics for F_y

Source	Testing Lab	$\overline{F_y}$ (MPa)	V_{Fy}	Min (MPa)	Max (MPa)	#
A and B	UWO	380.6	0.073	342.1	480.4	88
	UM	388.8	0.072	343.4	487.2	88
A – Only	UWO	374.8	0.056	342.1	445.7	79
	UM	384.8	0.058	343.4	449.5	81
B – Only	UWO	431.9	0.063	402.3	480.4	9
	UM	435.1	0.091	363.3	487.2	7

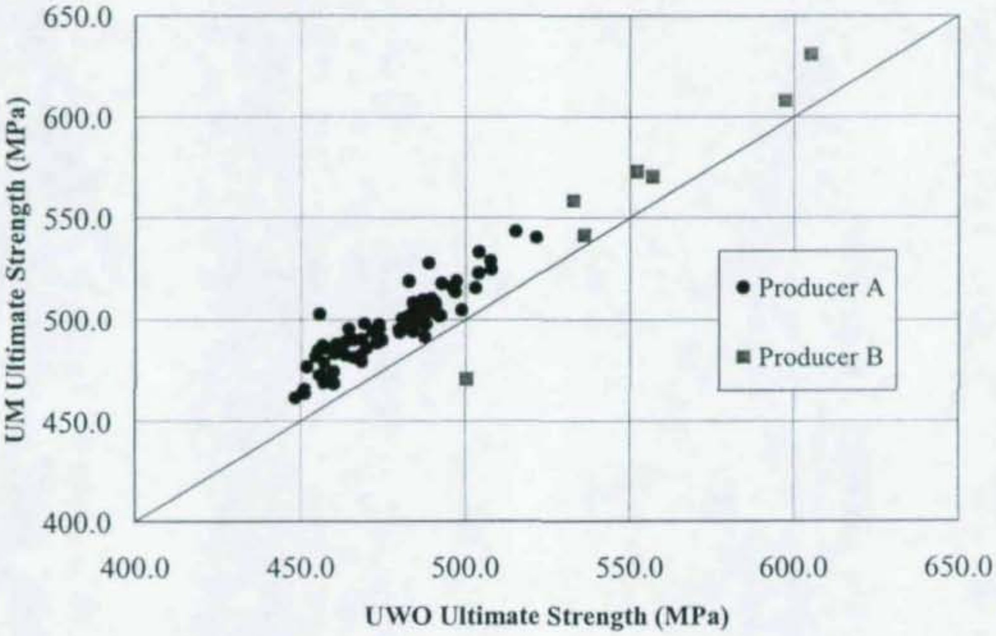

Figure 3.2.3: Comparison of UWO and UM Ultimate Strengths

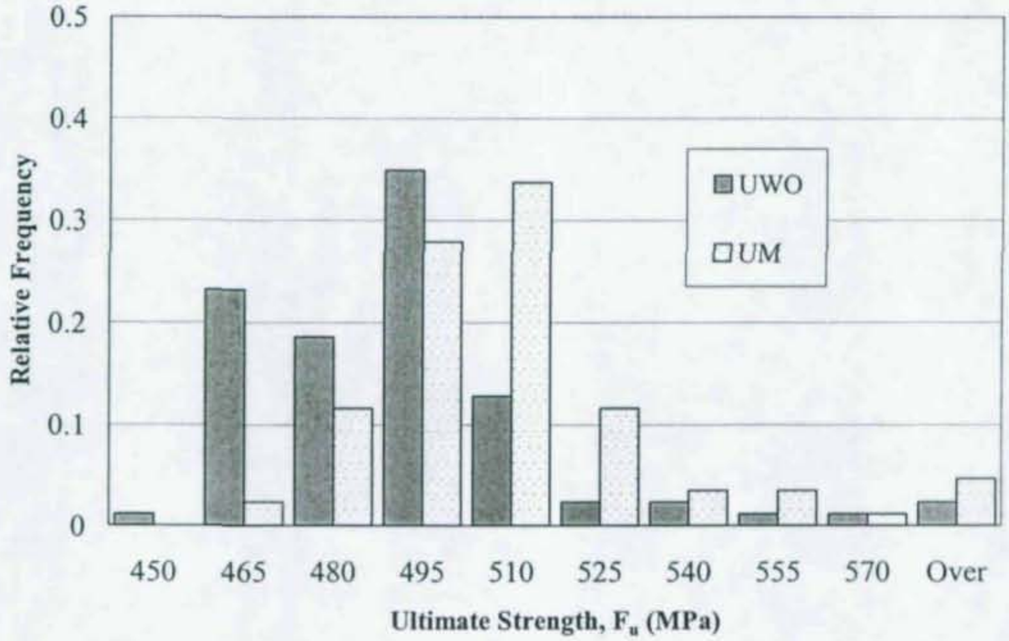

Figure 3.2.4: Histogram of F_u For Each Laboratory

Table 3.2.2: Comparative Summary of Statistics for F_u

Source	Testing Lab	$\overline{F_u}$ (MPa)	V_{Fu}	Min (MPa)	Max (MPa)	#
A and B	UWO	486.5	0.062	448.4	605.1	88
	UM	502.9	0.056	461.2	631.2	88
A – Only	UWO	478.5	0.035	448.4	521.5	79
	UM	497.6	0.034	461.2	543.2	81
B – Only	UWO	556.2	0.055	500.1	605.1	9
	UM	564.8	0.084	470.7	631.2	7

Table 3.2.3: Summary of Mean k Values

Strength	UWO	UM
Yield	0.78	1.03
Ultimate	0.69	1.14

Table 3.2.4: Summary of COV Values for Precision Statements

Strength	V_r (%)	V_R (%)
Yield (0.2% Offset)	0.71	2.59
Ultimate	1.36	2.17

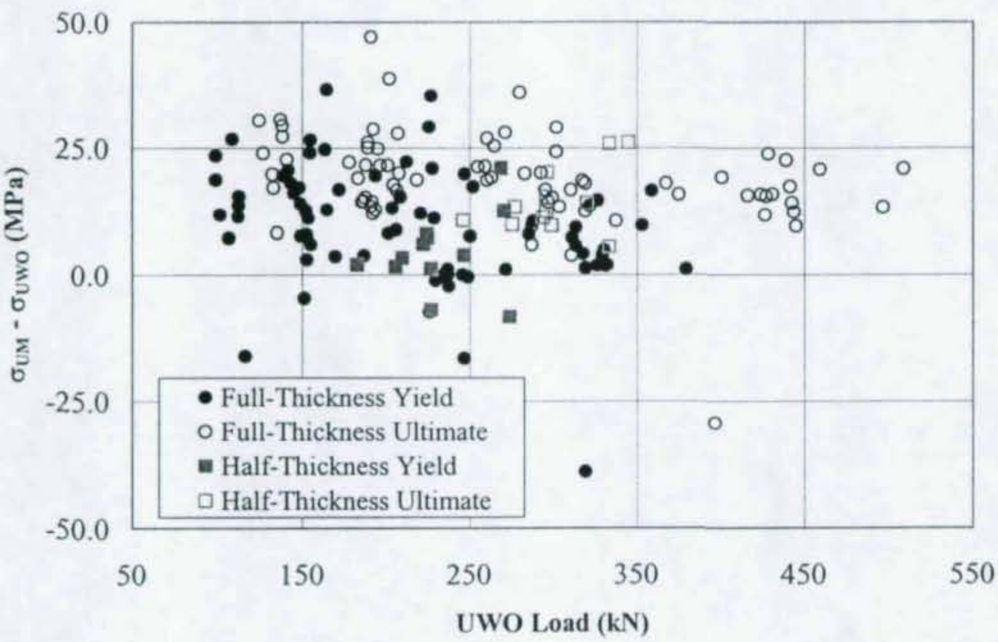

Figure 3.2.5: Stress Difference vs UWO Load

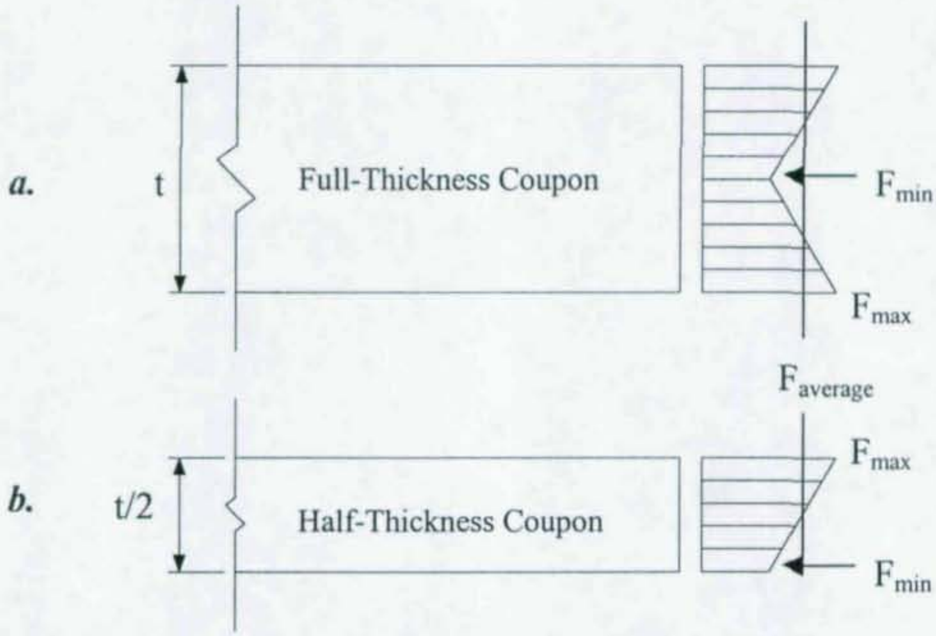

Figure 3.3.1: Strength Distribution Through Coupon Thickness

Table 3.3.1: Yield Strength of Half and Full-Thickness Coupons

Coupon UWO	Coupon UM	$F_{y\text{-}UWO}$ (MPa)	$F_{y\text{-}UM}$ (MPa)	$F_{y\text{-}UM}-F_{y\text{-}UWO}$ (MPa)	$F_{y\text{-}UM}/F_{y\text{-}UWO}$
141A2	141A1	374.7	378.6	3.9	1.010
141A3	141A4	375.9	369.0	-6.9	0.982
141B2	141B1	368.5	375.8	7.3	1.020
141B3	141B4	365.0	371.1	6.1	1.017
141C1	141C2	370.7	378.7	8.0	1.022
141C3	141C4	373.2	374.4	1.2	1.003
142A6	142A5	367.9	371.3	3.4	1.009
142B6	142B5	347.7	349.7	2.0	1.006
142C6	142C5	361.6	363.2	1.6	1.004
JA6	JA5	474.6	487.2	12.6	1.027
JB2	JB1	439.9	431.6	-8.3	0.981
JB3	JB4	428.9	449.9	21	1.049
			Average	4.3	1.011

Table 3.3.2: Ultimate Strength of Half and Full-Thickness Coupons

Coupon UWO	Coupon UM	$F_{u\text{-}UWO}$ (MPa)	$F_{u\text{-}UM}$ (MPa)	$F_{u\text{-}UM}-F_{y\text{-}UWO}$ (MPa)	$F_{u\text{-}UM}/F_{y\text{-}UWO}$
141A2	141A1	486.3	500.4	14.1	1.029
141A3	141A4	486.5	497.8	11.3	1.023
141B2	141B1	486.0	506.2	20.2	1.042
141B3	141B4	485.6	498.1	12.5	1.026
141C1	141C2	488.5	503.9	15.4	1.032
141C3	141C4	491.9	501.6	9.7	1.020
142A6	142A5	485.7	499.1	13.4	1.028
142B6	142B5	468.3	479.1	10.8	1.023
142C6	142C5	483.8	493.8	10.0	1.021
JA6	JA5	605.1	631.2	26.1	1.043
JB2	JB1	536.0	541.5	5.5	1.010
JB3	JB4	532.7	558.5	25.8	1.048
			Average	14.6	1.029

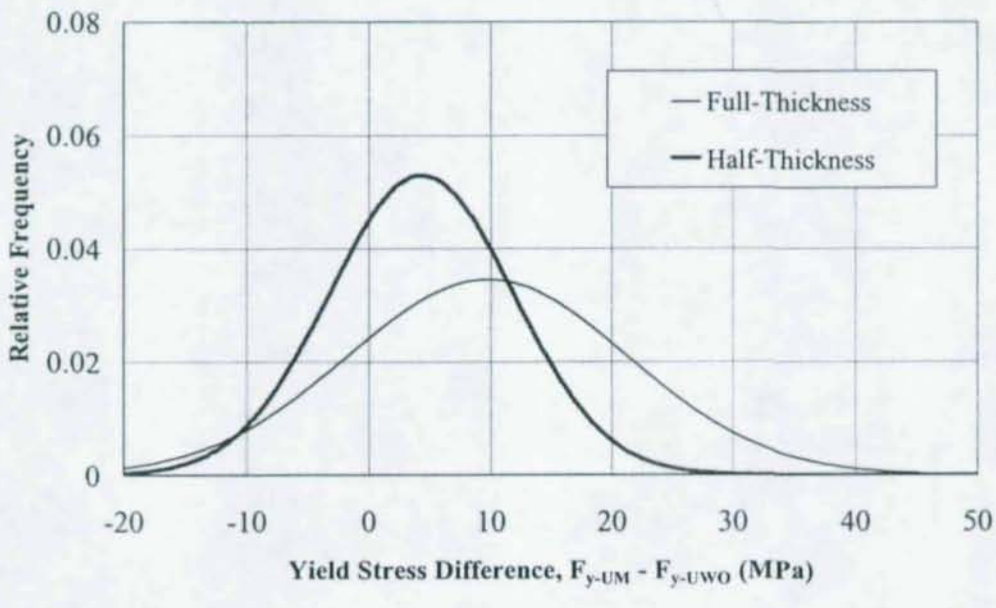

Figure 3.3.2: Distributions of Yield Stress Difference for Half and Full-Thickness Coupons

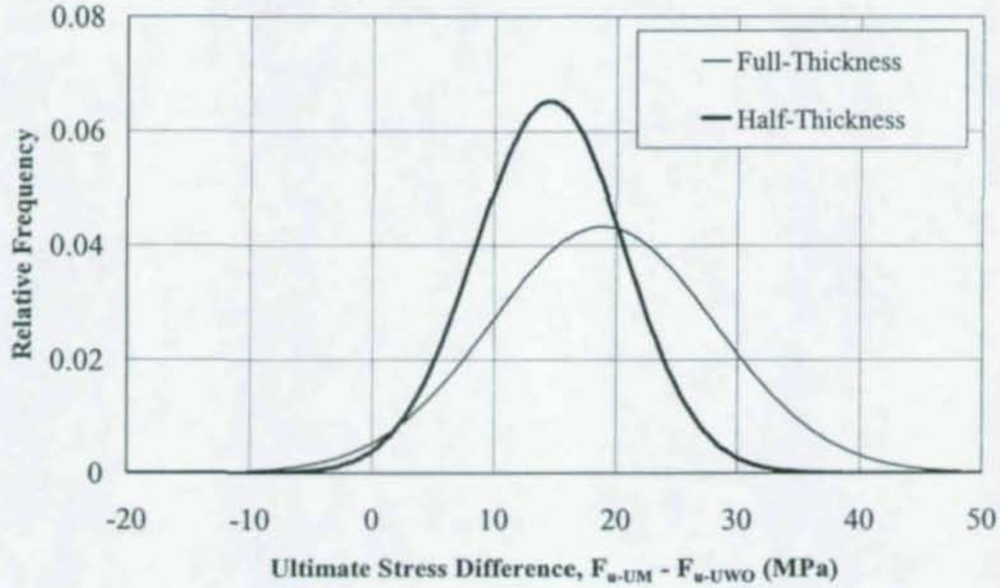

Figure 3.3.3: Distributions of Ultimate Stress Difference for Half and Full-Thickness Coupons

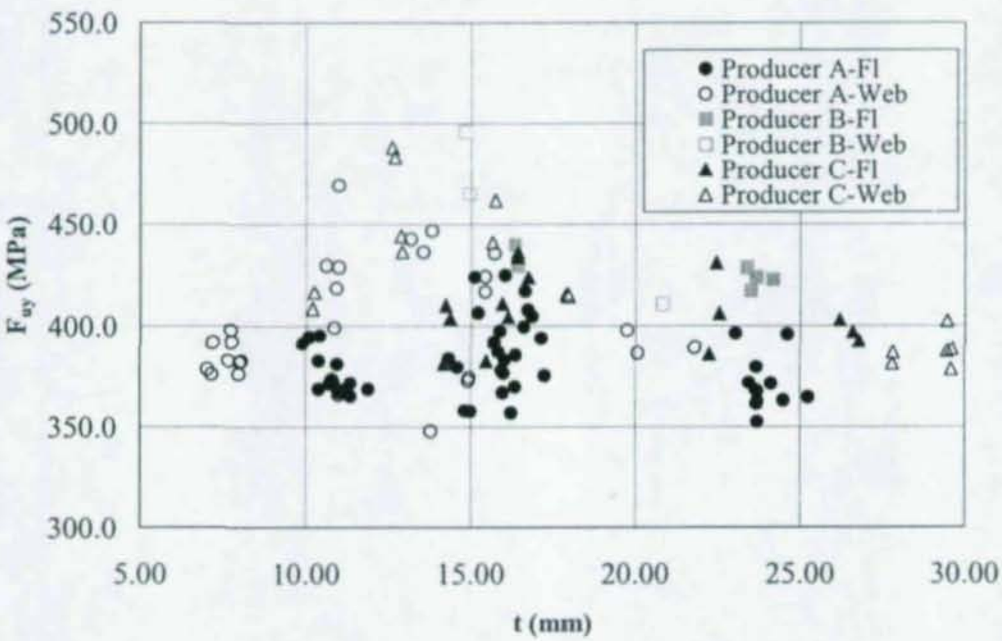

Figure 3.4.1: Plot of F_{uy} Versus Thickness

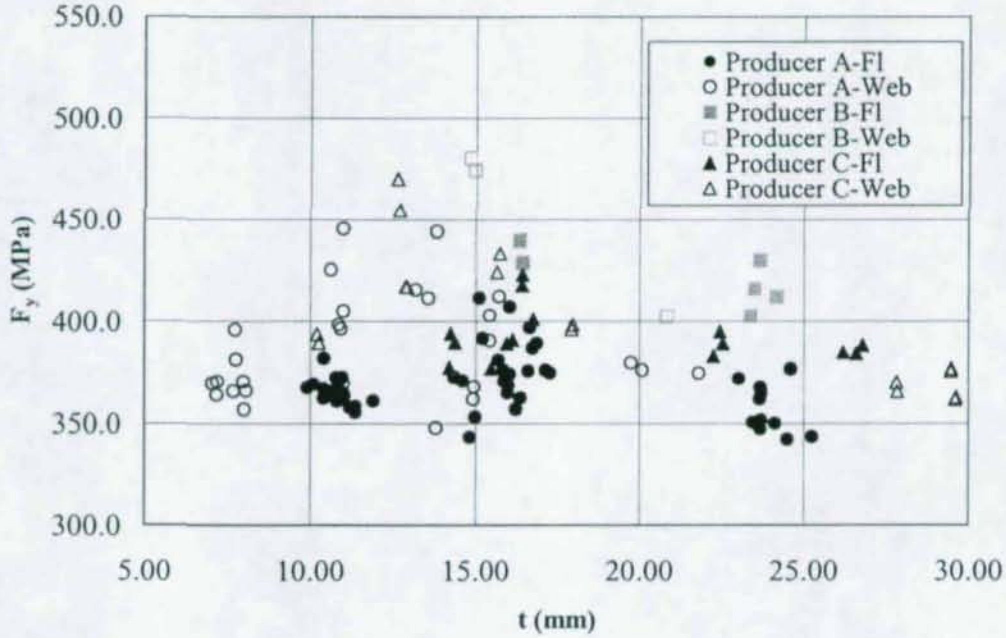

Figure 3.4.2: Plot of F_y Versus Thickness

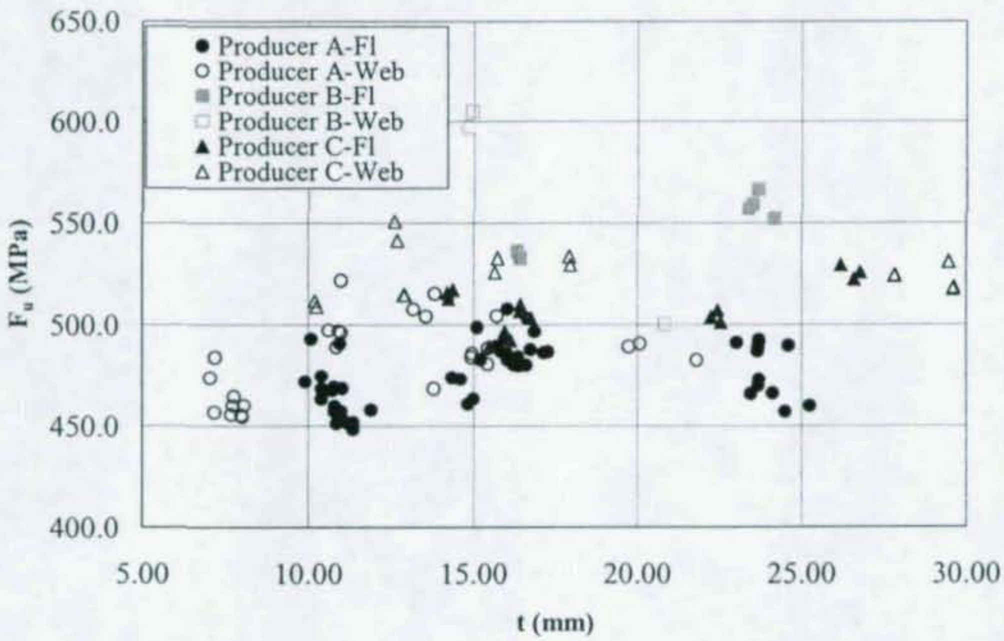

Figure 3.4.3: Plot of F_u Versus Thickness

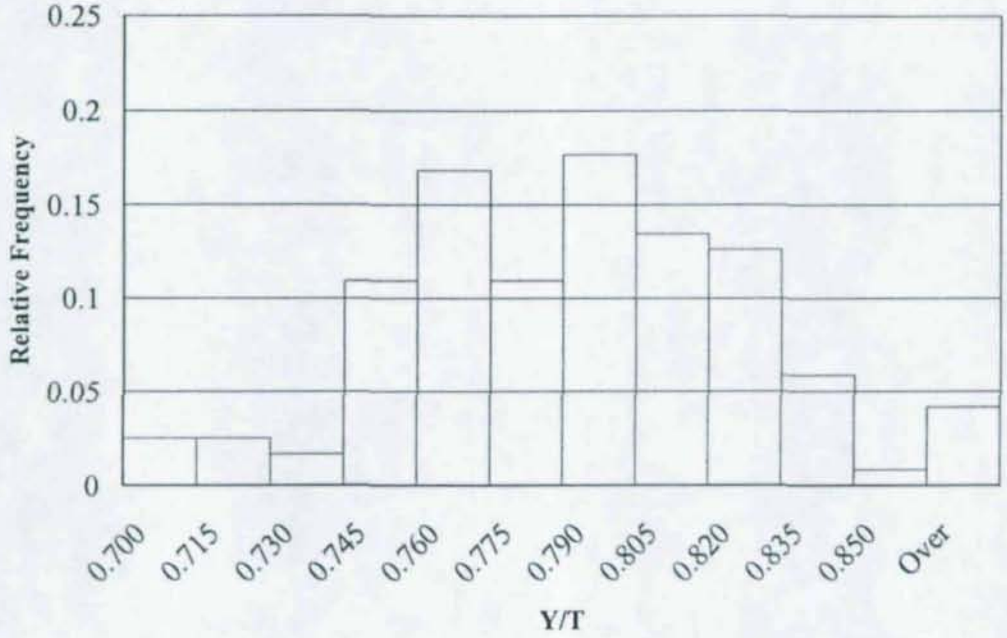

Figure 3.5.1: Histogram of Y/T

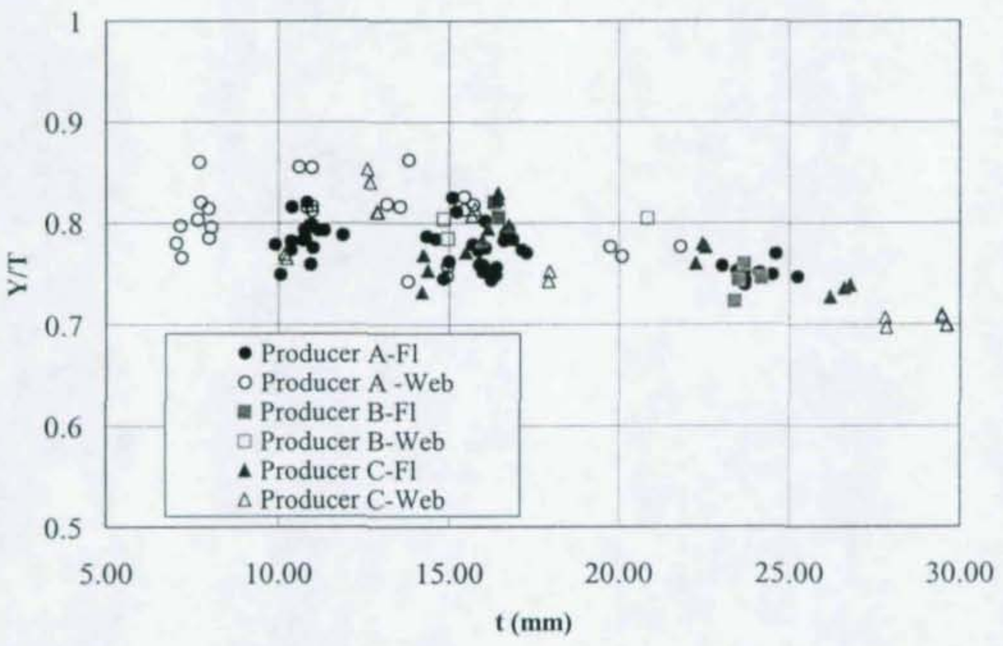

Figure 3.5.2: Plot of Y/T Versus Thickness

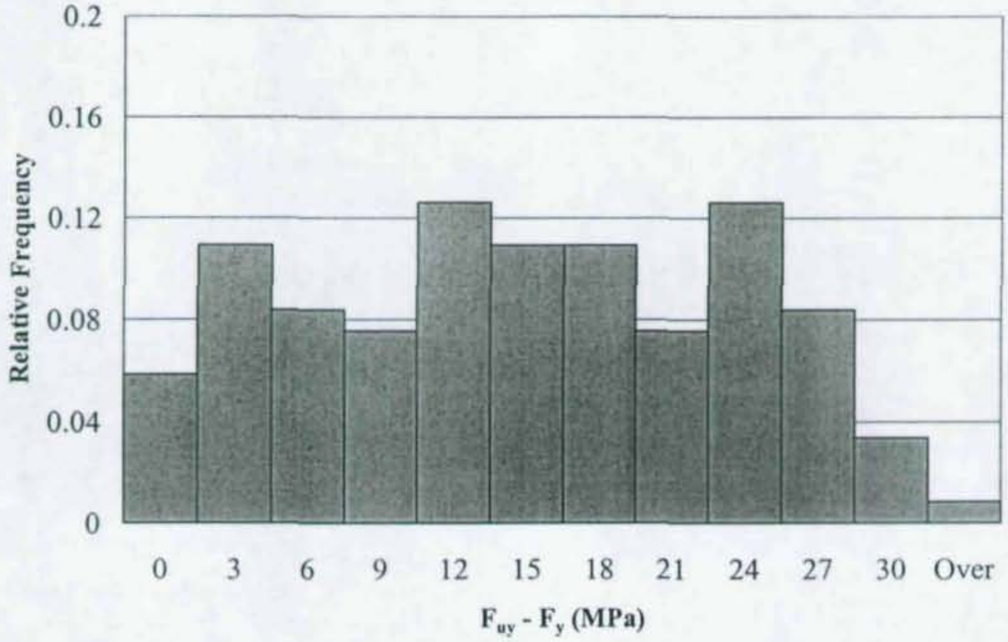

Figure 3.6.1: Histogram of Upper Yield Strength Minus Yield Strength

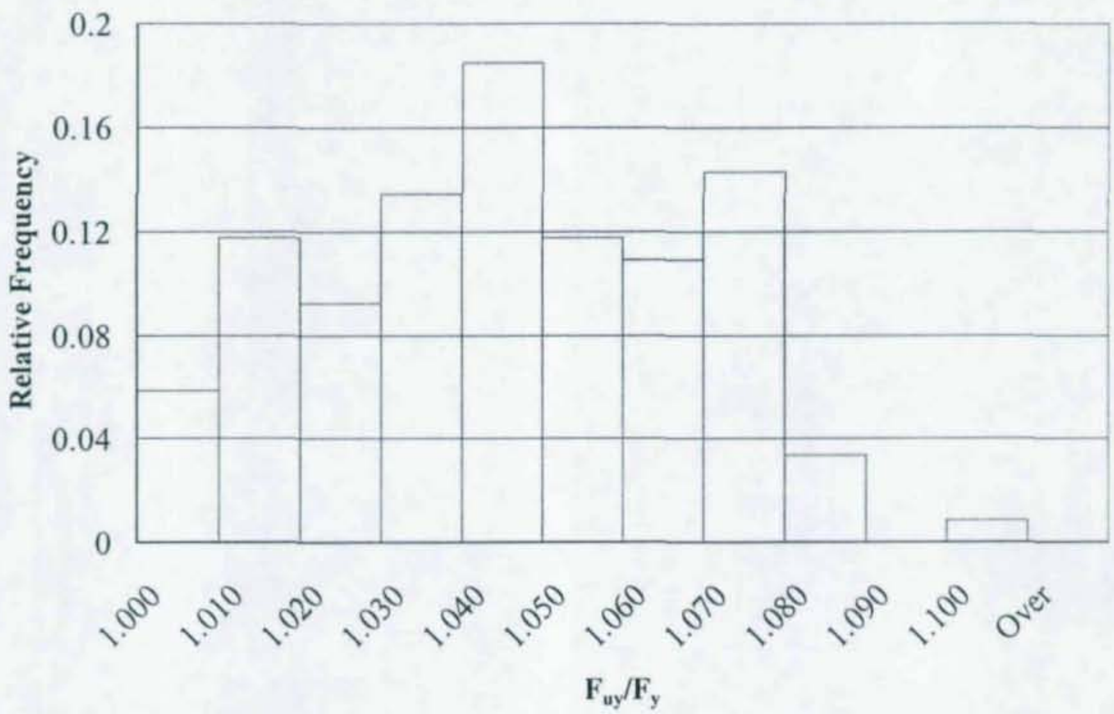

Figure 3.6.2: Histogram of Upper Yield Strength Divided by Yield Strength

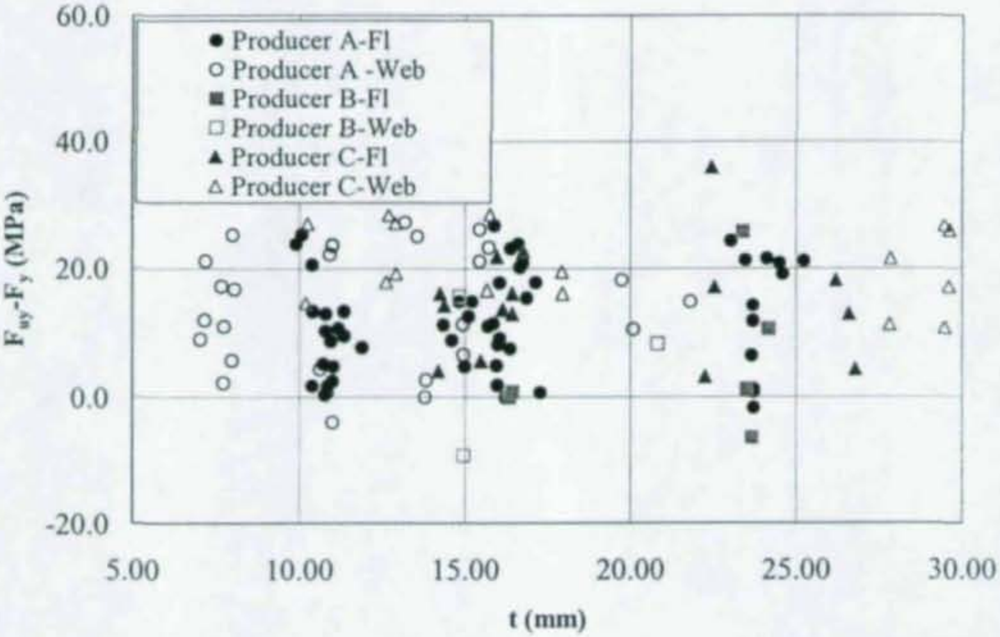

Figure 3.6.3: Plot of Upper Yield Strength Minus Yield Strength Versus Thickness

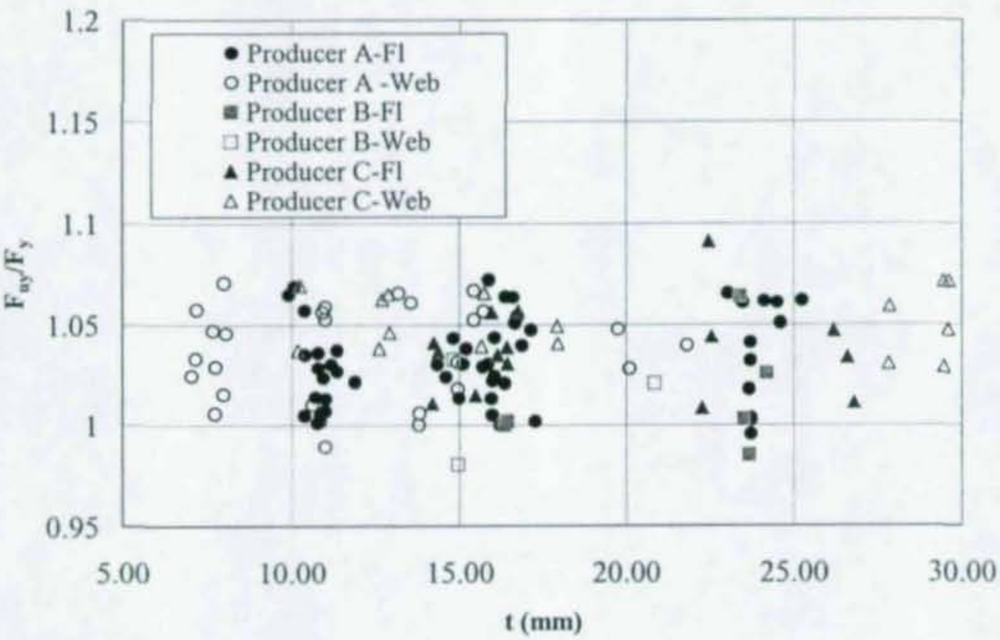

Figure 3.6.4: Plot of Upper Yield Strength Divided By Yield Strength Versus Thickness

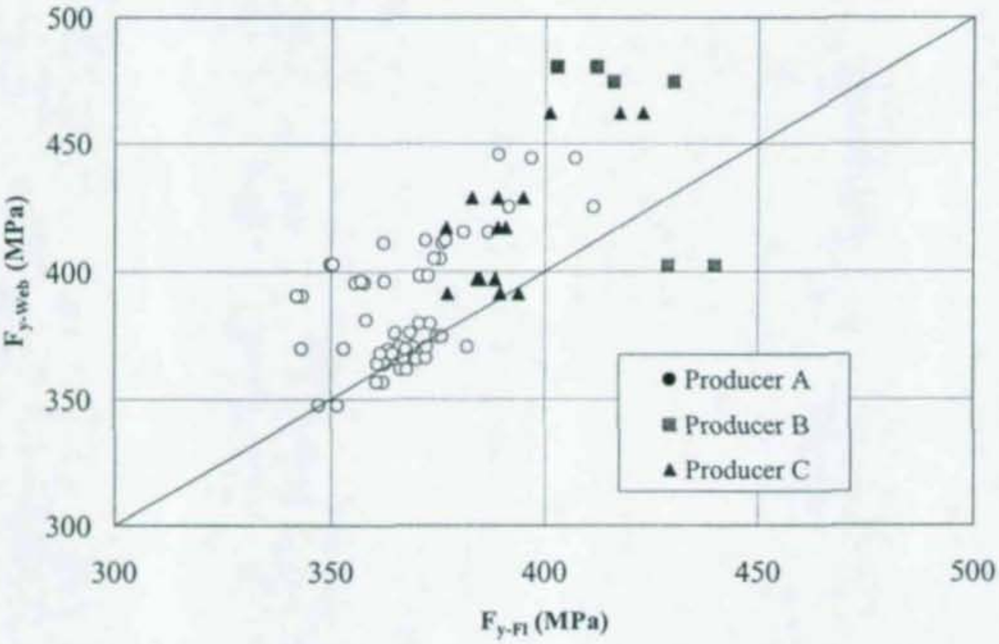

Figure 3.7.1: Web Yield Strengths Versus Flange Yield Strengths

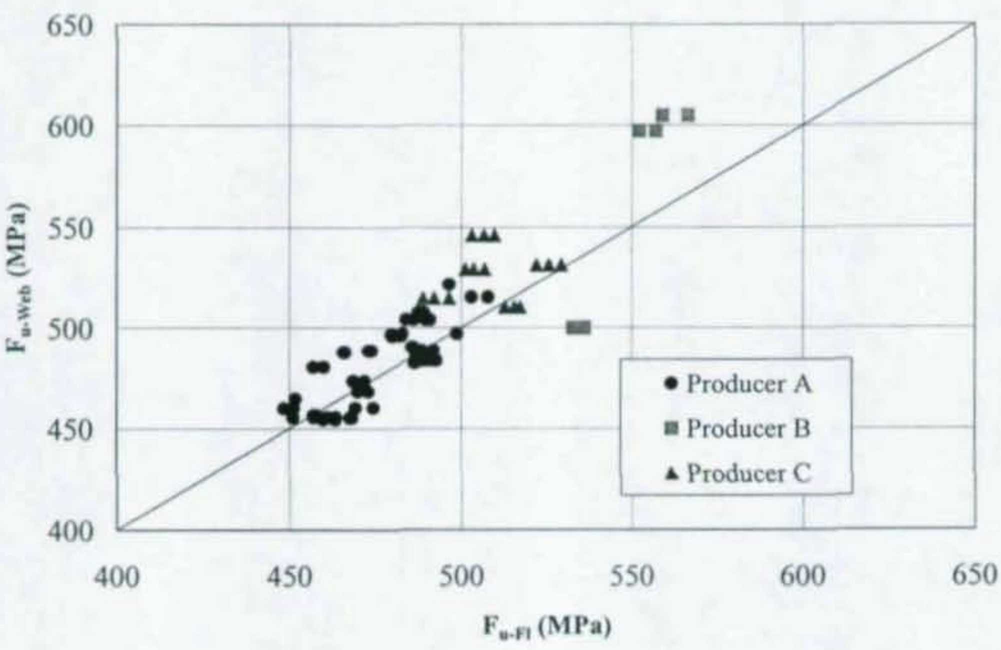

Figure 3.7.2: Web Ultimate Strengths Versus Flange Ultimate Strengths

Table 3.7.1: Web and Flange Strength Comparison By Producer

Quantity	Parameter	All Data	Producer A	Producer B	Producer C
$F_{y\text{-}web} - F_{y\text{-}fl}$	Mean	21.2 MPa	18.4 MPa	30.8 MPa	27.3 MPa
	COV	1.092	1.078	1.484	0.654
$F_{y\text{-}web}/F_{y\text{-}fl}$	Mean	1.056	1.050	1.076	1.069
	COV	0.057	0.052	0.102	0.042
$F_{u\text{-}web} - F_{u\text{-}fl}$	Mean	8.7 MPa	5.1 MPa	17.0 MPa	17.6 MPa
	COV	1.936	2.197	2.139	0.898
$F_{u\text{-}web}/F_{u\text{-}fl}$	Mean	1.017	1.011	1.030	1.035
	COV	0.032	0.023	0.064	0.030

Table 3.8.1: Summary of Producer Data for Yield Strengths

	Producer A			Producer B			Producer C		
	All	Fl	Web	All	Fl	Web	All	Fl	Web
Mean (MPa)	374.8	368.2	387.5	431.9	421.6	452.4	396.4	392.2	400.4
COV	0.056	0.039	0.066	0.063	0.030	0.079	0.063	0.032	0.080
Min (MPa)	342.1	342.1	347.7	402.3	402.7	402.3	361.5	376.9	361.5
Max (MPa)	445.7	411.4	445.7	480.4	439.9	480.4	470.2	423.0	470.2
# Samples	79	52	27	9	6	3	31	15	16

Table 3.8.2: Summary of Producer Data for Ultimate Strengths

	Producer A			Producer B			Producer C		
	All	Fl	Web	All	Fl	Web	All	Fl	Web
Mean (MPa)	478.5	476.6	482.2	556.2	550.6	567.5	517.4	508.7	525.5
COV	0.035	0.031	0.040	0.055	0.022	0.084	0.027	0.023	0.021
Min (MPa)	448.5	448.4	454.4	500.1	532.7	500.1	488.9	488.9	508.8
Max (MPa)	521.5	507.7	521.5	605.1	566.5	605.1	550.8	529.3	550.8
# Samples	79	52	27	9	6	3	31	15	16

Table 3.8.3: Yield Strength Summary By Shape Size Group

Group	All Producers			Producer A			Producer B			Producer C		
	#	$\overline{F_y}$ (MPa)	V_{Fy}	#	$\overline{F_y}$ (MPa)	V_{Fy}	#	$\overline{F_y}$ (MPa)	V_{Fy}	#	$\overline{F_y}$ (MPa)	V_{Fy}
1	26	367.4	0.023	26	367.4	0.023	0	-	-	0	-	-
2	58	394.5	0.076	35	384.6	0.070	3	431.7	0.080	20	406.3	0.061
3	17	387.1	0.052	9	373.1	0.011	3	423.7	0.037	5	390.3	0.015
4	18	376.1	0.084	9	359.6	0.022	3	440.3	0.057	6	368.7	0.016

Table 3.8.4: Ultimate Strength Summary By Shape Size Group

Group	All Producers			Producer A			Producer B			Producer C		
	#	$\overline{F_u}$ (MPa)	V_{Fu}	#	$\overline{F_u}$ (MPa)	V_{Fu}	#	$\overline{F_u}$ (MPa)	V_{Fu}	#	$\overline{F_u}$ (MPa)	V_{Fu}
1	26	464.0	0.025	26	464.0	0.025	0	-	-	0	-	-
2	58	499.5	0.052	35	486.1	0.034	3	568.8	0.036	20	512.7	0.029
3	17	505.6	0.041	9	487.4	0.006	3	522.9	0.031	5	527.9	0.007
4	18	512.0	0.071	9	482.2	0.018	3	576.9	0.035	6	524.2	0.010

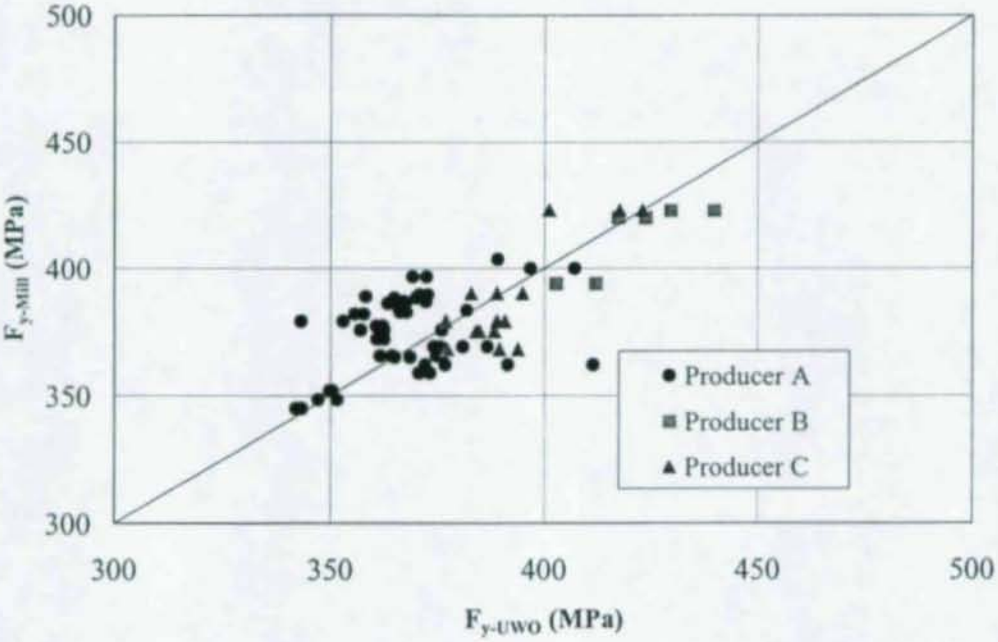

Figure 3.9.1: Plot of Yield Strength As Tested Versus Mill Certificate Yield Strength

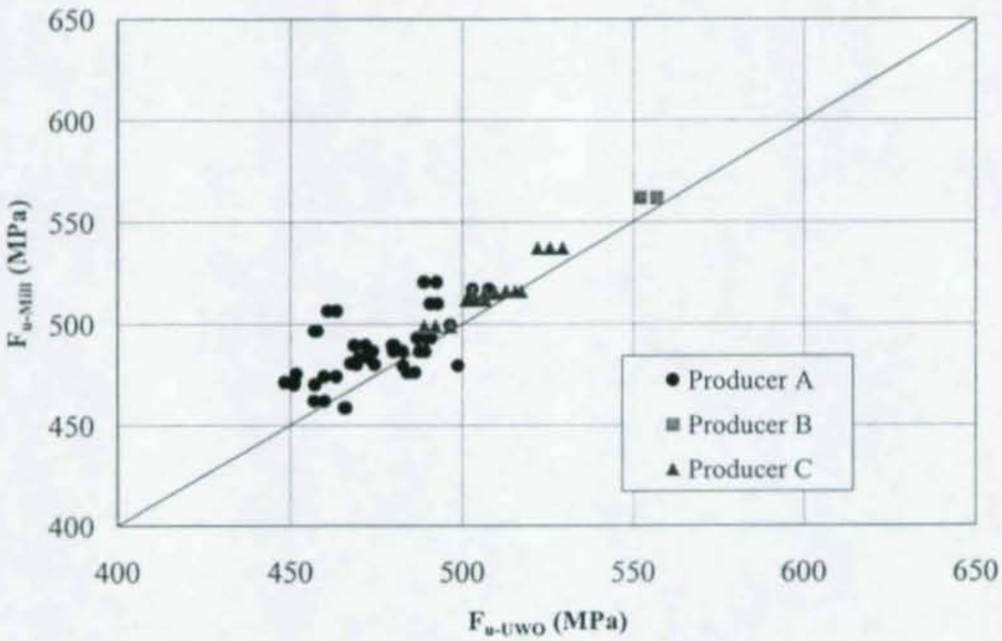

Figure 3.9.2: Plot of Ultimate Strength as Tested Versus Mill Certificate Ultimate Strength

Table 3.9.1: Summary of Mill Report Strengths Versus As Tested Strengths

	All Data		All Data	
	$F_{y\text{-mill}}-F_{y\text{-UWO}}$	$F_{y\text{-mill}}/F_{y\text{-UWO}}$	$F_{u\text{-mill}}-F_{u\text{-UWO}}$	$F_{u\text{-mill}}/F_{u\text{-UWO}}$
Mean (MPa)	2.6	1.008	9.9	1.021
COV	6.078	0.042	1.178	0.024
Min (MPa)	-49.4	0.880	-19.2	0.961
Max (MPa)	35.8	1.104	45.7	1.099
#	73	73	73	73

4.1 Summary and Conclusions

A total of 119 tensile coupons fabricated from ASTM A992 structural steel were tested at the University of Western Ontario (UWO). Another 88 coupons were tested in a parallel study at the University of Minnesota (UM).

This study has yielded the following conclusions:

1. The statistical parameters for the material properties of the steel tested at UWO to be used for subsequent reliability analysis, are as shown in Table 3.1.1.
2. On average, UM yield strengths were 9.0 MPa (1.3 ksi) higher than the UWO yield strengths for coupons from the same sample. Similarly, the UM ultimate strengths averaged 18.3 MPa (2.7 ksi) higher than the corresponding UWO ultimate strengths.
3. The effect of testing half-thickness specimens instead of full-thickness specimens was statistically insignificant for both the yield and ultimate strengths.
4. Both F_{uy} and F_y decreased slightly with an increase in the coupon thickness, although the trend was statistically significant. F_u was relatively invariant with thickness.
5. The mean value of Y/T was found to be 0.778. There were 5 web coupons with larger than the 0.85 stipulated for flange coupons in ASTM A992 with a maximum value of 0.862.
6. The yield plateau strength was on average 13.4 MPa (1.9 ksi) less than the upper yield point for loading rates between 42 and 171 $\mu\varepsilon$/s.
7. The yield strength of a web coupon was higher than the yield strength of the corresponding flange coupon by an average of 21.2 MPa (3.1 ksi) or a factor of 1.056. This consistent with the assumptions made by Kennedy and Gad Aly (1980)

in their original derivation of the resistance factor, ϕ. The ultimate strength of a web coupon was higher than the ultimate strength of the corresponding flange coupon by an average of 8.7 MPa (1.3 ksi) or a factor of 1.007.

8. F_y and F_u are dependent on producer.
9. The reported yield strengths on mill test certificates were 2.9 MPa (0.4 ksi), or 1.008 times, higher than those obtained in the lab. The ultimate strengths reported on mill certificates were higher than those obtained in the lab by an average of 9.9 MPa (1.4 ksi), or a factor of 1.021.

References

1. ASTM Specification A6 (1997): *Standard Specification for General Requirements for Rolled Structural Steel Bars, Plates, Shapes, and Sheet Piling*. West Conshohocken, PA.

2. ASTM Specification A370 (1996): *Standard Test Methods and Definitions for Mechanical Testing of Steel Products*. West Conshohocken, PA.

3. ASTM Specification A992 (1998): *Standard Specification for Steel for Structural Shapes For Use in Building Framing*. West Conshohocken, PA.

4. ASTM Specification E8 (1996a): *Standard Test Methods for Tension Testing of Metallic Materials*. West Conshohocken, PA.

5. ASTM Specification E178 (1994): *Standard Practice for Dealing With Outlying Observations*. West Conshohocken, PA.

6. ASTM Specification E691 (1992): *Standard Practice for Conducting an Interlaboratory Study to Determine the Precision of a Test Method*. West Conshohocken, PA.

7. CSA Standard CAN/CSA S16.1-94 (1994): *Limit States Design of Steel Structures*. Rexdale, Ontario.

8. Jaquess, T. K., and Frank, K. (1999): "Characterization of the Material Properties of Rolled Sections". The University of Texas at Austin.

9. Kennedy, D. J. L., and Gad Aly, M. (1980): "Limit States Design of Steel Structures-Performance Factors". *Canadian Journal of Civil Engineering*. Vol. 7. pp. 45-77.

10. Larsen, R. J., and Marx, M. (1986): "An Introduction to Mathematical Statistics and its Applications". Prentice-Hall. Englewood Cliffs, NJ.

11. Rao, N. R. N., Lohrmann, M., Tall, L. (1966): "Effect of Strain Rate on the Yield Stress of Structural Steels". *Journal of Materials, ASCE*. Vol. 1 No. 1. pp. 241-262.

12. Schmidt, B. (2000): "Review of the Resistance Factor For Steel". Master's Thesis. The University of Western Ontario.

13. Soroushian, P., and Choi, K. (1987): "Steel Mechanical Properties at Different Strain Rates". *Journal of Structural Engineering, ASCE*. Vol. 113. No. 4. pp. 663-672.

Appendix A: UWO Data Summary

ID#	Type	t (mm)	F_{uy} (MPa)	F_y (MPa)	$F_{y\text{-mill}}$ (MPa)	F_u (MPa)	$F_{u\text{-mill}}$ (MPa)	E (GPa)	$d\varepsilon/dt$ ($\mu\varepsilon$/s)	ε_{sh} (%)	ε_u (%)	% Elong.
625D2	Flange	10.85	371.7	370.0	388.2	451.0	470.2	195.0	76.2	2.89	18.1	41.5
625D3	Flange	11.00	367.4	364.9	388.2	457.1	470.2	193.5	72.1	3.62	17.4	40.7
625D6	Web	7.67	382.9	365.7	-	455.4	-	207.0	74.7	3.54	18.4	41.8
625E2	Flange	11.35	365.2	355.7	381.9	448.4	471.3	203.0	45.6	3.26	18.2	41.5
625E3	Flange	11.18	368.5	357.8	381.9	451.3	471.3	211.1	52.0	3.54	18.8	42.2
625E6	Web	7.72	397.9	395.7	-	460.0	-	204.2	65.7	3.80	13.2	36.6
625F2	Flange	11.35	371.5	358.2	388.8	451.7	475.4	197.1	71.2	3.46	16.8	40.2
625F3	Flange	10.77	-	-	388.8	-	475.4	-	-	-	-	-
625F6	Web	7.75	392.0	381.0	-	464.5	-	211.0	42.1	3.51	17.0	40.4
831D2	Flange	10.39	382.8	362.2	377.2	463.3	474.0	204.6	58.5	2.39	14.8	38.1
831D3	Flange	10.80	373.6	360.7	377.2	459.8	474.0	200.8	78.7	2.52	16.9	40.2
831D6	Web	8.00	381.9	356.7	-	454.4	-	194.8	61.6	2.98	17.7	41.1
831E2	Flange	10.39	368.7	367.0	386.8	474.4	479.9	203.7	82.0	1.96	15.4	38.7
831E3	Flange	10.77	372.5	372.2	386.8	469.2	479.9	205.8	91.9	2.39	16.5	39.9
831E6	Web	8.05	382.8	366.1	-	460.1	-	208.4	97.1	2.99	16.6	40.0
831F2	Flange	10.41	395.1	381.8	383.4	468.2	480.6	200.3	101.4	2.29	14.9	38.3
831F3	Flange	10.72	371.2	366.1	383.4	467.5	480.6	198.2	91.2	2.21	14.9	38.2
831F6	Web	7.98	376.2	370.5	-	455.2	-	206.0	98.3	2.78	16.9	40.3
8A2	Flange	10.08	394.4	369.1	396.5	492.7	510.0	199.4	126.4	1.87	16.5	39.9
8A3	Flange	10.95	381.1	372.4	396.5	490.6	510.0	198.0	130.4	2.05	16.4	39.8
8A6	Web	7.19	391.6	370.4	-	483.7	-	201.4	56.2	2.11	16.3	39.7
8B2	Flange	9.91	391.3	367.5	386.0	471.8	489.5	198.4	138.0	2.74	17.2	40.6
8B3	Flange	11.02	368.1	363.4	386.0	468.5	489.5	199.6	102.2	2.89	17.3	40.6
8B6	Web	7.04	378.5	369.5	-	473.6	-	206.5	98.1	2.66	16.7	40.0
8C2	Flange	10.80	372.8	362.5	372.0	457.0	496.5	197.8	123.3	3.08	17.6	41.0
8C3	Flange	11.89	368.6	360.9	372.0	457.8	496.5	196.0	134.8	2.83	17.4	40.7
8C6	Web	7.16	375.9	363.9	-	456.5	-	199.5	90.5	2.83	16.4	39.8
12A2	Flange	15.11	423.9	411.4	362.0	498.7	479.5	200.4	57.2	2.43	12.9	36.2
12A3	Flange	15.21	406.3	391.5	362.0	482.7	479.5	193.1	69.8	2.54	15.5	38.8
12A6	Web	10.62	429.6	425.3	-	497.2	-	204.5	46.4	2.47	13.2	36.6
12B2	Flange	14.60	379.6	370.8	389.5	473.0	486.5	194.5	72.9	2.95	17.8	41.1
12B3	Flange	14.35	383.9	372.7	389.5	473.8	486.5	201.6	93.3	3.02	17.4	40.7
12B6	Web	10.85	399.0	398.3	-	488.7	-	170.3	73.3	2.23	14.3	37.7
12C2	Flange	14.83	358.0	343.2	379.0	460.8	506.5	196.5	84.4	2.62	18.3	41.7
12C3	Flange	14.99	357.7	353.0	379.0	463.4	506.5	188.6	107.3	2.73	18.4	41.8
12C6	Web	11.00	365.8	369.8	-	455.6	-	179.1	83.6	2.74	12.2	35.5

Appendix A: UWO Data Summary Continued

ID#	Type	t (mm)	F_{uy} (MPa)	F_y (MPa)	$F_{y\text{-mill}}$ (MPa)	F_u (MPa)	$F_{u\text{-mill}}$ (MPa)	E (GPa)	$d\varepsilon/dt$ ($\mu\varepsilon$/s)	ε_{sh} (%)	ε_u (%)	% Elong.
141A2	Flange	17.27	375.4	374.7	365.5	486.3	496.5	187.0	60.3	1.84	14.5	37.8
141A3	Flange	15.85	387.3	375.9	365.5	486.5	496.5	201.7	93.0	1.97	15.0	38.4
141A6	Web	21.82	389.3	374.5	-	482.4	-	205.7	121.3	2.20	15.3	38.6
141B2	Flange	16.00	376.6	368.5	365.0	486.0	483.0	202.0	90.2	1.86	16.4	39.8
141B3	Flange	15.98	366.8	365.0	365.0	485.6	483.0	197.3	100.5	1.46	15.5	38.9
141B6	Web	20.09	386.5	376.0	-	490.4	-	203.4	106.7	2.23	15.9	39.3
141C1	Flange	15.88	397.4	370.7	358.5	488.5	489.5	200.8	137.0	1.53	15.0	38.4
141C3	Flange	15.95	378.1	373.2	358.5	491.9	489.5	205.8	119.2	1.44	14.7	37.9
141C6	Web	19.74	397.7	379.6	-	488.9	-	196.7	105.4	1.97	14.5	37.9
142A2	Flange	23.72	362.7	364.4	365.5	490.9	493.0	197.3	129.5	1.39	13.5	36.9
142A3	Flange	23.67	368.0	361.6	365.5	486.8	493.0	193.8	152.2	1.50	15.0	38.3
142A6	Web	14.96	374.5	367.9	-	485.7	-	206.9	141.0	1.87	15.0	38.2
142B2	Flange	23.72	352.4	351.6	348.5	472.9	483.0	202.0	120.5	1.55	15.3	38.7
142B3	Flange	23.70	361.4	347.2	348.5	469.8	483.0	198.5	118.1	1.64	15.9	39.3
142B6	Web	13.79	347.7	347.7	-	468.3	-	199.0	151.4	1.66	15.8	39.2
142C2	Flange	23.72	367.5	366.3	382.5	492.4	520.5	196.2	59.9	1.54	14.0	37.3
142C3	Flange	23.70	379.6	367.8	382.5	488.8	520.5	204.6	86.4	1.74	14.6	37.9
142C6	Web	14.94	372.9	361.6	-	483.8	-	199.5	131.6	1.86	15.6	39.0
24A2	Flange	16.87	404.5	389.1	403.5	496.4	499.5	198.6	70.4	1.83	15.4	38.7
24A3	Flange	-	-	-	403.5	-	499.5	-	-	-	-	-
24A6	Web	11.00	469.2	445.7	-	521.5	-	199.6	140.8	3.13	13.6	37.0
24B2	Flange	16.38	385.6	362.5	375.5	479.6	489.5	192.5	67.6	2.23	16.2	39.5
24B3	Flange	16.23	356.9	357.0	375.5	480.1	489.5	183.0	69.8	1.91	16.5	39.8
24B6	Web	10.92	418.4	396.2	-	496.8	-	189.3	162.6	2.78	16.4	39.7
24C2	Flange	16.61	399.3	375.5	369.0	479.9	486.5	202.1	93.1	2.42	15.9	39.2
24C3	Flange	16.05	383.2	374.1	369.0	482.6	486.5	202.2	96.7	2.00	15.5	38.9
24C6	Web	11.00	428.8	405.1	-	496.0	-	200.4	146.0	2.90	15.7	39.1
30A2	Flange	17.14	393.8	376.0	375.5	486.1	476.0	206.7	143.0	2.67	16.9	40.3
30A3	Flange	16.36	369.8	362.3	375.5	484.0	476.0	200.9	104.7	1.68	15.9	39.3
30A6	Web	13.56	436.2	411.2	-	504.0	-	198.4	60.5	2.72	14.7	38.0
30B2	Flange	16.74	407.6	386.7	369.0	487.5	486.5	204.1	74.5	2.89	16.8	40.1
30B3	Flange	15.70	391.9	380.9	369.0	489.1	486.5	194.6	78.6	2.31	16.5	39.9
30B6	Web	13.18	442.6	415.4	-	507.5	-	194.1	87.3	2.63	14.4	37.8
30C2	Flange	16.05	424.8	407.1	400.0	507.7	517.0	196.7	116.8	2.79	15.3	38.6
30C3	Flange	16.66	417.0	396.8	400.0	502.9	517.0	195.4	145.9	2.16	15.0	38.3
30C6	Web	13.82	446.8	444.2	-	515.2	-	205.2	85.1	2.67	14.5	37.8

Appendix A: UWO Data Summary Continued

ID#	Type	t (mm)	F_{uy} (MPa)	F_y (MPa)	$F_{y\text{-mill}}$ (MPa)	F_u (MPa)	$F_{u\text{-mill}}$ (MPa)	E (GPa)	$d\varepsilon/dt$ ($\mu\varepsilon$/s)	ε_{sh} (%)	ε_u (%)	% Elong.
36A2	Flange	24.13	371.4	349.9	352.0	466.1	458.5	194.6	117.6	2.02	16.2	39.6
36A3	Flange	23.47	371.8	350.5	352.0	465.7	458.5	202.9	170.6	1.96	16.7	40.1
36A6	Web	15.44	424.0	402.9	-	488.0	-	191.8	168.5	2.71	15.2	38.6
36B2	Flange	23.04	396.3	372.0	362.0	490.9	493.0	184.4	167.2	1.78	14.5	37.7
36B3	Flange	24.61	395.8	376.7	362.0	489.5	493.0	196.1	120.8	2.01	15.0	38.3
36B6	Web	15.72	435.5	412.2	-	504.1	-	193.5	159.1	2.85	15.4	38.7
36C2	Flange	25.25	364.6	343.4	345.0	459.9	462.0	184.3	111.5	1.99	16.7	40.0
36C3	Flange	24.51	362.9	342.1	345.0	456.9	462.0	191.4	93.7	2.06	16.9	40.3
36C6	Web	15.44	416.6	390.5	-	480.6	-	189.1	154.7	2.83	15.7	39.0
JA2	Flange	23.50	417.2	416.0	419.9	559.0	580.8	181.6	47.6	0.85	12.9	36.3
JA3	Flange	23.67	423.8	430.2	419.9	566.5	580.8	181.5	62.0	0.73	11.6	34.9
JA6	Web	14.96	465.3	474.6	-	605.1	-	195.7	68.4	0.27	10.3	33.6
JB2	Flange	16.33	439.9	439.9	422.9	536.0	543.9	194.7	61.2	1.35	11.2	34.5
JB3	Flange	16.43	429.7	428.9	422.9	532.7	543.9	201.3	65.7	1.32	12.0	35.4
JB6	Web	20.83	410.6	402.3	-	500.1	-	196.0	81.1	1.74	12.5	35.9
JC2	Flange	23.39	428.5	402.7	393.9	557.0	561.9	196.4	75.6	1.73	15.7	39.0
JC3	Flange	24.18	422.6	412.0	393.9	552.1	561.9	203.9	94.8	1.77	15.3	38.6
JC6	Web	14.83	496.0	480.4	-	597.4	-	189.4	129.7	2.07	12.4	35.7
606589-3	Web	29.46	402.3	375.6	-	530.8	-	203.6	114.9	1.23	14.6	45.6
606589-4	Web	29.47	387.6	376.8	-	530.6	-	202.7	110.1	1.31	14.5	45.3
615871-3	Web	27.81	381.4	370.1	-	523.8	-	212.9	100.9	1.14	14.1	45.6
615871-4	Web	27.84	387.1	365.5	-	524.2	-	201.6	78.1	1.23	14.4	45.7
616117-1	Flange	14.24	410.0	393.9	368.0	512.7	516.0	201.6	135.2	2.28	16.3	41.0
616117-2	Flange	14.20	381.2	377.2	368.0	515.5	516.0	204.1	114.2	1.74	15.5	37.5
616117-3	Web	10.19	408.3	393.7	-	511.6	-	199.5	130.9	2.64	16.0	-
616117-4	Web	10.25	416.4	389.4	-	508.8	-	207.0	91.9	2.53	16.5	33.1
616117-5	Flange	14.37	403.7	389.5	368.0	517.2	516.0	198.1	164.3	2.00	16.3	40.5
617633-3	Web	29.61	388.6	362.7	-	518.5	-	203.0	111.9	1.24	14.7	47.0
617633-4	Web	29.59	378.6	361.5	-	517.3	-	200.5	77.0	1.26	15.3	47.1
623446-1	Flange	15.96	410.7	388.9	379.0	496.4	499.0	204.8	121.2	2.67	16.6	43.1
623446-2	Flange	15.48	382.5	376.9	379.0	488.9	499.0	206.5	160.3	2.35	16.3	41.5
623446-3	Web	12.88	444.3	417.2	-	514.6	-	197.8	81.6	2.70	15.2	39.0
623446-4	Web	12.91	436.3	417.1	-	514.6	-	201.2	76.0	2.71	15.4	40.0
623446-5	Flange	16.14	404.4	390.8	379.0	492.1	499.0	197.9	113.3	2.59	16.9	44.0

Appendix A: UWO Data Summary Continued

ID#	Type	t (mm)	F_{uy} (MPa)	F_y (MPa)	$F_{y\text{-mill}}$ (MPa)	F_u (MPa)	$F_{u\text{-mill}}$ (MPa)	E (GPa)	$d\varepsilon/dt$ ($\mu\varepsilon$/s)	ε_{sh} (%)	ε_u (%)	% Elong.
624388-1	Flange	26.59	397.0	384.1	375.0	522.0	537.0	202.9	102.2	1.88	15.1	46.7
624388-2	Flange	26.19	402.9	384.8	375.0	529.3	537.0	204.7	121.0	1.43	14.6	45.6
624388-3	Web	17.95	414.3	398.2	-	529.3	-	198.6	94.5	1.99	15.9	42.3
624388-4	Web	17.92	415.6	396.1	-	533.4	-	201.6	74.3	1.72	14.8	37.2
624388-5	Flange	26.78	392.6	388.3	375.0	525.6	537.0	199.9	125.5	1.92	15.6	47.0
626534-1	Flange	22.55	406.0	388.9	390.0	501.1	512.0	196.5	161.5	2.37	16.0	45.7
626534-2	Flange	22.26	386.1	382.9	390.0	503.6	512.0	190.2	128.8	2.16	16.3	47.4
626534-3	Web	15.75	462.0	433.5	-	532.7	-	200.8	139.7	2.86	15.0	40.8
626534-4	Web	15.66	440.9	424.3	-	525.6	-	194.4	116.6	2.86	16.2	42.5
626534-5	Flange	22.46	430.8	394.9	390.0	506.8	512.0	202.2	133.9	2.33	16.4	47.1
626709-1	Flange	16.43	435.9	423.0	423.0	509.7	515.0	198.2	134.7	3.31	16.5	46.8
626709-2	Flange	16.76	423.8	401.1	423.0	503.0	515.0	198.1	138.7	2.71	16.5	45.9
626709-3	Web	12.69	483.3	454.9	-	541.2	-	197.7	157.5	2.55	13.9	37.8
626709-4	Web	12.61	488.1	470.2	-	550.8	-	196.9	143.9	2.52	12.3	36.1
626709-5	Flange	16.42	433.7	417.6	423.0	506.6	515.0	198.1	95.8	3.38	16.2	44.9